Monitoring of Atmospheric Perturbations Caused by Various Geophysical Events Using VLF Signal

THESIS

Submitted for the Degree of

Doctor of Philosophy (Science)

of

Jadavpur University

By

Minu Sanfui

Department of Physics

Jadavpur University

Kolkata -700032, India

2022

CERTIFICATE FROM THE SUPERVISOR

This is to certify that the Thesis entitled "**Monitoring of Atmospheric Perturbations Caused by Various Geophysical Events Using VLF Signal"** submitted by **Minu Sanfui** who got her name registered on 26/09/2013 for the award of Ph.D. (Science), Degree of Jadavpur University, is absolutely based upon her own work under the supervision of **Prof. Debasish Biswas** and that neither this thesis or any part of it has been submitted for either any Degree / Diploma or any other academic award anywhere before.

(Signature of the Supervisor and Date with official seal)

Prof. Debasish Biswas

Department of Physics
Jadavpur University
Kolkata, India

DECLARATION

I declare that the work described in the thesis entitled, **"Monitoring of Atmospheric Perturbations Caused by Various Geophysical Events Using VLF Signal"** is the result of investigation carried out by me under the supervision of Prof. Debasish Biswas, Department of Physics, Jadavpur University, Jadavpur, Kolkata-700032, India and that it has not been submitted elsewhere for the award of any degree or diploma. I declare that this written document represents my ideas, in my own words and I have adhered to all principles of academic honesty and integrity and have not misrepresented or fabricated or falsified any idea/data/fact/source in my submission.

In keeping with the general practice in reporting scientific observations, due acknowledgement and citation has been made whenever the work described based on the findings of other investigators. Any omission that might have occurred by oversight or error of judgment is regretted

Date : MINU SANFUI

ACKNOWLEDGEMENT

The author expresses her indebtedness to her supervisor, Prof. Debasish Biswas for inspiring her in this research field and for suggesting her different research problems. Without his continuous inspiration, guidance and all supports, it would never be possible for her to complete this thesis.

Thanks are due to other co-workers, Dr. Dilip Halder, Dr. Goutami Chattopadhaya, Dr. Suman Paul, Prof. S. S. De who acted as the co-authors in different published papers included / not included in this thesis.

The author is also thankful to the library staff of the Department of Physics, JU for their valuable co-operation sought in the work and in the preparation of the thesis.

Minu Sanfui

Department of Physics
Jadavpur University
Kolkata, India

PREFACE

Schumann resonance and some its important characteristics uses and monitoring of atmospheric perturbation caused by various geophysical and extra-terrestrial events using VLF signals have been presented in this thesis. From the observational records over Kolkata the variation of frequency of the first mode SR spectra during solar proton event on 6-7 March 2012 have been presented in this work. The result shows that the decrease in frequency during the period of occurrence. The severe solar X-ray bursts occur just before the proton event shows enhancement of the first mode SR frequency. The influences of solar proton event and X-ray bursts upon the SR frequency fluctuation in the result in some other locations are also exhibited. The variation may be explained in terms of changes of ionization produced by the events. From the observational records over Kolkata, Agartala (Tripura), a few specific characteristic of SR like the changes due to global thunderstorm activity, the amplitude and frequency changes of different modes due to earthquake, solar eclipse and also change of frequency and amplitude of transmitted signal and sferic signal due to lightning storm, meteor shower, solar eclipse, earthquake, effects of different geophysical and extra-terrestrial event within the earth ionosphere cavity in terms of ULF/ELF/VLF radio waves etc. are discussed in this thesis.

Other than the studies of variation of frequency of SR first mode due to solar proton event, global circuit, effect of geophysical and extra-terrestrial event within the earth-ionosphere cavity in terms of ELF/ULF/VLF/Radio waves the candidate was engaged to also explore different atmospheric electricity parameters.

The results of observations from different experimental setups in connections with the stated phenomena are analyzed and in some cases results are interpreted graphically and

compared with earlier work. It is observed that the result are almost same. The most of the results are published in the form of research articles in various peer-reviewed reputed national and international journal. A list is attached herewith.

Further works in most of the topic of the stated areas are being investigated. It is contemplated the outcome that some works to will be published in the near future.

The results of investigation in the thesis about some characteristic of SR and variation of SR first mode frequency due to solar proton event 2012 and effects of some geophysical and extra-terrestrial event upon transmitted sub ionospheric VLF signals, it is hoped, will be of some use to the different experimental groups.

Date:

MINU SANFUI

Departmnet of Physics
Jadavpur University
Jadavpur, Kolkata 700032

Dedicated to

My supervisor

Prof. Debasish Biswas

ABSTRACT

The spherical shell of the atmosphere ionized by the solar X-ray and γ -ray radiation in the range of 50 – 1000 km altitude is called the ionosphere. Below this altitude medium is ionized only by highly energetic galactic cosmic rays. The ionosphere consists of different layers, viz., D-layer (60–90 km), E-layer (90–120 km), E_s -layer, F -layer (120– 500 km) and above this the topside ionosphere. The day side F -layer is sub-divided further into F_1 and F_2 layers. The space above ionosphere around the planet, where magnetic field lines are dominant is called the magnetosphere which is controlled by the planet's magnetic field. Earth surface and lower boundary of the ionosphere (50– 60 km altitude) is dielectric in nature, and eventually becomes a spherical waveguide for the low frequency radio wave.

Earth-ionsphere waveguide acts as a global circuit. Schumann resonances occur in this waveguide. It is an electromagnetic resonance phenonmenon generated by global lightning discharges within the resonator formed between the earth and the ionosphere.

Chapter 1 gives an introduction and a review of the studies reported in the literature in this field.

Chapter 2 explains the rudimentary theoretical background and the experimental techniques employed in the measurement and analyses carried out.

Chapter 3 provides the details about the severe X-ray flare occurred on 06 - 07 March 2012 followed by a solar proton event (SPE). During this event the variation in frequency of the first Schumann resonance (SR) spectra mode from the recorded data over Kolkata (22.56°N, 88.5°E) was studied. The first mode frequency enhanced (~8.14 Hz, 3.85%) during the solar X-ray bursts and immediately after its value decreased (~7.44 Hz, 5.13%) during the proton event. The influences of SPE and X-ray bursts upon the SR frequency fluctuation are

explained in terms of the changes in medium ionization, i.e., the change in dielectric property and two layer reflection height variation in the waveguide. The geomagnetic storm effect on the modification of this frequency variation occurring during that time was also considered.

Chapter 4 presents the details about earth-ionosphere waveguide. In this chapter earthquake research, meteor shower effect, solar proton event, earthquake prediction, Hiss emission etc. have been explained in detail. The space between the two spherical conducting shells, Earth surface and the lower boundary of the ionosphere, behaves as a spherical cavity in which some electromagnetic signals can propagate a long distance and is called Earth-ionosphere waveguide. Through this waveguide ultralow frequency (ULF), extremely low frequency (ELF) and very low frequency (VLF) signals can propagate efficiently with low attenuation. Resonances which occur for ELF waves due to round-the-world propagation interfering with $2n\pi$ phase difference are called Schumann resonances. Lightnings are the main sources of energy continuously producing these electromagnetic radiations from the troposphere. Some fixed frequency signals are also transmitted through the waveguide from different stations for navigation purposes. The intensity and phase of these signals at a particular position depend on the waveguide characteristics which are highly influenced by different natural events. Thus the signatures of different geophysical and extra-terrestrial events may be investigated by studying these signals through proper monitoring of the time series data using suitable techniques. In this work, we provided a review on ULF, ELF and VLF signals within the waveguide in terms of different geophysical and extra-terrestrial events like lightning, earthquakes, Leonid meteor shower, solar flares, solar eclipse, geomagnetic storms, and TLEs etc.

Chapter 5 summarizes the works presented in the thesis. It also described the scope of the future researches in this field.

LIST OF PUBLICATION

Included in the thesis :

1. **Minu Sanfui,** Debasish Biswas: First mode Schumann resonance frequency variation during a solar proton event. Terr. Atmos. Ocean. Sci. vol-**27** No 2,253-259, April 2016
2. **Minu Sanfui,** D. K. Halder, Debasish Biswas: Studies on the ULF/ELF/VLF Radio wave propagations in terms of different Geophysical and extra–terrestrial events within the earth–ionosphere cavity, Astrophys Space Sci 2016, 361:325

Not included in the thesis:

Published in International & National Journals:

1. S S De, Suman Paul, D. K. Haldar, S Barui, **Minu Sanfui** and B Bandyopadhyay : The effects of recent solar eclipse upon a subionospheric transmitted signal, Indian J. Phys. **83** 1245, 2009
2. B. K. De, Pinaki Pal, B. Bandyopadhyay, S. Barui, D.K.Haldar, Suman Paul, **Minu Sanfui** and Goutami Chattopadhyay: Detection of 2009 Leonid, Perseid and Geminid Meteor Showers through its effects on Transmitted VLF Signals. Astrophys. Space Sci. (Netherlands), 2010,
3. B. K. De, B. Bandyopadhyay, Suman Paul, S. S. De, S. Barui, **Minu Sanfui**, Pinaki Pal and T. K. Das: Studies on the precursors of an earthquake as the VLF electromagnetic sferics. Rom. Journ. Phys., **56,** 1208–1227, 2011

4. S. S. De, B. Bandyopadhyay, T. K. Das, Suman Paul, D. K. Haldar, B. K. De, S. Barui, **Minu Sanfui,** Pinaki Pal and Goutami Chattopadhyay: Studies on the anomalies in the behaviour of transmitted subionospheric VLF electromagnetic signals and the changes in the fourth Schumann resonance mode as signatures of two pending Earthquakes, Indian J. Phys., **85,** 447, 2011

5. B. K. De, B. Bandyopadhyay, S. Paul, S. Barui, D. K. Haldar, **Minu Sanfui**, T. K. Das, G. Chattopadhyay and P. Pal: The effects of solar eclipse on long path VLF transmission, Bulg. J. Phys. (Bulgaria), **38,** 206-215. 2011

6. S.S. De, **Minu Sanfui** etal,: Studies on the variations of ELF Atmospherics over Kolkata, Bulg. J. Phys. **37** (2010) 37 – 74. 2010

International Seminar & Conference Paper

1. S. S. De, B. K. De, B. Bandyopadhyay, Suman Paul, **Minu Sanfui**, D. K. Haldar, M. Bose and Goutami Chattopadhyay: Studies on non-linear Travelling Ionospheric Disturbances and mode coupling within the auroral region, Proceedings of the IEEE Xplore: International Conference on Computers and Devices for communication (CODEC – 2009) organized by University of Calcutta held at Kolkata, India during December 14-16, 2009 (INSPEC Accession Number: 11107217)

2. S. S. De, B. Bandyopadhyay, Suman Paul, D. K. Haldar, S. Nandi, **Minu Sanfui**, S. Barui and Goutami Chattopadhyay: AILA-2009 and its effects on VLF sferics, Proceedings of the IEEE Xplore: International Conference on Computers and Devices for communication (CODEC – 2009) organized by University of Calcutta held at Kolkata, India during December 14-16, 2009 (INSPEC Accession Number: 11107218)

3. S. S. De, B. K. De, B. Bandyopadhyay, Suman Paul, D. K. Haldar, S. Barui, **Minu Sanfui**, A. Bhowmick, Pinaki Pal, S. Nandi and T K Das: On some effects of perturbations in the ionosphere due to electromagnetic precursory signals from earthquake, Proceedings of the IEEE Xplore: International Conference on Computers and Devices for communication (CODEC – 2009) organized by University of Calcutta held at Kolkata, India during December 14-16, 2009 (INSPEC Accession Number: 11107219)

CONTENTS

CHAPTER - 1

1.1 INTRODUCTION:

The atmosphere is comprised of layers based on temperature. These layers are the troposphere, stratosphere, mesosphere and thermosphere. A further region at about 500 km above the Earth's surface is called the exosphere. Le Monnier first demonstrated that the atmosphere was electrified, even in fare weather. The source of the ions is dominated by galactic cosmic rays with energies typically 100 GeV or more, each of which slams into the atmosphere, leaving a trail of highly ionized gas in its wake. The peak ion pair production rate is a function of altitude. The peak production rate occurs between 10-30 Km. The rate decreases above this layer because lower density layer in the upper atmosphere presents less of a target for cosmic rays.

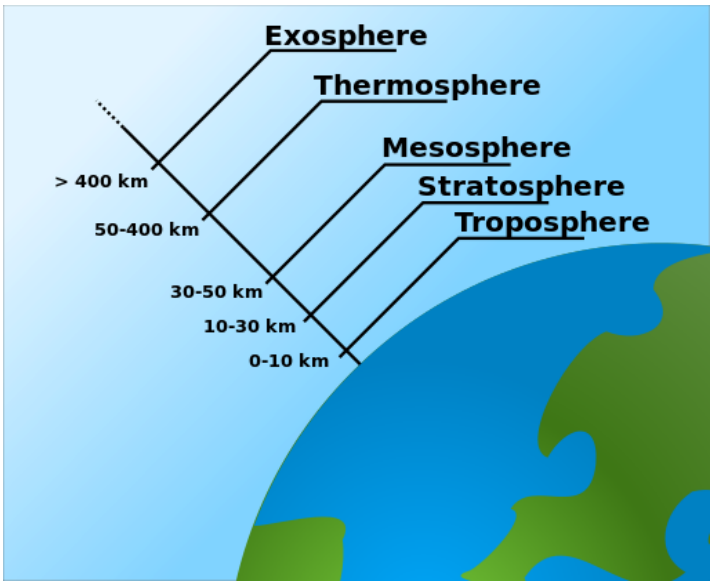

Fig 1.1 : Layers of earth’s atmosphere

The waves in the range of 3 Hz - 30 Hz is known as ELF frequency, 300 Hz - 3 KHz is known as ULF frequency, 3 KHz - 30 KHz is known as VLF frequency, 30 KHz - 300 KHz is known as LF frequency. Schumann Resonances are electromagnetic oscillations of

the earth-ionosphere cavity [1a]. To analyze ELF wave propagation in the earth-ionosphere cavity, a flat earth approximation may be derived from the exact equations, which are applicable to the spherical cavity, by introducing a second-order or Debye approximation for the spherical Hankel functions. In the frequency range 3 - 30 Hz, however, the assumed conditions for the Debye approximation are not satisfied. For this reason an exact evaluation of the spherical Hankel functions is used to study the effects of the flat earth approximation on various propagation and resonance parameters [1b].

Schumann resonance frequencies are excited by lightning strokes and maintained by worldwide thunderstorm activity. In this way the global lightning activity can be monitored by measuring its intensity, as numerous studies have shown [2 - 9]. According to the SR theory, [10] the SR intensities at a given location depends not only on the lightning source parameters (current movements) but also on the cavity properties (Ionospheric D region conditions).

The Schumann Resonance is the electro-magnetic resonance phenomenon generated by global lightning discharges within the resonator formed between the earth and ionosphere. The various aspects of Schumann Resonance phenomena have been explained [11 - 27] over the years.

The seasonal and day to day variability in SR intensities, frequencies and quality factors are reported with possible explanation for such changes [28 - 38]. The specific linkage between the SR peak frequencies values with global and regional temperature is well known. The variation in SR peak frequency has been proven to be useful in indicating the variation in the tropical and global temperature [16, 39].

A powerful radio noise burst radiating over a wide frequency ranges from few Hz to several MHz during lightning discharges within the thunder clouds, which can propagate over

a long distance through the earth-ionosphere waveguide. Attenuation of the EM waves with frequencies less than 50 Hz is extremely low [40] which can encircle round the globe few times through the earth-ionosphere cavity. Resonances are occurred when these waves are interfering with 2π phase difference, i.e, the wave length is of the order of dimension of the cavity around 40 mm. This phenomenon is known as the Schumann Resonance [1a]. Some other electrical noises generated from the difference sources, i.e, from electric railways, mechanical variation of the antennas, surrounding vegetations, drifting electrically charge clouds and power line transients, EM signals from earthquake etc. also interfear with these resonance phenomena and perturb the signal intensity. Presently Schumann resonance are being used to monitor global lightning activity [41]. Global variability of lightning activity [42], and Sprite activity [41, 43 - 45] showed the influence the solar proton events as the increment in frequency, Q factor and amplitude of the SR modes. SR has also been used for the earthquake forecursorie studies [46 - 50].

The parametric measurements of SR occurances can be used to study the inter annual variability in global thunder storm activity centres in the three different continental regions. The maximum frequency variations of about 0.3, 0.4 and 0.7 Hz waves were observed in the first second and third mode respectively and has been explained in terms of the ionospheric electron density variation in the Himalaya Region India.

Due to the geomagnetic field the anisotropic conductivity of the cavity influences the wave propagation in the earth-ionosphere cavity. Within the cavity disturbances like random fluctuation of irregularities are corresponding regularly along with other causalities such as polar cap absorption, x-ray bursts. The inhomogeneity and anisotropy of the cavity are supposed to introduce line splitting of the SR spectra [51 - 53]. Vertical properties of the electric and magnetic fields of the first global SR in the earth-ionosphere cavity are

investigated numerically with various vertical profiles of the ionospheric electron concentration [54].

Information about the influence of geomagnetic disturbances on values of SR frequencies is scarce and contradictory using magnetic components measurements for three months. Sao et.al [13] investigated the dependence of the first and second mode frequencies on Heliogeo physical activity. They detected some similarities in the course of variation of the first mode frequency and intensity of the solar rays. The comparison of frequency variation with AP index (The Ap index is defined as the earliest occurring maximum 24-hour value obtained by computing an 8-point running average of successive 3-hour Ap indices during a geomagnetic storm event) displays there small negative corelation, Satori et.al [55] found an opposite result : first mode frequency may be higher by nearly 01. to 0.3 Hz for geomagnetically disturbed days ($K_P \geq 4$) as compared with quiet conditions ($K_P \leq 1$). (Where The planetary 3-hour-range index **Kp** is the mean standardized K-index from 13 geomagnetic observatories between 44 degrees and 60 degrees northern or southern geomagnetic latitude).

The waves in the earth-ionosphere cavity are generated by lightning discharges. At the same time the Schumann resonance is controlled not only by thunderstorms but also by the solar and geomagnetic activities. Sentman et.al [56] showed the dependence of the observed resonace power on the effective height of the ionospheric D region at the observation point. The dependence of the first and second order Schumann resonance modes on solar activity was discovered by Fullekrug et.al [57]. They found 27 days amplitude variation co-incident in phase with solar spot number. From measurement made Marsx et.al [58] found similarities between the resonance amplitude and the atmospheric electric field despite the local character of the later.

The resonances of earth-ionosphere cavity are analyzed by considering the difference propagation characteristic of day and night hemispheres. A uniform model of earth-ionosphere cavity accounts for some of the observations [59] but more accurate theoretical models were recently develop the work of Madden et.al and Hobara et.al [12, 60]. They represented the lower Ionospheric boundary by a surface impedance that accounts for different between day time and night time conditions and for the magnetic field effect at various latitudes.

Due to the global nature the SR represents a proxy for global lightning activity [61], and can also be reliably monitored from a single location on the earth surface [52, 63 - 65]. In addition changes in the diurnal SR frequency ranges are related to the areal variation of thunder- storm regions around the globe [66, 67]. In recent years there has been increasing interest in the SR as an indicator of global and regional lightning activity. One of the reasons for this interest is due to the possible connection between the earth climate and global lightning activity and the possibility of studying this connection used in single station SR measurement [12, 64, 69].

The earth-ionosphere cavity is sharply bounded by two concentric spherical shells. The space between two shells each is assumed to be vacuum with dielectric permittivity ε_0, the homogeneous earth of radius 'a' is characterized by conductivity σ_g and permittivity ε_g while the homogeneous ionosphere ($r>a+h$) has a conductivity σ_i and permittivity ε_i. The problem is formulated in spherical coordinates (r,θ,ϕ) and excitation by a vertical dipole located on the ground surface at $\theta=0$ is assumed.

A high altitude nuclear explosion has been shown to affect the earth-ionosphere cavity resonance by simultaneous lowering all the resonance frequencies [70-72].

The lowering of the resonance frequency following a nuclear explosion has been attributed by Chapman et.al [73] in their two layer ionosphere model solely to decreasing conductivity of the E region. After measuring a change of the resonance frequency following a nuclear explosion it is possible to advance simple ionosphere model for explaining a particular change. However, no attempt has been reported to predict resonance shifts for different nuclear yields. This rather complex problem requires a quantative evaluation of the various nuclear mechanism that may shift to ionosphere perturbations. In such information is available for the computation of the resonances shifts which is relatively simple. It would be also of interest to investigate the effects of the sudden ionosphere disturbances (SID) and to discriminate between SIDs and nuclear effects.

The resonance frequency changes can be considerated more accurately with non uniform models of the propagation geometry. A perturbation method [74] or neumerical techniques [12] has been used for solving such problems.

Based on theoretical consideration Schumann et.al [75 - 78] postulated resonances of the earth-ionosphere cavity. Koenig et.al [79 - 81] obtained the first experimental indication of Schumann resonances by observing noise waveforms in the output of a narrow band amplifier. Detailed frequency spectra of this noise were first obtained by Balser and Wagner [11]. Other measurements have been reported by various scientists [82–91]. Fundamental theory of Schumann resonance [76 - 78] is discussed in books by Wait and others et.al [92 - 94]. They considered the observable noise spectra as the response of the earth-ionosphere cavity due to lightning flashes of the earth-ionosphere cavity all over the world, but the homogeneous sharply bounded ionosphere model of Raemer introduced high losses and he did not succeed in reproducing the spherical measurement of [11]. Galejs [95,96] used an isotopic ionosphere model of exponentially increasing conductivity which is based on measured or calculated characteristic of the lower ionosphere. The model permits a close

reproduction of the noise spectra measurement in the earth-ionosphere region and it also provided an agreement with measured ELF attenuation rates. Some scientists [97-101] computed the local surface impedance and propagation constant for a uniform cylindrical shell between anisotophic ionosphere and the earth using matrix multiplication techniques. The resonance frequencies and Q factors are computed numerically using a lumped parameter approximation of the two dimensional transmission line. In the theoretical model for explaining the resonance frequencies and the Q factor measurement [102-104], it is necessary to consider the boundary property of the spherical shell.

Models of the anisotropic ionosphere are difficult to apply to the problem of earth-ionosphere cavity. Resonance occur for the variation of the magnetic field vector along the surface of the earth [59].. The propagation parameter can be estimated in the presence of a horizontal magnetic field component from the works of [99,100] and the earth-ionosphere cavity resonances have been analyzed for a inhomogeneous ionosphere in the presence of a radial magnetic field by Thompson [105]. A thin shell approximation of the ionosphere with a super imposed radial magnetic field have been considerate by Wait [106]. Some other works [107,108] although intended for a difference frequency range could also be applied to the earth to ionosphere resonance problem in the presence of a radial magnetic field.

In wide band recording of atmospheric signal an ELF component or Slow Tail follows the initial VLF component of the transient [109 - 113] and oscillatory structure of the signal becomes noticeable by passing it through a band pass filter. The two horizontal magnetic field component have been observed simultaneously in Canada and in Antarctica [59].

A resonance frequency and Q factor may be determined from spectral measurement. Analytically it is also possible to compute the power spectrum of the noise waveform.

However, it is more analytically determined propagation parameters and the radial electrical field due to the vertical dipole excitation can be represented by

$$E_r = - \frac{iIds}{4\omega\varepsilon ha2} \frac{v\,(v+1)}{\sin v\pi} P_v\,(-\cos\theta) \;\ldots\ldots\ldots\ldots\ldots\ldots\ldots\ldots\ldots\ldots\ldots\ldots\ldots(1)$$

where

$$v(v + 1) = (k_0aS)^2$$

For a wave that propagates in the spherical shell between the earth and the ionosphere, S is defined as the ratio of the complex wave number K to free space wave number K_0 where $S=K/K_0$. The real part S can be seen to be inversely proportional to the phase velocity, and the imaginary part of S is proportional to the attenuation constant. This parameters S is determined form solving the appropriate boundary value problem of the earth, the air space and the chosen ionosphere model [93, 103]. The frequency of the nth mode are determined from the minima of sin νπ. In equation 2 [103, 115] which gives

$$f_n \approx \frac{7.5\sqrt{n(\,n+1)}}{ReS} \;\ldots\ldots\ldots\ldots\ldots\ldots\ldots\ldots\ldots\ldots\ldots\ldots\ldots\ldots\ldots(2)$$

Tripical value of R_{es} is 1.4 to 1.2 for frequencies in the resonance region.

The cavity Q may be determined as a ratio between the stored energy and energy loss per cycle or simply by the width of resonance curve.

The cavity between the earth and ionosphere is a resonator for electromagnetic waves. The Schumann resonance frequency cover several Hz. The simplest vacuum model confined with two concentric perfectly conducting spheres yields the frequency [1a]

$$\omega_n = \frac{c}{a}\sqrt{n\,(n+1)(1-\frac{h}{a})} \;\ldots\ldots\ldots\ldots\ldots\ldots\ldots\ldots\ldots\ldots\ldots\ldots\ldots (3)$$

where n is an integer number, c is the light velocity, a is the radius of the inner sphere, h = (a-b), is the distance from the inner sphere to the outer one and b is the radius of the outer sphere. Above expression 3 can be rewritten as follows taking into consideration h << a

$$f_n = \frac{\omega_n}{2\pi} \approx \frac{c}{2\pi a}\sqrt{n\,(n+1)} = 10.6\sqrt{\frac{n\,(n+1)}{2}}\ \text{Hz} \quad \ldots\ldots\ldots(4)$$

The simplest model credits the first order frequency f_1 = 10.6 Hz. Observations yields on average f_1 = 7.8 Hz [3]. The frequency became smaller because the ionosphere is not a perfect conductor. Introducing the impedance Z of the upper edge (r=b), the following equation result for the resonance frequencies (providing IzI <<1, h<<a) [117]

$$\omega_n = \frac{c}{a}\left(\sqrt{n\,(n+1) - \frac{z^2\,a^2}{4h^3}} + \frac{iZa}{2h}\right) \quad \ldots\ldots\ldots\ldots(5)$$

If the dielectric permeability at r>b and ε=constant then the impedance is

$$Z = \frac{1}{\sqrt{\epsilon}}$$

For an isotopic ionosphere the dielectric permeability has the following from [32].

$$\varepsilon = 1 - \frac{\omega_0^2}{\omega\,(\omega - i\nu)}$$

where ω is the wave frequency, $\nu = (4\pi e^2\ N/m^2)\ 2^{1/2}$ is the electron plasma frequency, e and m are the electron charge and mass respectively, N is the electron number density, ω is the frequency of collision of electron with neutral and ions. One can choose such values of Z and h that several resonance harmonies calculated with the help of equation 3 coincide sufficiently well with the observed 1. Observe once come complicated distribution of Q with

the height allows us to explain the observed width of the resonance band related to the resonator quality. The ionospheric D region (Heights from 60 to 90 Km) appears to determine the resonance spectrum.

Solar terminator fx (where Solar terminator is defined as the locus of points on a planet or moon where the line through the center of its parent star is tangent layer) are found in SR magnetic and electric field characteristics [118]. SPE (Solar proton events) are measured through infrequent space weather phenomena that can produce hazardous effects in the near earth space environment.

Madden and Thompson 1964 [101[computed the local surface impedance and propagation constant for a uniform cylindrical shell between the anisotropic ionosphere and by using matrix multiplication techniques. The resonance frequencies and Q factors are computed numerically using a lumped parameter approximation of the two dimensional transmission line. In the theoretical model that are advanced for explaining the resonance frequencies and the Q factor measurement [92, 103, 104]. It is necessary to consider the boundary property of the spherical shell.

Two layer ionospheric models give more accurate values of the resonance frequency and of cavity Q or of the complex propagation parameter S. Such models are usually derived by trial and error procedures and they are difficult to corelate with continuous ionosphere profiles. The ionospheric exponential model gives a reasonable approximation to the ionospheric conductivity versus height profile through the lower ionosphere layer and the propagation parameter of the model can be determined from closed form expression of the surface impedance [114], .The Q factor considered also the effects of cosmic ray ionization that gives a nearly exponential conductivity versus height variation as indicated by Galejs

[115]. The cosmic ray ionization decreases the effective Q in particular for the lower frequency.

The single layer ionosphere model [93, 94] assumes the boundary height of the ionosphere to be constant but the conductivity to change with frequency so as to obtain the correct resonant frequencies. However, the result in Q factor are approximately two time lower than measurement. Same difficulties are experienced with an ionospheric model of constant conductivity but frequency depends on boundary height and at ionospheric boundary at h=80 km the deficiency of a single layer ionosphere model is less pronounced if it is attempted to achieve only a partial match of resonance frequency as shown from [104]. However the Q factor will be two low in particular at the higher resonance frequency.

The magnetic field effects for a homogeneous sharply bounded ionosphere model have been discussed by Wait [92] in a quasilongitudinal approximation for a super imposed radial magnetic field and also for a transverse magnetic field. The earth-ionosphere cavity resonance frequencies have been considered in the thesis from [105] for a radial magnetic field. Thompson used a multi layer ionosphere model that approximate the continuous altitude variation of the conductivity tensor.

Solar flares, coronal mass ejections, high-speed solar wind, and solar energetic particles are all forms of solar activity. All solar activity is driven by the solar magnetic field.

A solar flare is an intense burst of radiation coming from the release of magnetic energy associated with sunspots. Flares are our solar system's largest explosive events. They are seen as bright areas on the sun and they can last from minutes to hours. We typically see a solar flare by the photons (or light) it releases, at most every wavelength of the spectrum. The primary ways we monitor flares are in X-rays and optical light. Flares are also sites where particles (electrons, protons, and heavier particles) are accelerated.

The outer solar atmosphere, the corona, is structured by strong magnetic fields. Where these fields are closed, often above sunspot groups, the confined solar atmosphere can suddenly and violently release bubbles of gas and magnetic fields called coronal mass ejections (CME). A large CME can contain a billion tons of matter that can be accelerated to several million miles per hour in a spectacular explosion. Solar material streams out through the interplanetary medium, impacting any planet or spacecraft in its path. CMEs are sometimes associated with flares but can occur independently.

Systematic description of theoretical and experimental research of this geophysical phenomenon, e.g., calculation of natural frequency of the cavity resonator based on different modes of ionosphere, study of excitation of the resonator by terrestrial and cosmic sources, lightning discharges, magnetosphere phenomena have been presented by Bliokh and co-workers [117]. They also discussed about location of lightning discharge, properties of the lower ionosphere, connection between resonances and magnetic disturbances, solar activity etc. in detail in connection with ELF signals. Presently Schumann resonances are being used to monitor global lightning activity [119 - 122], in characterizing the main African thunderstorm center [123] global variability of lightning activity [124] and sprite activity [120, 125]. A characteristic customary outline of the amplitude spectra has been exploited for evaluating the source-observer distance [126]. The relations between lightning and ELF noise levels on the global basis have been used to study the space-time dynamics of worldwide lightning activity [127]. ELF measurements can be used in the studies of TLEs [128 - 130]. The field decomposition method was used in a spherical cavity by Kulak et.al [131] to determine the source observer distance, by separating the resonant field from the traveling waves Dyrda et.al [123] studied the African thunderstorms by solving the inverse problem and by using the SR power spectrum templates derived analytically. They calculated the distances to the most powerful thunderstorm centers and presented the simplified 1-D

thunderstorm lightning activity 'maps' in absolute units C^2m^2/s. Schlegel et.al [132] showed the influence of solar proton events as an increment in frequency, Q-factor and amplitude of the SR modes. SR has also been used for the earthquake precursory studies [133 - 135], Nickolaenko and co-workers [136] computed the idealistic and realistic radio signals in the frequency and time domains and discussed features significant to the Earth-ionosphere cavity with low losses for the discrete ELF transients (Q-bursts) considering the special model of atmospheric conductivity.

Some fixed frequencies man-made VLF signals are also transmitted from different stations like Alpha, VTX, NWC, NPM etc. which are used for the global navigation system, detection of ionospheric irregularities and various other purposes. The intensity and phase of these signals are modulated by the waveguide characteristics, i.e., reflection height variation, dielectric constant of the medium etc. [137]. Different geophysical events, e.g., earthquake, thunderstorms and lightning, meteor showers etc. modify the Earth-ionosphere cavity by introducing huge energy which contributes additional ionization in the lower-ionospheric region. Thus the waveguide characteristics like reflection height, dielectric permeability etc. are changed by different natural sources. During the Lithosphere-Atmosphere- Ionosphere coupling, through the simultaneous effects of (1) chemical channel, (2) wave channel and (3) electric field channel, the seismic energy transport to the ionospheric height can modify the waveguide characteristics by extra ionization [138]. It produces the Seismo-induced ionospheric instabilities and modifies the charge density distribution which changes the reflection height and perturbs the over-horizon radio wave propagation within the earth- ionosphere waveguide [138 – 142]

Solar X-rays ionize the ionospheric layers on a regular basis and over the solar cycle but a kind of inhomogeneity can arise due to unequal extra-ionization in different layers during solar X-ray flares (SXF) and solar proton events (SPE). Thus the flares and

~

astronomical events like gama ray flare modify the ionosphere and are detected by the sub-ionospheric VLF propagation and ELF waves [143, 144]. Protons with energy up to 100 MeV are most often emitted from the Sun in conjunction with solar flares which can penetrate deeply (40 km) into the *D*-region and can cause additional ionization leading to conductivity changes thereby modifying the SR parameters [48, 49, 145–150]. Meteor showers also introduce perturbations in ion composition, temperature and other physical parameters within the ionospheric medium at different altitudes extending from the *D*-region to the ionospheric altitude [50, 151-154].

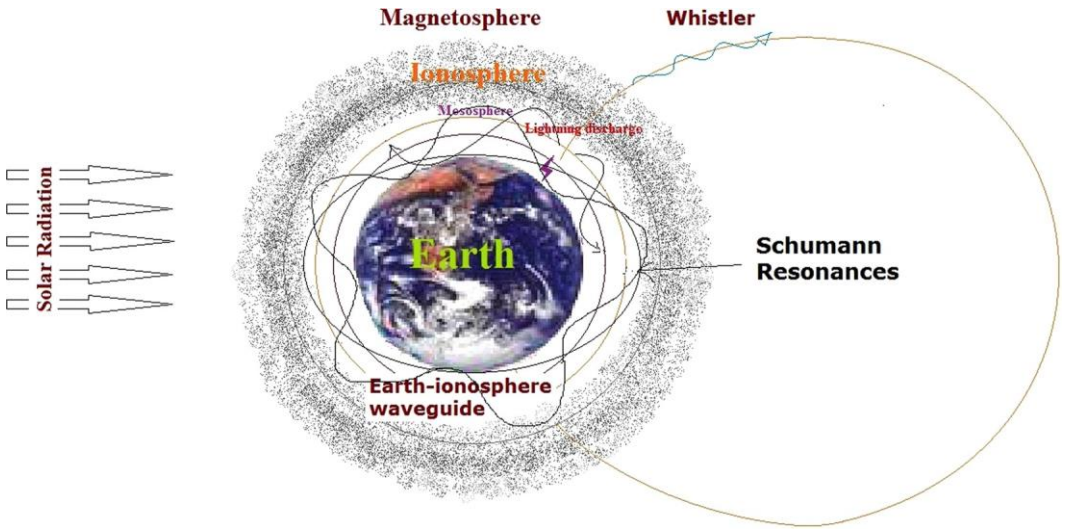

Figure – 1.2

A brief overview of atmospheric layers and the earth-ionosphere waveguide with a model diagram is given in Fig. 1.2. The troposphere extends up to 12 km on average from the ground surface, 9 km at pole and 17 km at Equator with some variations. All kind of meteorological phenomena, e.g., thunderstorms and lightning, wind, and rainfall, occur in this spherical shell. 80 % of the total atmospheric mass 5.1480 x 10^{18} kg is present in this zone. Upper boundary of the troposphere, where an abrupt change in lapse rate usually decreases to 2 °C/km or less is called tropopause. Stratosphere starts from the top of the

troposphere, i.e., tropopause and extends up to 50 km altitude. The altitude span of the mesosphere 50–85 km is basically the *D*-region of ionosphere. Different transient luminous events (e.g., elves, red sprites etc.) predominantly occur in this altitude during severe thunderstorm. All meteors of mass <50 kg break apart and dissipate energy in this zone. The spherical shell of the atmosphere ionized by the solar X-ray and γ -ray radiation in the range of 50 – 1000 km altitude is called the ionosphere. Below this altitude medium is ionized only by highly energetic galactic cosmic rays. The ionosphere consists of different layers, viz., *D*-layer (60–90 km), *E*-layer (90–120 km), E_s -layer, *F* -layer (120– 500 km) and above this the topside ionosphere. The day side *F* -layer is sub-divided into F_1 and F_2 layers. The space above ionosphere around the planet, where magnetic field lines are dominant is called the magnetosphere which is controlled by the planet's magnetic field. The solar wind is primarily responsible for the teardrop shape of the Earth's magnetosphere which prevents most of the particles from the Sun from reaching the Earth. In the day side atmosphere the magnetosphere extends up to 10 R_E (Earth's radius) whereas for the night side it extends up to 100 R_E. Various literatures are available regarding the magnetosphere of the earth [155- 157]. The medium confined within the spherical shell between the conductors, i.e., Earth surface and lower boundary of the ionosphere (50– 60 km altitude) is dielectric in nature, and eventually becomes a spherical waveguide for the low frequency radio wave.

The thunderstorm is the main process through which charge separation occurs in the troposphere under all circumstances which produces stratified charge distribution in the different layers and creates different charge centers. Electrical discharges occur between these opposite polarity charge centers in the form of lightning. Numerous processes operate synergistically within the environment of a mature convective cloud, and different processes with varying effectiveness and time-dependencies affect cloud electrification [158 - 163].

The charging of thunderstorms takes place via inductive or non-inductive process. An

inductive charging process requires pre-existing electric fields to induce charges on a particle so that when it rebounds from another charge particle charge gets separated and the field is enhanced. The fair weather electric field resulting from positive charges in the atmosphere and negative charges on the ground could be considered as the pre-existing field which has been verified by laboratory experiments [164].

Non-inductive processes are independent of external electric field(s) and are based only on a collision mechanism between group with cloud-ice particles and the selective transfer of charge of a certain polarity to the larger particle. This mechanism is dominant in the charging of thunderstorms [165]. In an ordinary thundercloud, the smaller ice crystals are charged positively and move upward, whereas larger graupel particles charged negatively descend down relative to the smaller particles. Depending on the prevailing conditions of temperature, liquid water content and mixing in the thunderstorm is the normal situation. A variant of this situation may lead to the reverse condition. Charging of solid particles can engage trio electric charging by fractoemission and photoelectric charging, as discussed in detail in different articles [166,167] The presence of soluble ionic substances in the liquid and ice phases have a significant effect on the charging processes and may significantly alter the outcome of particle interaction and the charging processes. In the non-inductive mechanism Sunders [167] has discussed drop break up, ion charging (atmospheric ions produced by cosmic rays, or radioactivity) and convective mechanisms, etc. Some scientists [168 - 170] recommended in other cases that the small fraction of flashes striking ground was caused by a severe storm's very strong updraft. The strong updraft lifts the formation and growth of the frozen hydrometeor charge carriers to higher altitudes than usual height of storms, and causes the resulting charge to remain relatively high for substantial period. It has also been noted that cloud-to-ground lightning creation may be inverted in severe storms by the time required to form and bring downward the precipitation

carrying the low-level charge region that is needed to initiate lightning from the mid-level oppositely charged region [168 – 170].

The spherical cavity between the Earth's surface and lower ionosphere acts as a resonator in which the standing electromagnetic waves are generated due to excitation energy from lightning. The resonance occurs when the wavelength is of the order of the dimension of the resonator. The observed discrete peak frequencies are 8, 14, 20, 26 . . . Hz in the ELF range. Winfried Otto Schumann first theoretically predicted this electromagnetic resonance phenomenon in 1952 and calculated their eigen frequencies in the spherical Earth-ionosphere cavity as 10.6, 18.4, etc . . . Hz [1b]. The characteristic Schumann resonance spectra are shown in Fig. 1.3. This was recorded at Kolkata on April 2, 2000 [171].

The experimental evidences of this phenomenon came later, with subsequently developed more realistic analytical models taking into account the inhomogeneities due to asymmetry of the day and night-time ionospheres, variations of conductivity of the ionosphere, the distribution of sources etc. However, these factors in the lower ionosphere

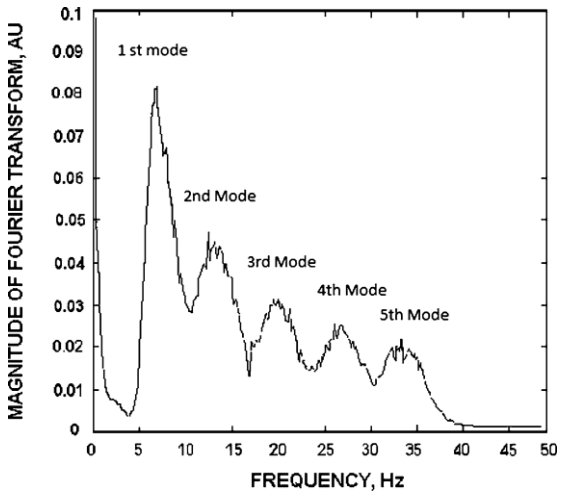

Fig. 1.3 Frequency response of Schumann resonance signal recorded at Kolkata on April 2, 2000 [171]

have relatively small influence over the resonance frequencies to decrease to the experimentally observed value. The fact that the observed frequencies are 8 Hz, 14 Hz etc. in- stead of 10.6 Hz, 18.4 Hz etc., is primarily due to the low propagation speed of radio waves in the Earth-ionosphere cavity compared to that of light in vacuum. Hence the observed peak frequencies are lower than the eigen frequencies for a perfect cavity. The ratio of velocity of propagation in vacuum and within the waveguide is *c/v* 1.36 at 10 Hz [172]. Considering this velocity ratio the calculated resonant frequency will be reduced to the observed SR peak frequency at the Earth surface. Different aspects of Schumann resonance phenomenon as well as their observation and measurement techniques are presented by different workers, e.g., SR signal as the global thermometer [16] for the detection of upper tropospheric water vapor content [64] detection of pre- seismic anomalies during large earthquake [173 - 176] etc. Some frequency changes about the peak values and some amplitude changes were found to be present in the observed spectra, which may be attributed to the uncertainties arising from spatial distribution of lightning sources exciting the SR modes [177].

The diurnal variation of peak frequencies and amplitudes of different modes were utilized to know (i) the characteristics of global thunderstorm activities, and (ii) the electron number density of the ionosphere. The seasonal and day-to-day variability of SR intensities, frequencies, line splitting and quality factors have been reported by many authors along with the possible explanations for such changes [3, 12, 29, 30, 118, 178, 180]. Schumann resonance frequency variations have been established as an indicator of the thunderstorm distribution over the globe [30]. Both linear and non-linear combinations of average power spectra of electric and magnetic fields are used successfully in the solution of the inverse problem [122, 181,182].

SR frequencies are modified by the interaction of energetic precipitating particles

within the lower ionosphere due to extra ionization. Solar proton precipitations cause the lower ionospheric boundary to move downward, e.g., lower ionospheric refection height decreases that manifests a change in the frequency of the first SR mode to lower values [32, 34]. A noticeable change, approximately 50 % of the mean on short time scale, in amplitude as well as in peak frequencies of the first two modes during the 30-min period γ -ray burst was observed. The normal variability of the peak frequency is about 0.5 Hz for the first mode and approximately 1 Hz for the second mode before, during and after the burst [183-185].

A change has been detected successfully in the Schumann resonance spectra during the intense γ ray flare SGR (Soft Gamma Repeater) 1806-20 (27 December 2004), recorded at the Moshiri observatory, Japan (44.365°N and 142.24°E) [186] It was compared with the experimental records at the same observatory with the model calculated approximately for the parametric ELF pulse produced by the γ ray flare [143, 187 - 189].

Inhomogeneity can arise due to unequal extra ionization in different layers during solar X-ray flares (SF) and solar proton events (SPE) [190]. The variation in the first and second mode Schumann resonance frequency occurred during the intense solar X-ray burst by 0.2 Hz and 0.3 Hz, respectively [191]. The observed maximum of first, second and third SR mode frequencies during sudden ionospheric disturbance were 8.51 Hz, 14.71 Hz and 21.22 Hz respectively [192].

During solar activity, there may be two kinds of changes to the lower boundary of the Earth-ionosphere waveguide:

(i) ionization enhancement at the normal *D*-region reflection heights, and (ii) the variation of *D*-region's lower edge [32] According to the simplest vacuum model [192] the variation of the first SR frequency can be written as [32].

$$\nabla f_1 / f_1 \approx 0.36(\nabla N / 2N + \nabla h / h) \ldots\ldots (1)$$

Where symbols have their usual meaning

It is established that solar X-ray radiation causes extra ionization mainly in the height range of 70–80 km, whereas SPE can cause extra ionization up to the depth of 40–50 km.

To explain the effect of this kind of inhomogeneity on SR, the two-layer waveguide model has been proposed by Greifinger et.al [145] for the lower layer $\sigma=\varepsilon_0\omega$, i.e., where displacement and conduction currents are equal to each other. The other, relatively upper layer is that at which $\mu_0\omega\sigma\zeta^2 > 1$ where ζ is the conductivity scale height at the altitude for reflection of ELF wave. The unequal ionization of these two layers by solar extra radiation, i.e., by both X-ray and γ-rays can give rise to vertical inhomogeneity which modifies the SR frequency. The SR frequencies can be expressed as [52, 192].

$$f_n = \frac{1}{\sqrt{2\pi}}\frac{c}{r_e}\sqrt{n\,(n+1)}\,\sqrt{\frac{h_1}{h_2}} \quad \ldots\ldots\ldots\ldots(2)$$

where n is the mode number (n = 1, the first harmonic is regarded here); c, the velocity of light; r_e, mean radius of the earth; h_1 and h_2 are the two characteristic heights in the D-region. For n = 1,

$$f_1 = \frac{1}{\sqrt{\pi}}\frac{c}{r_e}\sqrt{\frac{h_1}{h_2}} \quad \ldots\ldots\ldots\ldots(3)$$

During solar flare, the lower height h_1 is almost unaffected because it causes extra-ionization mainly around 70 km, i.e., the reduced upper reflection height δ_2 modified the first SR frequency and thus the first SR frequency increases. During solar proton events, energetic protons can penetrate deeply into the ionosphere upto 50 km and possibly even deeper and can ionize regions lower than the normal D-region [32]. Thus, the δ_1 decrement over h_1 lower

reflection height modifies the first mode SR frequency resulting in a diminishment of SR frequency.

$$(f_1)_{SR} = \sqrt{1/\pi}\,(c/r_e)\,\sqrt{h_1/(h_2 - \delta_2)}$$

……..(4)

Significant solar terminator effects are found in SR magnetic and electric field characteristics [118]. The larger the area coverage by the ionospheric disturbances, the greater is its influence on SR characteristics. Thus, from the nature of variation of SR characteristics, the vastness of the magnitude of disturbance of solar terminator time can be determined. Hence, lateral ionospheric gradients across the terminator region have sufficient influences on ELF wave propagation along with the diurnal-seasonal lightning sources [193]. Effects of the solar terminator time on the diurnal frequency variation of Schumann resonance frequency had been studied at Garhwal Himalayan region, India, during March 10–May 23 in 2006 [194].

A general approach suggested by Williams E.R. [16] based on the analogy between ELF propagation within a waveguide and wave propagation in a transmission line with two dimensional telegraph equation (TDTE) technique, has been developed later on [181, 195], where TDTE allows incorporation of any conductivity profile. Mushtak et.al [196] introduced the 'knee' approximation on the basis of the TDTE formalism to obtain both realistic resonance frequencies and quality factors which overcomes the shortcoming of the two-exponential approach.

Large amount of water vapor is transported into the upper troposphere due to continental deep convection. This water vapor is the key element of Earth's climate. It has direct impact as a greenhouse gas as well as indirect effect through interaction with cloud,

aerosols and tropospheric chemistry for the generation of the charge centers. The relatively small amount of water vapor in the upper troposphere has a large impact on climate variation [197]. The retrieval of upper tropospheric water vapor concentration can be achieved through the continuous magnetic intensity measurements of SR spectra. Due to the presence of water vapor with some Aitkin particles through the formation of group, there will be more charge separation at the expense of thermal energy and thereby producing stratified charge centers. Instantaneous discharge processes between opposite charge center will emit EM radiation during the process of recombination of charges. This excess EM energy from the tropospheric zone will influence the SR magnetic records in a varying manner depending upon the intensity of the charge separation process.

It is known that ELF data, NASA water vapor project and upper-tropospheric water-vapor (UTWV) data are in good agreement with each other (correlation co-efficient, $r=0.76$) [198]. The sensitivity of this relationship implies that for every 0.25 mm increase in UTWV (1% of total column), the ELF signal will increase by approximately 25%. A relatively simple and inexpensive method for continuous observation of global lightning variability is the use of the Schumann resonances. Thus monitoring of SR signal may provide a tool for time-tracking of the upper-tropospheric water-vapor changes which will be made useful to the processes involving climate change. That is, SR data → water vapor content → climate forecasting.

Disturbances of the daytime ionosphere are well seen in the records of the amplitude and phase of very low-frequency (VLF) radio signals (10–30 kHz) if their propagation path passes through the dayside hemisphere. Signals at the frequencies of the global electromagnetic resonance have a number of features. The first of them is connected with the fact that in this case the concept of a day or night time propagation path is inappropriate. Indeed, at the first resonance frequency of 8 Hz, the wavelength of

a radio wave is equal to the circumference of the Earth's equator 4 x 10^4 km; therefore, the entire surface of the Earth is inside the first Fresnel zone for an arbitrary location of the source and the observer. In other words, the propagation "path" certainly covers the entire planet, i. e., both its day and night-side hemispheres. At a typical distance of 5 x 10^3 km from the observer to the signal source, this occurs for the first (lower) resonance modes. Therefore, the day–night asymmetry and its variations have little effect on the signal parameters, and only variations in the cavity parameters can, on the average, affect the Schumann resonance.[183,199,200].

The second feature of the Schumann resonance is related to two characteristic altitudes in the vertical profile of the ionospheric conductivity [201]. The peak frequency f_n of the *n*th resonance can be determined from the equation 2 [202,203].

The attempts to detect the effect of solar flares on the parameters of the Schumann resonance have repeatedly been undertaken [204 - 208]. The difficulties in detecting the expected changes are due to the fact that are hidden by fluctuations of a natural extremely low-frequency (ELF, 3–3000 Hz) radio signal, which are due to the noise nature of its sources (global thunderstorms). Until now, it has not been possible to clearly demonstrate the connection between the solar flares and the parameters of ELF radio signals and then to evaluate the corresponding changes in the state of the ionosphere [209].

Los Alamos energetic proton instruments at geosynchronous orbit observed more major solar energetic particle events during 1989 than any other year since this series of detectors began observations in 1976. The temporal flux profiles of four intervals, which contain six distinct events, are compared illustrating the uniqueness of each event. Characteristic rise time and decay time are computed for each event. During two of these

events, brief order of magnitude increases of the proton flux are observed. They are associated with sudden commencement events and dramatic changes in the solar wind [210].

The 23–30 January and 7–11 March 2012 solar proton event (SPE) periods were substantial and caused significant impacts on the middle atmosphere. These were probably the two largest SPE periods of solar cycle 24 so far. The highly energetic solar protons produced considerable ionization of the neutral atmosphere as well as HO_x (H, OH, HO_2) and NO_x (N, NO, NO_2). We computed a NO_x production of 1.9 and 2.1 Gigamoles due to these SPE periods in January and March 2012, respectively, which places these SPE periods among the 12 largest in the past 50 years. Aura Microwave Limb Sounder (MLS) observations of the peroxy radical, HO_2, show significant enhancements of > 0.9 ppbv in the northern polar mesosphere as a result of these SPE period [211].

The impact of solar proton events (SPEs) on noctilucent clouds (NLCs) is studied using the 30-year NLC data set based on measurements with SBUV instruments on NIMBUS 7 and the NOAA 9-17 satellites. A cross-correlation analysis was performed between GOES proton flux time series and NLC occurrence rate (albedo) time series to investigate, whether a depletion of NLCs is frequently observed during SPEs. It was focused on the analysis of the years when SPEs occurred during the core NLC season (days 0-40 with respect to solstice). For energetic protons in the 5-10 MeV energy range of the majority of SPEs statistically significant anti-correlations between NLC occurrence rate (albedo) and proton flux time series with time lags of up to 8 days. For the two strong SPEs in July 2000 and January 2005 the sensitivity of the results to the proton energy range was investigated. The main results do not depend on proton energy. Together with a recently proposed physical mechanism leading to a SPE-induced warming of the polar summer menopause region, the results may indicate that NLCs are frequently depleted during SPE [212].

Nitrate ion spikes in polar ice cores are contentiously used to estimate the intensity, frequency, and probability of historical solar proton events, quantities that are needed to prepare for potentially society-crippling space weather events. The Whole Atmosphere Community Climate Model was used to calculate how large an event would have to be to produce enough odd nitrogen throughout the atmosphere to be discernible as nitrate peaks at the Earth's surface. These hypothetically large events are compared with probability of occurrence estimates derived from measured events, sunspot records, and Cosmogenic radionuclides archives. We conclude that the flounce and spectrum of solar proton events necessary to produce odd nitrogen enhancements equivalent to the spikes of nitrate ions in Greenland ice cores are unlikely to have occurred throughout the Holocene, confirming that nitrate ions in ice cores are not suitable proxies for historical individual solar proton events [213].

Solar energetic particles ionize the atmosphere, leading to production of nitrogen oxides. It has been suggested that such events are visible as layers of nitrate in ice cores, yielding archives of energetic, high-flounce solar proton events (SPEs). This has been controversial, due to slowness of transport for these species down from the upper stratosphere; past numerical simulations based on an analytic calculation have shown very little ionization below the midstratosphere. These simulations suffer from deficiencies: they consider only soft SPEs and narrow energy ranges; spectral fits are poorly chosen; and with few exceptions secondary particles in air showers are ignored [214].

Recent observations have shown that coronal shocks driven by coronal mass ejections can develop and accelerate particles within several solar radii in large solar energetic particle (SEP) events. The acceleration of protons is modeled by numerically solving the Parker transport equation with spatial diffusion both along and across the magnetic field. We show

that particles can be sufficiently accelerated to up to several hundred MeV within 2-3 solar radii. When the shock propagates through a streamer-like magnetic field, particles are more efficiently accelerated compared to the case with a simple radial magnetic field, mainly due to perpendicular shock geometry and the natural trapping effect of closed magnetic fields [215].

The procedure for compilation of a new proton catalog is presented here. The focus is on the SOHO/ERNE instrument for the period 1996 to 2016 (entire solar cycle 23 and the ongoing solar cycle 24). The main steps of the data analysis are outlined. Namely, as a first approach it is selected that 5-min averaged data will be used to identify the peak proton intensity. Contributions due to local shock acceleration close to Earth are not taken into account. In this report, the main properties of the proton sample in the energy channel 17-22 MeV are presented and discussed [216].

There is unique indicator that a specific solar flare will generate a significant solar proton event. At times solar emission expected to be associated with solar particle acceleration seem to be weak even for significant solar particle event [217]. Even the popular belief that energetic solar particle are always associated with large solar flares has some under serious attack with the measurement of E >50 Mev protons at the earth associated with a disappearing filament without and accompanying flare [218]. .

The solar proton event of July 1982 was the largest to date the current solar cycle proton fluxes observed by the NOAA_6 Satellite have been used to calculate ionization rates during the events which have been found to be almost as large as those of august 1972 near 70 km but much smaller at lower altitude [219].

Solar proton events have been routinely detected by satellites since the 20th solar cycle; however, before that time only very major proton events were detected at the earth. Even though the detection thresholds differed between the 19th and more recent cycles, more than 200 solar proton events with a flux of over 10 particles/(sq cms) above 10 MeV have been recorded at the earth in the last three solar cycles. At least 15 percent of these events had protons with energies greater than 450 MeV detected at the earth. Other than an increase in solar proton event occurrence with increasing solar cycle, no recognizable pattern could be identified between the occurrence of solar proton events and the solar cycle. The knowledge gained from the data acquired over the past 40 years illustrates the difficulty in extrapolating back in time to infer the number and intensity of major solar proton events at the earth [220].

Solar protons present a major problem to space systems because of the ionization and displacement effects which arise from their interaction with matter. This is likely to become a greater problem in the future due to the use of more sensitive electronic components and the proposed expansion of manned activities in space. An outline of the physical processes associated with individual solar events, the solar activity cycle and the transport of solar particles between the Sun and the Earth is provided. The problems of predicting solar event flounces, both over short- and long-term periods, are discussed. The currently available solar proton event models used for long-term forecasting are briefly reviewed, and the advantages and deficiencies of each model are investigated. Predictions using the models are compared to measurements made by the GOES-7 satellite during the rising phase of the current solar cycle. These measurements are also used to illustrate the sensitivity of the models to the choice of confidence level and to the spectral form used for extrapolation over the solar proton energy range [221].

It was found 20 SEP source regions in the northern hemisphere and 15 SEP source regions in the southern hemisphere confirm the North-South asymmetry in the SEP locations during our study period. We noticed that majority of source region are located in the northern hemisphere [222].

A new catalogue of 253 solar proton events (SPEs) with energy >10MeV and peak intensity >10 protons/cm^2.s.sr (pfu) at the Earth's orbit for three complete 11-year solar cycles (1970-2002) is given. A statistical analysis of this data set of SPEs and their associated flares that occurred during this time period is presented. It is outlined that 231 of these proton events are flare related and only 22 of them are not associated with Ha flares. It is also noteworthy that 42 of these events are registered as Ground Level Enhancements (GLEs) in neutron monitors. The longitudinal distribution of the associated flares shows that a great number of these events are connected with west flares. This analysis enables one to understand the long-term dependence of the SPEs and the related flare characteristics on the solar cycle which are useful for space weather prediction [223].

The finalized catalog of solar energetic proton events detected by Wind/EPACT instrument over the period 1996-2016. Onset times, peak times, peak proton intensity and onset-to-peak proton fluence are evaluated for the two available energy channels, at about 25 and 50 MeV. We describe the procedure utilized to identify the proton events and to relate them to their solar origin (in terms of flares and coronal mass ejections). The statistical relationships between the energetic protons and their origin (linear and partial correlation analysis) are reported and discussed in view of earlier findings. Finally, the different trends found in the first eight years of solar cycles 23 and 24 are discussed [224].

Majority of SEP events source regions are located in the western hemisphere. Some are in eastern part and their speed is high relative to western event. Majority of major SEP events are associated with halo and high speed CMEs. The minor and weak

SEPs are associated with relatively poor CMEs speeds. Most of the SEPs source regions are in northern hemisphere, which indicates north-south asymmetry in SEPs source locations. The correlation is slow between X-ray flux and SEP intensity. The correlation looks better between CME speed and SEP intensity,

The topical collection demonstrates the power of combination methodology at work and provides new results on i) type I solar radio bursts and thermal emission to study active regions; ii) type II and IV bursts to better understand the structure of coronal mass ejections; and iii) non-thermal gyro-synchrotron and/or type III bursts to improve the characterisation of particle acceleration in solar flares [225]. A principal component analysis (PCA) on a set of six solar variables (*i.e.*width/size (ss) and velocity (uu) of a coronal mass ejection, logarithm of the solar flare (SF), magnitude, SF longitude (lonlon), duration (DTDT), and rise time (RTRT)). The solar energetic particle (SEP) event radiation impact (in terms of the National Oceanic and Atmospheric Administration scales) with respect to the characteristics of their parent solar events. Further attempt to infer the possible prediction of SEP events 126 SEP were completely analysised from 1997 to 2013. Each SEP event is a vector in six dimensions (corresponding to the six solar variables used in this work). The PCA transforms the input vectors into a set of orthogonal components. By mapping the characteristics of the parent solar events, a new base defined by these components led to the classification of the SEP events [226].

A new catalogue of solar energetic particle events near the Earth, covering solar cycle 23 and the majority of solar cycle 24 (1996-2016), based on the 55-80 MeV proton intensity data gathered by the SOHO/ERNE experiment. In addition to ERNE proton and heavy ion observations, data from the ACE/EPAM (near-relativistic electrons), SOHO/EPHIN (relativistic electrons), SOHO/LASCO (coronal mass ejections, CMEs), and GOES soft X-ray experiments are also considered and the associations between the particle and CME/X-ray

events deduced to obtain a better understanding of each event. A total of 176 SEP events have been identified as having occurred during the time period of interest; their onset and solar release times have been estimated using both velocity dispersion analysis (VDA) and time-shifting analysis (TSA) for protons, as well as TSA for near-relativistic electrons [227].

Different aspect of SR phenomena as well as their observation and measurement technique have been presented by many workers during the last five decades. Towards the developmental stage of SR phenomena the diurnal variation of peak frequencies and amplitude of different modes were utilize to know the characteristic of global thunderstorm activity, The electron number density of the Ionosphere. These two application of SR continues for more than 3 decades from its year of prediction in 1952 without any additional finding. During 1990 and later the scenario of these sub ionospheric ELF waves changed an different new phenomena of SR emerged. Some of those are uncertentiy in frequency/amplitude of lightning which is due to its connectivity with the spectral distribution of lightning sources exciting the modes. The variation in Schumann resonance amplitude and variations in global tropical surface temperature suggest that such measurement can serve as diagnostic of temperature.

Due to deep convection in the topical atmosphere, intensity of SR signal is found to be linked through logical change to tropical surface temperature of the earth. Thus SR behaves as a sensitive global topical thermometer on diurnal, seasonal time scale.

Schumann resonance is generally detected by ball antenna for vertical electric field and two induction coil-type antennas (magnetometers) for two horizontal magnetic field components set at remote locations far from artificial electrical interaction and any other types of electro magnetic noises. The intensity of SR field produced by thunderstorm activity is strong enough to give rise to non-linear effects in the D-layer. As a result, there will be

heating of electrons by the ELF oscillations of SR fields. Fair-weather electric field gives a linear dependence of electron temperature fluctuations on the field strength of SR. These lead to non-linear effects comprising the variations of electron temperature, effective collision frequency and conductivity of the medium. The variation arises due to the variation in the value of fair-weather field and electron-neutral particle collision frequency at the upper D-region height range.

Earth is very sensitive to the water vapor content in the upper troposphere. Small changes in upper troposphere water vapor can have large implications for the earth climate. Continental deep convections pump water vapor into the upper troposphere that generate storms thereby producting the majority of Earth's lightning discharges and major source of ELF electromagnetic waves in the Earth-ionosphere cavity.

Global water vapor measurement reveal the apparent co relations in time and space between (a) Lightning activity, (b) SR measurements and (c) Atmospheric water vapor content. SR may thus be of use in monitoring changes in atmospheric water vapor content, an extremely important parameter related to global climate change. From statistical analysis of long time water vapor data, global climate change may be predicted.

Some SR transients (Q-bursts) are released as the transient luminous events; sprites, elves, blue jets etc. Sprites are produced by positive cloud-to-ground (CG) lightning occurring in the thunderstorm strati form region. It is accompanied by Q-burst in the SR band. SR data is useful for the estimation of global occurrence rate of sprites. Return stroke current in the lightning discharge from the ground, in some cases, does not end in the cloud, but continues to move upward and terminate in the lower ionosphere. This transient current/field is associated with optical emissions (sprites, elves, blue jets, blue starters), in the

space between the top of the cloud and the lower ionosphere, known as Transient Luminous Event (TLE).

Observed variations of both frequency and amplitude in Schumann resonance phenomena are related to changes in global thunderstorm activity as well as the consequence of complex effects in the Earth-ionosphere cavity. Inhomogeneities in the earth-Ionosphere cavity and the anisotropy due to geomagnetic field are supposed to introduce conductivity perturbation in the medium which modify the attenuation depending on the location of the source.

During high power transmitter operations, there will be interaction between electromagnetic wave and medium particles within the ionosphere. As a result, the average energy received by the electrons from the field will gradually heat up the medium. This in turn changes the equilibrium distribution of the temperature within the medium. The electrons receive a considerable amount of energy from the field because of its large free-path length. For this, dialectic constant becomes a function of electric field, and thus there will be modification in the electromagnetic processes within the atmosphere. The dynamical response of various phenomena to transient heating has been studied by different authors [228-234, 235-240] from which perturbation of density, composition and electron-ion-temperature with in the ionosphere during high power radio wave propagation are known. In these works, numerous efforts have been made to explore different properties and physical processes responsible for ionospheric modifications. Further investigations can be made to know the medium parameters and other aspects of the ionosphere during modification.

Perturbations within the upper atmosphere have been investigated by different workers for the determination of the physical processes involved in the mechanism [233, 240].

There exists a considerable amount of data from ground and rocket and satellite based measurements to interpret the physical processes within the medium. Among various formulations, the description of the medium characteristics may be made in terms of susceptibility. The theory of wave propagation in a homogeneous magneto-plasma in term of susceptibility dyadic and its extension to inhomogeneous magneto-plasma with static pressure gradient have been developed. An expression for the susceptibility dyadic appropriate for the D and lower E-region can be derived using the field equations and the equation for the conservation of momentum. The influence due to convection current density may be taken into account in the formulation whereas that due to the conduction current can be omitted for high frequency propagation. The various effects of the medium could be incorporated in the momentum transfer equation. Coupled wave equations can be obtained though the dyadic. The nature of dispersion of the wave may be studied.

In various field Schumann Resonance is used :

- SR for climate research
- SR for Earthquake research [241]
- SR for lightning research
- SR for solar flare research
- SR for solar eclipse research [102, 114]
- SR for solar weather prediction [68]
- SR in space [148]
- SR at planet Mars [66, 166, 178]
- SR for new remote sensing capabilities [242]
- SR for bio-physical mechanism [243 , 244]
- SR influence Brain wave research [245 , 246]
- SR as a global thermometer [16]

Schumann Resonance can perturbed with the different geo physical and extra-terrestrial events within the earth-ionosphere cavity. They are solar X-ray flare, Solar proton event lightning, earthquake, solar eclipse meteor shower effect, storm, global thunderstorm, tsunami etc.

Record of the peak frequencies of the first four modes of the Schumann Resonance in a solar flare at 16:19 UT of march 11, 2015 [209] have been discussed. Again variation of the frequency for the first mode SR during solar flare on July, 14 2000 was recorded over Kolkata have discussed in different articles [48,49]. Same experiment was conducted by Roldugin et.al [32]. Changes of the first mode Schumann resonance frequency during relativistic solar proton specification in the 6 th Nov, 1997 event [34], changes of Schumann resonance parameters during the solar proton event of 14 th July, 2000 [33], decrease of the first Schumann resonance frequency during solar proton event [179], Schumann resonance frequency increase during solar X-ray brust in reports presented in all the above papers. Schlegel et.al [247] also shows that Schumann resonance parameter changes during high energy particle specification.

The present thesis embodies the result of some investigation in the area indicated that is on the variation of the first mode Schumann resonance frequency during a solar proton event on 6 to 7 th March, 2012, studies on different geophysical and extraterrestrial events within the earth-ionosphere cavity in terms of ULF/ELF/VLF.

Many more theoretical and experimental aspect of the stated phenomena had yet to be investigated. With a view to fill up some of the case remain in the investigation reported on the different aspects of SR and atmospheric electricity. The author carried out researches on some of the stated areas at JU during the period 2013 to till date.

In all the above experimental results it is concluded that at the time of solar X-ray flare the first mode Schumann resonance frequency intensity will increase and after the preceding of solar flare solar proton event occur. As the result the SR first mode frequency decreases immediately, that is all the results on the above research work almost same and the reason is discussed in chapter III.

There are studies on the variation of VLF atmospheric over Kolkata, variation of atmospheric vertical electric potential gradient at Kolkata during solar eclipse. The effects of solar eclipse on long part VLF transmission, the effect of recent solar eclipse upon a sub ionospheric transmitted signal, the analysis of the effect of Leonid, Parsed and Geminid Meteor Showers through it is effect on transmitted VLF signal 2009. Studies on the precursors of an earthquake as the VLF electromagnetic sferics, studies on nonlinear travelling ionospheric disturbances and more coupling within the auroral reason, AILA 2009 and its effect on VLF sferics on some effects of perturbations in the ionosphere due to electromagnetic precursory signals from earthquake which are published in reputed international and national journals and seminar or conference.

Various investigations have contributed a lot to the understanding of the propagation of electromagnetic wavelength through different regions of the atmosphere. It is worth mentioning that the electromagnetic waves are due to the vibration of the electrons of the medium, in short due to elementary Hertzian oscillation. The direction of vibration of the electrons are solely determined by the direction of the forces experienced by them. Within the ionosphere plasma, in the presence of collision and geomagnetic field, the directions of the forces are the direction of the displacement vectors which are however not identical with the direction of the electric vector. So the polarization angle will depend on the orientation of the displacement vector instead of electric vector for which the form of the electric permittivity will be tonsorial in nature there by developing plasma anisotropy.

The exploration of different phenomena within such anisotropic plasma contributors a lot to due understanding of the physical states and properties of the medium and on the other hand, yielded results that found applications in various physical problems.

In the presence of geometric field irregularities, there are various types of interactions within the ionosphere. If an intense electromagnetic wave, modulated in amplitude be incident within the upper atmospheric plasma, the perturbation which are caused in the plasma are also modulated and thus, so for waves which pass through the perturbed region. Propagation of intense unperturbed waves perturbed the plasma medium and introduce certain changes in the electron temperature, electron number density and therefore also in the conductivity and permittivity of the medium.

Electric field at a point on the earth's surface depends on the major thunderstorm activities of the globe and on the local environmental factors. Various models for thundercloud electric field have been developed to investigate their characteristics and connectivity with different global electric parameters into the regions between the surface of the earth and the upper D-region of the ionosphere.

In vast electric field from solar X-ray flares, solar proton events, meteor showers, scismo-associated electromagnetic waves, global thunderstorms and lightning., while entering the Earth's atmosphere produce electromagnetic radiations in the ELF to LF ranges due to their interaction with the medium. Any of those sources introduces anomalous and significant perturbations in the amplitude of VLF sferic signals during their propagation through such disturbed regions. Any such source also produces changes in the amplitude of VLF sferic signals, and amplitude and phase of the transmitted sub-ionosphereic VLF signals. The investigations of solar flare and solar cycle induced lower ionospheric changes are well known.

1.2 REFERENCE:

[1a] Schumann, W. O. (1952), Uber die strahlungslosen Eigenschwingungen einer leitenden Kugel, die von einer Luftschicht und einer Ionospha¨renhu¨ lle umgeben ist, Z. Naturforsch. A, **7**, 149–154.

[1b] A. Tran, C. Polk (1976), The Earth-ionosphere Cavity, Radio Science, Vol -**11**, No. 10, Page – 803.

[2] Raemer, E. T. (1961), On the extra low frequency spectrum of the Earth-ionosphere cavity response to electrical storms, J. Geophys. Res., **66**, 1580–1583.

[3] Balser, M., and C. A. Wagner (1962), Diurnal power variations in the Earth-ionosphere cavity modes and their relationship to worldwide thunderstorm activity, J. Geophys. Res., **67**, 619–625.

[4] Pierce, E. T. (1963), Excitation of Earth-ionosphere resonances by lightning flashes, J. Geophys. Res., **68**, 4125– 4127.

[5] Galejs, J. (1972), Terrestrial Propagation of Long Electromagnetic Waves, Elsevier, New York.

[6] Ogawa, T., Y. Tanaka, and M. Yasuhara (1969), Schumann resonances and worldwide thunderstorm activity, in Planetary Electrodynamics, vol. **2**, edited by S. Coroniti and J. Hughes, pp. 85–91, Gordon and Breach, New York.

[7] Bliokh, P. V., A. P. Nickolaenko, and Y. F. Filippov (1980), Schumann Resonances in the Earth-Ionosphere Cavity, IEE Electromagn. Wave Ser., vol. **8**, Peter Peregrinus, London.

[8] Heckman, S. (1998), The day-night asymmetry, paper presented at Schumann Resonance Symposium and Workshop, U. S.-Hung. Sci. and Technol. Joint Fund, Sopron, Hungary, 7–10 Sept.

[9] Nickolaenko, A. P., G. Satori, B. Zieger, L. M. Rabinowicz, and I. G. Kudintseva (1998), Parameters of global thunderstorm activity deduced from the long-term Schumann resonance records, J. Atmos. Sol. Terr. Phys., **60**, 387–399.

[10] Wait, J. R. (1996), Electromagnetic Waves in Stratified Media, IEEE Press, Piscataway, N. J.

[11] Balser, M. and C. A. Wagner, 1960: Observations of earth-ionosphere cavity resonances. *Nature*, **188**, 638-641,

[12] Madden, T. and W. Thompson, 1965: Low-frequency electromagnetic oscillations of the Earth-ionosphere cavity. Rev. Geophys., **3**, 211-254,

[13] Sao, K., M. Yamashita, S. Tanahashi, H. Jindoh, and K. Ohta, 1973: Experimental investigations of Schumann resonance frequencies. J. Atmos. Terr. Phys., **35**, 2047-2053,

[14] Tanahashi, S., 1976: Detection of line splitting of Schumann resonances from ordinary data. J. Atmos. Terr. Phys., **38**, 135-142,

[15] Sentman, D. D., 1983: Schumann resonance effects of electrical conductivity perturbations in an exponential atmospheric/ionospheric profile. J. Atmos. Terr. Phys., **45**, 55-65,

[16] Williams, E. R., 1992: The Schumann resonance: A global tropical thermometer. Science, **256**, 1184-1187,

[17] Füllekrug, M., 1995: Schumann resonances in magnetic field components. J. Atmos. Terr. Phys., **57**, 479-484,

[18] Füllekrug, M. and A. C. Fraser-Smith, 1996: Further evidence for a global correlation of the earth-ionosphere cavity resonances. Geophys. Res. Lett., **23**, 2773-2776,

[19] Yampolski, Y. M., P. V. Bliokh, V. S. Beley, V. G. Galushko, and S. B. Kascheev, 1997: Non-linear interaction between Schumann resonances and HF signals. J. Atmos. Sol.-Terr. Phys., **59**, 335-342,

[20] Heckman, S. J., E. Williams, and B. Boldi, 1998: Total global lightning inferred from Schumann resonance measurements. J. Geophys. Res., **103**, 31775-31779,

[21] Balling, R. C. and M. Hildebrandt, 2000: Evaluation of the linkage between Schumann Resonance peak frequency values and global and regional temperatures. Clim. *Res.*, **16**, 31-36,

[22] Hobara, Y., N. Iwasaki, T. Hayashida, N. Tsuchiya, E. R. Williams, M. Sera, Y. Ikegami, and M. Hayakawa, 2000: New ELF observation site in Moshiri, Hokkaido Japan and the results of preliminary data analysis. J. Atmos. Electr., **20**, 99-109.

[23] Shvets, A. V., 2001: A technique for reconstruction of global lightning distance profile from background Schumann resonance signal. J. Atmos. Sol.-Terr. Phys., **63**, 1061-1074,

[24] Nickolaenko, A. P. and M. Hayakawa, 2002: Resonances in the Earth-Ionosphere Cavity, Modern Approaches in Geophysics, Vol. **19**, Springer Science & Business Media, New York, 380 pp

[25] Nickolaenko, A. P. and M. Hayakawa, 2007: Recent studies of Schumann resonance and ELF transients. J. Atmos. Electr., **27**, 19-39.

[26] Nickolaenko, A. P. and M. Hayakawa, 2014: Spectra and waveforms of ELF transients in the earth-ionosphere cavity with small losses. Radio Sci., **49**, 118-130,.

[27] Sekiguchi, M., M. Hayakawa, A. P. Nickolaenko, and Y. Hobara, 2006: Evidence on a link between the intensity of Schumann resonance and global surface temperature. Ann. Geophys., **24**, 1809-1817,

[28] Galejs, J., 1970: Frequency variations of Schumann resonances. J. Geophys. Res., **75**, 3237-3251,

[29] Cannon, P. S. and M. J. Rycroft, 1982: Schumann resonance frequency variations during sudden ionospheric disturbances. J. Atmos. Terr. Phys., **44**, 201-206,

[30] Nickolaenko, A. P. and L. M. Rabinowicz, 1995: Study of the annual changes of global lightning distribution and frequency variations of the first Schumann resonance mode. J. Atmos. Terr. Phys., **57**, 1345-1348,

[31] Sátori, G., 1996: Monitoring Schumann resonances--II. Daily and seasonal frequency variations. J. Atmos. Terr. Phys., **58**, 1483-1488,

[32] Roldugin, V. C., Y. P. Maltsev, A. N. Vasiljev, and E. V. Vashenyuk, 1999: Changes of the first Schumann resonance frequency during relativistic solar proton precipitation in the 6 November 1997 event. Ann. Geophys., **17**, 1293-1297,

[33] Roldugin, V. C., Y. P. Maltsev, G. A. Petrova, and A. N. Vasiljev, 2001: Decrease of the first Schumann resonance frequency during solar proton events. J. Geophys. Res., **106**, 18555-18562,

[34] Roldugin, V. C., Y. P. Maltsev, A. N. Vasiljev, A. V. Shvets, and A. P. Nikolaenko, 2003: Changes of Schumann resonance parameters during the solar proton event of 14 July 2000. J. Geophys. Res., **108**, 1103,

[35] Roldugin, V. C., Y. P. Maltsev, A. N. Vasiljev, A. Y. Schokotov, and G. G. Belyajev, 2004: Schumann resonance frequency increase during solar X-ray bursts. J. Geophys. Res., **109**, A01216,

[36] Price, C. and A. Melnikov, 2004: Diurnal, seasonal and inter-annual variations in the Schumann resonance parameters. J. Atmos. Sol.-Terr. Phys., **66**, 1179-1185,

[37] Melnikov, A., C. Price, G. Sátori, and M. Füllekrug, 2004: Influence of solar terminator passages on Schumann resonance parameters. J. Atmos. Sol.-Terr. Phys., **66**, 1187-1194,

[38] Sekiguchi, M., Y. Hobara, and M. Hayakawa, 2008: Diurnal and seasonal variations in the Schumann resonance parameters at Moshiri, Japan. J. Atmos. Electr., **28**, 1-10.

[39] Balling, R. C. and M. Hildebrandt, 2000: Evaluation of the linkage between Schumann Resonance peak frequency values and global and regional temperatures. Clim. Res., **16**, 31-36,

[40] Kułak, A., Młynarczyk, J.: ELF propagation parameters for the Ground-Ionosphere waveguide with finite ground conductivity. IEEE Trans. Antennas Propag. **61**(4), 2269 (2013)

[41] Rycroft, M.J., Israelsson, S., Price, C.: The global atmospheric electric circuit, solar activity and climate change. J. Atmos. Sol.-Terr. Phys. **62**, 1563 (2000)

[42] Nickolaenko, A. P., G. Sátori, B. Zieger, L. M. Rabinowicz, and I. G. Kudintseva, 1998: Parameters of global thunderstorm activity deduced from the long-term Schumann resonance records. J. Atmos. Sol.-Terr. Phys., **60**, 387-399,

[43] Cummer, S.A., Inan, U.S., Bell, T.F., Barrington-Leigh, C.P.: ELF radiation produced by electrical currents in sprites. Geophys. Res. Lett. **25**(8), 1281 (1998)

[44] Cummer, S.A., Li, J., Han, F., Lu, G., Jaugey, N., Lyons, W.A., Nel- son, T.E.: Quantification of the troposphere-to-ionosphere charge transfer in a gigantic jet. Nat. Geosci. **2**(9), 617 (2009)

[45] Schlegel, K., Füllekrug, M.: Schumann resonance parameter changes during high-energy particle precipitation. J. Geophys. Res. **104**(A5), 10111 (1999)

[46] Molchanov, O.A., Schekotov, A.Yu., Solovieva, M., et al.: Nearseismic effects in ULF fields and seismo-acoustic emission: statistics and explanation. Nat. Hazards Earth Syst. Sci. **5**, 1 (2005)

[47] Yuanqing, M., Xuemin, Z., Xuhui, S., Xinyan, O.: Pre-earthquake Schumann resonance anomaly in Yunnan. Earthq. Res. China **27**(1), 101 (2013)

[48] De, S.S., De, B.K., Bandyopadhyay, B., Paul, S., Haldar, D.K., Barui, S.: Studies on the shift in the frequency of the first Schumann resonance mode during a solar proton event. J. Atmos. Sol.-Terr. Phys. **72**, 829 (2010a)

[49] De, S.S., De, B.K., Bandyopadhyay, B., Paul, S., Haldar, D.K., Bhowmick, A., Barui, S., Ali, R.: Effects on atmospherics at 6 kHz and 9 kHz recorded at Tripura during the India-Pakistan Border earthquake. Nat. Hazards Earth Syst. Sci. **10**, 843 (2010b)

[50] De, S.S., De, B.K., Pal, P., Bandyopadhyay, B., Barui, S., Haldar, D.K., Paul, S., Sanfui, M., Chattopadhyay, G.: Detection of 2009 Leonid, Perseid and Geminid Meteor Showers through its effects on transmitted VLF signals. Astrophys. Space Sci. **332**(2), 353 (2011a)

[51] Bliokh, P.V., Nicholaenko, A.P., Filtippov, Yu.F., Llanwyn Jones, D.: Schumann Resonances in the Earth-Ionosphere Cavity. Stevenage [England], Peter Peregrinus, New York (1980)

[52] Sentman, D.D.: Approximate Schumann resonance parameters for a two-scale-height ionosphere. J. Atmos. Terr. Phys. **52**(1), 35 (1990)

[53] Labendz, D., 1998: Investigation of Schumann resonance polarization parameters. J. Atmos. Sol.-Terr. Phys., **60**, 1779-1789,

[54] Grimalsky, V., S. Koshevaya, A. Kotsarenko, and R. P. Enriquez, 2005: Penetration of the electric and magnetic field components of Schumann resonances into the ionosphere. Ann. Geophys., **23**, 2559-2564,

[55] Sátori, G., William, E.R., Boccippio, D.J.: On the dynamics of the north-south seasonal migration of global lightning, AE32A-0166, AGU Fall meeting, San Francisco, December, 8–12 (2003)

[56] Sentman, D. D., and B. J. Fraser, Simultaneous observations of Schumann resonances in California and Australia: evidence for intensity modulation by local height of the D-region, J. Geophys. Res., **96** (A9), 15 973±15 984, 1991.

[57] Fullekrug, M., and A. C. Fraser-Smith, Further evidence for a global correlation of the earth-ionosphere cavity resonances, Geophys. Res. Lett., **23** (20), 2773 -2776, 1996.

[58] Marsx, F., G. Satori, and B. Zieger, Variations in Schumann resonances and their relation to atmospheric electric parameters at Nagycenk station, Annalez Geophyzicae, **15** (12), 1604−1614, 1997.

[59] Garaj, S., Vinković, D., Zgrablić, G., Kovačić, D., Gradečak, S., Biliškov, N., Grbac, N., Andreić, Ž.: Observational detection of meteor-produced VLF electromagnetic radiation. Fizika A **8**(3), 91 (1999)

[60] Heckman, S. J., E. Williams, and B. Boldi, 1998: Total global lightning inferred from Schumann resonance measurements. J. Geophys. Res., **103**, 31775-31779,

[61] Hobara, Y., N. Iwasaki, T. Hayashida, N. Tsuchiya, E. R. Williams, M. Sera, Y. Ikegami, and M. Hayakawa, 2000: New ELF observation site in Moshiri, Hokkaido Japan and the results of preliminary data analysis. J. Atmos. Electr., **20**, 99-109

[62] M Sekiguchi, Y Hobara and M Hayakawa J. Atmos. Elec. **28** 1 (2008)

[63] Füllekrug, M. and A. C. Fraser-Smith, 1996: Further evidence for a global correlation of the Earth-ionosphere cavity resonances. Geophys. Res. Lett., **23**, 2773-2776,

[64] Price, C.: Evidence for a link between global lightning activity and upper tropospheric water vapour. Nature **406**, 290 (2000)

[65] Price, C., Mushtak, V.: The impact of the August 27, 1998, γ -ray burst on the Schumann resonances. J. Atmos. Sol.-Terr. Phys. **63**(10), 1043 (2001)

[66] On the Schumann resonances on Mars Author links open overlay panel A .I .Sukhorukov December 1991, Pages 1673-1676

[67] Nickolaenko, A. P., G. Sátori, B. Zieger, L. M. Rabinowicz, and I. G. Kudintseva, 1998: Parameters of global thunderstorm activity deduced from the long-term

Schumann resonance records. J. Atmos. Sol.-Terr. Phys., **60**, 387-399,

[68] Schumann resonance: A latest wonder for climate forecast! September 2011

[69] Sátori, G., 1996: Monitoring Schumann resonances--II. Daily and seasonal frequency variations. J. Atmos. Terr. Phys., **58**, 1483-1488,

[70] Gendrin, R., and R. Stefant (Sept. 1962a), Magnetic records between 0.2 and 30 cis, AGARD Conference on Propagation of Radio Frequencies Below 300 kc/s, Munich, Germany.

[71] Gendrin, R., and R. Stefant (1962b), Effects of the very high altitude nuclear explosion of the July 9, 1962 on the earth-ionosphere cavity resonances, experimental results and interpretation, C. R.Acad. Sci. **255**, 2273-2275 and 2493-2495.

[72] Tepley, L., R. C. Wentworth, K. G. Lambert, H. V. Prentiss, K. D. Amundsen and D. R. Hillendahl (26 Dec. 1963), Sub ELF geomagnetic fluctuations, III final report Contract AF **19**(628)-462, Lockheed Missile and Space Co., PaJo Alto, Calif.

[73] Chapman, F. W., and D. L. Jones (M,!y 16, 1964a), earth-ionosphere cavity resonances and the propagation of extremely low frequency radio waves. Nature **202**, 654-657.

[74] Wait, J. R. (1964b), earth-ionosphere cavity resonances and the propagation of ELF radio waves, ULF Symposium, Boulder, Colo., Aug. 17-20. Also Radio Sci. J. NBS 69D, No. **8**.

[75] Balser, M., and C. A. Wagner (July 1, 1963), Effect of a high-altitude nuclear detonation on the earth.ionosphere cavity, 1. Geophys. Res. 68, No. **13**, 4115-4118.

[76] Schumann, W. O. (1952a), Uber die strahlungslosen Eigenschwingun. geneiner leitenden Kugel, die voneiner Luftschicht und einer Ionospharenhiille umgeben .i.st, Z. Naturforsch, **72**, 149-154.

[77] Schumann, W. O. (l952b), Uber die Dampfung der elektromag· ne tischen Eigenschwingungen des Systems Erde·Luft·Ionosphare, Z. Naturforsch **72**. 250-252.

[78] Schumann, W. O. (Aug. 1957), Elektri sche Eigen schwingungen des Hohlraumes Erde.Luft-Ionosphare, Z. Angew. Phys. **9**, 373-378.

[79] Koenig,. H. (Dec. 1958), Atmospherics geringster frequenzen, DissertatIOn an der Technischen Hochschule Miinchen.

[80] Koenig, H. (July 1959), Atmospherics ger ingster frequenzen, Z.Angew. Phys. II, No.**7**, 264-274.

[81] Koenig, H., E. Haine, and C. H. Antoniadis (Aug. 1961), Messung von 'atmospherics' geringster frequenzen in Bonn, Z. Angew. Phys. 13, No. **8**, 364-367.

[82] Fournier, lI. (Aug. 17, 1960), Some aspects of the first high-frequency geomagnetic recordings obtained at Garchy, C. R. Acad. Sci. (France) 251, No. **7**, 962- 964.

[83] Benoit, R., and A. Houri (1961), Propagation of very-low-frequencies in the earth-ionosphere system, Ann. Geophys. (France) 17, No.**4**, 370-373.

[84] Benoit, R., and A. Houri (Nov. 5, 1962), Power spectrum measurements of geophysical noise. Application to earth-ionosphere cavity, C. R. Acad. Sci. (France) **255**, 2496-2498.

[85] Lokken, J. E., 1. A. Schand, and C. S. Wright (1962), A note on the classification of geomagnetic signals below 30 cis, Can. J. Phys. **40**, 1000-1009.

[86] Polk, c., and F. Fitchen '(May-June 1962), Schumann resonances of the ea;th-ionosphere cavity-extremely low frequency reception at Kingston, R.I., 1. Res. NBS 66D (Radio Prop.) No. **3,** 313-318.

[87] Gendrin, R., and R. Stefant (Sept. 1962a), Magnetic records between 0.2 and 30 cis, AGARD Conference on Propagation of Radio Frequencies Below 300 kc/s, Munich, Germany.

[88] Balser, M., and C. A. Wagner (Feb. 1962a), Diurnal power variations of the earth-ionosphere cavity modes and their relationship to worldwide thunderstorm activity, 1. Geophys. Res. 67, No.**2**, 619-625.

[89] Balser, M., and C. A. Wagner (July 1, 1963), Effect of a high-altitude nuclear detonation on the earth.ionosphere cavity, 1. Geophys. Res. 68, No. **13**, 4115-4118.

[90] Rycroft, M. J. (Dec. 1963), Low frequency disturbances of natural origin of the electric and magnetic fi elds of the earth, Ph.D. Thesis, University of Ca.IPbridge.

[91] Chapman, F. W. and D. L. Jones, Observations of earth-ionosphere cavity resonances and theIr interpretation in terms of a two-layer ionosphere model, Radio Sci., 1. Res. NBS **68D**, 1177-1185 (Nov. 1964b).

[92] Wait, 1. R. (1962), Electromagnetic waves in stratified media (Macmillan Co., New York, N.Y.).

[93] Raemer, H. R. (1961a), On the extremely-low-frequency spectrum of earth-ionosphere cavity response to electric storms, J. Geophys. Res 66, No.**5**, 1580-1583.

[94] Raemer, H. R. (Nov.-Dec. 1961b), On the spectrum of terrestrial radio noise at extremely low frequencies, 1. Res. NBS 65D (Radio Prop.), No. **6**, 581-594.

[95] Galejs, J. (1961a), Terrestrial extremely.low.frequency noise spectrum in the presence of exponential ionospheric conductivity profiles, J. Geophys. Res. 66, No.**9**, 2787-2792.

[96] Galejs, J. (Nov. 1961b), ELF waves in presence of exponential ionospheric conductivity profiles, IRE Trans. Ant. Prop. AP-**9**, 554-562.

[97] Chapman, F. W., and R. C. Macario (May 1956), Propagation of audio frequency radio waves to great distances, Nature **177**, 930-933.

[98] Jean, A. G., Jr., and A. C. Murphys, J. R. Wait, and D. F. Wasmundt (1961), Propagation attenuation rates at ELF, 1. Res NBS 65D (Radio Prop.), No.**5**, 475-479.

[99] Galejs, J., and R. V. Row (Jan. 1964), Propagation of ELF waves below an inhomogeneous anisotropic ionosphere, IEEE Trans. Ant. Prop. AP-12, No.**1**, 74-8:l.

[100] Galejs,1. (June 1964b), ELF and VLF waves below an inhomogeneous anisotropic ionosphere, Radio Sci. 1. Res. NBS 68D, No. **6**, 693-707.

[101] Madden, T: Rand, W. Thompson, Low-frequency electromagnetic oscillations of the earth-ionosphere cavity, Report on Project NRL 371-401, Geophysics Laboratory, MIT, Cambridge, Mass.(Sept. 22, 1964). Also Rev. Geophys. 3, No. **2** (May 1965)

[102] The impact of the July 22, 2009 solar eclipse on Schumann resonance observations in India July 2012

[103] Galejs, 1. (1964a), Terrestrial extremely-low frequency propagation, Proc. NATO Advanced Study Institute on Natural Electromagnetic Phenomena Below 30 kc/s, Bad Homburg, West Germany, July-Aug. 1963, pp. 205-258 (Plenum Press, New York, N.Y.).

[104] Wait, J. R. (April 1964a), On the theory of Schumann resonances in the earth-ionosphere cavity, Can. **1**. Phys. **42**, 575-582.

[105] Thompson, W. B. (Feb. 1963), A layered model approach to the earthionosphere cavity resonance problem, Ph.D. Thesis, Department of Geology and Geophys ics, MIT.

[106] Wait, J. R. (1964c), Cavity resonances for a spherical earth with a concentric anisotropic shell (private communication).

[107] Wait, J. R. (Feb. 1963a), The mode theory of VLF radio propagation for a spheric al earth and a concentric anisotropic. ionosphere, Can. J . Phys. **41**, 299-315.

[108] Wait, 1. R. (May- June 1963b), Concerning solutions of the VLF mode problem for an anisotropic curved ionosphere, J. Res. NBS 67D (Radio Prop.), No.**3**, 297-302.

[109] Hepburn; F., and E. T. Pierce (May 9, 1953), Atmospherics with very-low-frequency components, Nature (GB) **171**,837-838.

[110] Lieberma~n, L. (Dec. 1956a), Extremely-low-frequency electromagnetic waves: I. Reception from lightning, ./. App!. Phys. **27**, No. 12, 1473-1476.

[111] Liebermann, L. (Dec 1956b), Extremely-low-frequency electromagnetic waves: II. Propagation properties, 1. App!. Phys. **27**, No. 12, 1477-1483.

[112] Tepley, L. R. (Dec. 1959), A comparison of sferics as observed in the very-low·frequency and extremely-low-frequency bands, J. Geophys. Res. **64**, No. 12, 2315-2329.

[113] Pierce, E. T. (July-Aug. 1960), Some ELF phenomena, J. Res. NBS 64D (Radio Prop.), No. **4**, 383-386.

[114] Schumann resonance: a tool for investigating planetary atmospheric electricity and the origin and evolution of the solar system. F. Simoes1 , r. F. Pfaff1 , m. Hamelin2 , c. Béghin3 , j.j. Berthelier2 , p. Chamberlin4 , w. Farrell5 , h. Freudenreich

[115] Galejs, J. (July 1962a), A further note on terrestrial extremely-low frequency propagation in the presence of an isotropic ionosphere with an exponential conductivity-height profile, J Geophys. Res. **67**, No. **7**, 2715-2728.

[116] Balser, M., and C. A. Wagner on Frequency variations of the Earth-ionosphere cavity modes, J. Geophys. Res., **67** (10), 4081-4083, 1962.

[117] Bliokh, P.V., Nicholaenko, A.P., Filtippov, Yu.F., Llanwyn Jones, D.:Schumann Resonances in the Earth-Ionosphere Cavity. Stevenage [England], Peter Peregrinus, New York (1980)

[118] Melnikov, A., Price, C., Sátori, G., Füllekrug, M.: Influence of solar terminator passages on Schumann resonance parameters. J. At- mos. Sol.-Terr. Phys. **66**, 1187 (2004)

[119] Huang, E., Williams, E., Boldi, R., Heckman, S., Lyons, W., Taylor, M., Nelson, T., Wong, C.: Criteria for sprites and elves based on Schumann resonance observations. J. Geophys. Res. **104** (D14), 16943 (1999)

[120] Rycroft, M.J., Israelsson, S., Price, C.: The global atmospheric electric circuit, solar activity and climate change. J. Atmos. Sol.-Terr. Phys. **62**, 1563 (2000)

[121] Shvets, A.V., Hobara, Y., Hayakawa,M.: Variations of the global lightning distribution revealed from three-station Schumann resonance measurements. J. Geophys. Res. **115**(A12), A12316 (2010)

[122] Williams, E.R., Mareev, E.: Recent progress on the global electrical circuit. Atmos. Res. 135–136, **208** (2014)

[123] Dyrda, M., Kułak, A., Młynarczyk, J., Ostrowski, M., Kubisz, J., Michalec, A., Nieckarz, Z.: Application of the Schumann resonance spectral decomposition in characterizing the main African thunderstorm center. J. Geophys. Res. **119**(23), 13338 (2014)

[124] Nickolaenko, A.P., Sátori, G., Zieger, B., Rabinowicz, L.M., Kudintseva, I.G.: Parameters of global thunderstorm activity deduced from the long-term Schumann resonance records. J. Atmos. Sol.- Terr. Phys. **60**(3), 387 (1998)

[125] Cummer, S.A., Inan, U.S., Bell, T.F., Barrington-Leigh, C.P.: ELF radiation produced by electrical currents in sprites. Geophys. Res. Lett. **25**(8), 1281 (1998)

[126] Nickolaenko, A.P., Hayakawa,M.: Resonances in the Earth-Ionosphere Cavity. Kluwer Academic Publishers, Dordrecht (2002)

[127] Magunia, A.: The thunderstorm-driven diurnal variation of the ELF electromagnetic activity level. J. Atmos. Sol.-Terr. Phys. **58**(15), 1683 (1996)

[128] Cummer, S.A., Li, J., Han, F., Lu, G., Jaugey, N., Lyons, W.A., Nelson, T.E.: Quantification of the troposphere-to-ionosphere charge transfer in a gigantic jet. Nat. Geosci. **2**(9), 617 (2009)

[129] Pasko, V.P., Yair, Y., Kuo, C.-L.: Lightning related transient luminous events at high altitude in the Earth's atmosphere: henomenology, mechanisms and effects. Space Sci. Rev. **168**, 475 (2012)

[130] Młynarczyk, J., Bór, J., Kułak, A., Popek, M., Kubisz, J.: An unusual sequence of sprites followed by a secondary TLE: an analysis of ELF radio measurements and optical observations. J. Geophys. Res. **120**(3), 2241 (2015)

[131] Kułak, A., Młynarczyk, J., Zi˛eba, S., Micek, S., Nieckarz, Z.: Studies of ELF propagation in the spherical shell cavity using a field decomposition method based on asymmetry of Schumann resonance curves. J. Geophys. Res. **111**(A10), A10304 (2006)

[132] Schlegel, K., Füllekrug, M.: Schumann resonance parameter changes during high-energy particle precipitation. J. Geophys. Res. **104**(A5), 10111 (1999)

[133] Molchanov, O.A., Schekotov, A.Yu., Solovieva, M., et al.: Nearseismic effects in ULF fields and seismo-acoustic emission: statistics and explanation. Nat. Hazards Earth Syst. Sci. **5**, 1 (2005)

[134] Ohta, K., Izutsu, J., Furukawa, K., Hayakawa, M.: Anomalous excitation of Schumann resonances associated with huge earthquakes, ChiChi (China, 1999), Niigata-Chuetsu (Japan, 2004), NotoHantou (Japan, 2007) observed at Nakatsugawa in Japan. In: Proc. 7th International Conf. 'Problems of Geocosmos', p. 461 (2008)

[135] Yuanqing, M., Xuemin, Z., Xuhui, S., Xinyan, O.: Pre-earthquake Schumann resonance anomaly in Yunnan. Earthq. Res. China **27**(1), 101 (2013)

[136] Nickolaenko, A.P., Hayakawa, M.: Spectra and waveforms of ELF transients in the Earth-ionosphere cavity with small losses. Radio Sci. **49**, 118 (2014)

[137] Barr, R., Jones Llanwyn, D., Rodger, C.J.: ELF and VLF radio waves. J. Atmos. Sol.-Terr. Phys. **62**, 1689 (2000)

[138] Pulinets, S.A., Ouzounov, D.: Lithosphere-atmosphere-ionosphere coupling (LAIC) model an unified concept for earthquake recursors validation. J. Asian Earth Sci. **41**, 371 (2011)

[139] Molchanov, O.A., Fedorov, E., Schekotov, A., et al.: Lithosphereatmosphere-ionosphere coupling as governing mechanism for preseismic short-term events in atmosphere and ionosphere. Nat. Hazards Earth Syst. Sci. **4**, 757 (2004a)

[140] Molchanov, O.A., Schekotov, A.Yu., Fedorov, E.N., Hayakawa, M.: Ionospheric Alfvén resonance at middle latitudes: results of bservations at Kamchatka. Phys. Chem. Earth Parts A/B/C **29**, 649 (2004b)

[141] Abhijit Ghosh, Debasish Biswas, Pranab Hazra, Gautam Guha, S. S. De Studies on Schumann Resonance Phenomena and Some Recent Advancements Geomagnetism and Aeronomy (IF0.701), Pub Date : 2020-03-17,

[142] Meister, C.-V., Mayer, B., Dziendziel, P., Fülbert, F., Hoffmann, D.H.H., Liperovsky, V.A.: On the acoustic model of lithosphereatmosphere- ionosphere coupling before earthquakes. Nat. Hazards Earth Syst. Sci. **11**, 1011 (2011)

[143] Tanaka, Y.T., Hayakawa, M., Hobara, Y., Nickolaenko, A.P., Yamashita, K., Sato, M., Takahashi, Y., Terasawa, T., Takahashi, T.: Detection of transient ELF emission caused by the extremely intense cosmic gamma-ray flare of 27 December 2004. Geophys. Res. Lett. **38**(8), L08805 (2011)

[144] Pal, S., Maji, S.K., Chakrabarti, S.K.: First ever VLF monitoring of the lunar occultation of a solar flare during the 2010 annular solar eclipse and its effects on the D-region electron density profile. Planet. Space Sci. **73**(1), 310 (2012)

[145] Greifinger, C., Greifinger, P.: Approximate method for determining ELF eigenvalues in the Earth-ionosphere waveguide. Radio Sci. **13**(5), 831 (1978)

[146] Earth-ionosphere Wave guide dispersion Parameter Optical Fiber Communication, Page 125, John. M. Senior

[147] Sátori, G., Williams, E., Mushtak, V.: Response of the Earthionosphere cavity resonator to the 11-year solar cycle in Xradiation. J. Atmos. Sol.-Terr. Phys. **67**, 553 (2005)

[148] Satellite observations of Schumann resonances in the Earth's Ionosphere_F Simões, R Pfaff… - Geophysical Research, 2011

[149] DE, S. S., B. K. DE, B. K. SARKAR, B. BANDYOPADHYAY, D. K. HALDAR, SUMAN PAUL and S. BARUI (2009): Analyses of Schumann resonance spectra from Kolkata and their possible interpretations, *Indian J. Radio Space Phys.*, **38**, 208-214.

[150] Dyrda, M., Kułak, A., Młynarczyk, J., Ostrowski, M.: Novel analysis of a sudden ionospheric disturbance using Schumann resonance measurements. J. Geophys. Res. **120**(3), 2255 (2015)

[151] Garaj, S., Vinkovi´c, D., Zgrabli´c, G., Kovaˇci´c, D., Gradeˇcak, S., Biliškov, N., Grbac, N., Andrei´c, Ž.: Observational detection of meteor-produced VLF electromagnetic radiation. Fizika A **8**(3), 91 (1999)

[152] Rodger, C.J.: Subionospheric VLF perturbations associated with lightning discharges. J. Atmos. Sol.-Terr. Phys. **65**(5), 591 (2003)

[153] DE, S. S., B. K. DE, A. GUHA and P. K. MANDAL (2006): Detection of 2004 Leonid meteor shower by observing its effects on VLF transmission., Indian J. Radio Space Phys, 35, 396-400.

[154] De, S.S., Bandyopadhyay, B., Das, T.K., Paul, S., Haldar, D.K., De, B.K., Barui, S., Sanfui, M., Pal, P., Chattopadhyay, G.: Studies on the anomalies in the behaviour of transmitted subionospheric VLF electromagnetic signals and the changes in the fourth Schumann resonance mode as signatures of two pending earthquakes. Indian J. Phys. **85**(3), 447 (2011b)

[155] Merrill, R.T.: Our Magnetic Earth: The Science of Geomagnetism, p. 126. The University of Chicago Press, Chicago (2010)

[156] Parks, G.K.: Physics of Space Plasmas: An Introduction. Addison- Wesley, Reading (1991). ISBN 0201508214, Chap. 1

[157] Fabien, D., Johan, D.K., Philippe, E.C.: Cluster shows plasmasphere interacting with Van Allen belts. European Space Agency. http:// sci.esa.int/cluster/52802-cluster (2013)

[158] Takahashi, T.: Riming electrification as a charge generation mechanism in thunderstorms. J. Atmos. Sci. **35**, 1536 (1978)

[159] Uman, M.A.: The Lightning Discharge. Academic Press, Oxford (1987)

[160] MacGorman, D.R., Rust, W.D.: The Electrical Nature of Storms. Oxford University Press, London (1998)

[161] Rakov, V.A., Uman, M.A.: Lightning: Physics and Effects. Cambridge Univ. Press, Cambridge (2003)

[162] Stolzenburg, M., Marshall, T.C.: Charge structure and dynamics in 0thunderstorms. Space Sci. Rev. **137**, 355 (2008)

[163] Yair, Y.: Charge generation and separation processes. Space Sci. Rev.**137**(1), 119 (2008)

[164] Brooks, I.M., Saunders, C.P.R.: An experimental investigation of the inductive mechanism of thunderstorm electrification. J. Geophys. Res. **99**(D5), 10627 (1994)

[165] Harrison, R.G., Nicoll, K.A., Ambaum, M.H.P.: On the microphysical effects of observed cloud edge charging. Q. J. R. Meteorol. Soc. **141**(692), 2690 (2015)

[166] Constraints on the U-Pb isotopic systematics of Mars inferred from a combined U-Pb, Rb-Sr, and Sm-Nd isotopic study of the Martian meteorite Zagami LE Borg, JE Edmunson, Y Asmerom - Geochimica et Cosmochimica Acta, 2005

[167] Saunders, C.: Charge separation mechanisms in clouds. Space Sci. Rev. **137**, 335 (2008)

[168] MacGorman, D.R., Burgess, D.W., Mazur, V., Rust, W.D., Taylor, W.L., Johnson, B.C.: Lightning rates relative to tornadic stormevolution on 22 May 1981. J. Atmos. Sci. **46**, 221 (1989)

[169] MacGorman, D.R., Rust, W.D., Krehbiel, P., Rison, W., Bruning, E., Wiens, K.: The electrical structure of two supercell storms during STEPS. Mon. Weather Rev. **133**, 2583 (2005)

[170] MacGorman, D.R., Filiaggi, T., Holle, R.L., Brown, R.A.: Negative cloud-to-ground lightning flash rates relative to VIL, maximum reflectivity, cell height, and cell isolation. J. Lightning Res. **1**, 132 (2007)

[171] De, S.S., De, B.K., Sarkar, B.K., Bandyopadhyay, B., Haldar, D.K., Paul, S., Barui, S.: Analyses of Schumann resonance spectra from Kolkata and their possible interpretations. Indian J. Radio Space Phys. **38**(4), 208 (2009)

[172] Kułak, A., Młynarczyk, J.: ELF propagation parameters for the Ground-Ionosphere waveguide with finite ground conductivity. IEEE Trans. Antennas Propag. **61**(4), 2269 (2013)

[173] MacGorman, D.R., Emersic, C., Heinselman, P.L.: In: 22nd International Lightning Conference. Bromfield, Colorado (2012)

[174] Nickolaenko, A.P., Rabinowicz, L.M.: Possible Global Electromagnetic Resonances on the Planets of the Solar System. Plenum, New York (1982). Translated from Kosmicheskie Issledovaniya **20**(1), 82–88

[175] Nickolaenko, A.P., Hayakawa, M., Kudintseva, I.G., Myand, S.V., Rabinowicz, L.M.: ELF sub-ionospheric pulse in time domain. Geophys. Res. Lett. **26**, 999 (1999a)

[176] Nickolaenko, A.P., Hayakawa, M., Hobara, Y.: Long-term periodical variations in global lightning activity deduced from the Schumann resonance monitoring. J. Geophys. Res. **104**(D22), 27585 (1999b)

[177] Price, C., Pechony, O., Greenberg, E.: Schumann resonances in lightning research. J. Lightning Res. **1**, 1 (2007)

[178] Sr stable isotope composition of Earth, the Moon, Mars, Vesta and meteorites F Moynier, A Agranier, DC Hezel, A Bouvier - Earth and Planetary Science …, 2010

[179] Roldugin, V.C., Maltsev, Y.P., Vasiljev, A.N., Schokotov, A.Y., Belyajev, G.G.: Diurnal variations of Schumann resonance frequency in NS and EW magnetic components. J. Geophys. Res. **109**, A08304 (2004a)

[180] Sekiguchi, M., Hayakawa, M., Nickolaenko, A.P., Hobara, Y.: Evidence on a link between the intensity of Schumann resonance and global surface temperature. Ann. Geophys. **24**, 1809 (2006)

[181] Kirillov, V.V., Kopeykin, V.N., Mushtak, V.K.: Electromagnetic waves in ELF range in the Earth-ionosphere waveguide. Geomagn. Aeron. **37**(3), 114 (1997) (in Russian)

[182] Shvets, A.V.: A technique for reconstruction of global lightning distance profile from background Schumann resonance signal. J. Atmos. Sol.-Terr. Phys. **63**(10), 1061 (2001)

[183] Motz, H., Radio Sci., **69**D, 671, (1965)

[184] Roldugin, V.C., Maltsev, Ye.P., Vasiljev, A.N., Shvets, A.V., Nickolaenko, A.P.: Changes of Schumann resonance parameters during the solar proton event of 14 July 2000. J. Geophys. Res. **108** (A3), 1103 (2003)

[185] Price, C., Mushtak, V.: The impact of the August 27, 1998, γ -ray burst on the Schumann resonances. J. Atmos. Sol.-Terr. Phys. **63**(10), 1043 (2001)

[186] Nickolaenko, A.P., Kudintseva, I.G., Pechony, O., Hayakawa, M., Hobara, Y., Tanaka, Y.T.: The effect of a gamma ray flare on Schumann resonances. Ann. Geophys. **30**, 1321 (2012)

[187] Nickolaenko, A.P., Hayakawa, M.: Model disturbance of Schumann resonance by the SGR l806-20 γ -ray flare on December 27, 2004. J. Atmos. Electr. **30**(1), 1 (2010)

[188] Nickolaenko, A.P., Schekotov, A.Yu.: Experimental detection of an ELF radio pulse associated with the gamma-ray burst of December 27, 2004. Radiophys. Quantum Electron. **54**(1), 15 (2011a)

[189] Nickolaenko, A.P., Schekotov, A.Yu.: ELF Q-burst caused by galactic gamma ray burst, XXX URSI General Assembly, Istanbul Turkey, 13–20 August 2011, Abstract EGH-3 (2011b)

[190] Sátori, G., Williams, E., Mushtak, V.: Response of the Earth- ionosphere cavity resonator to the 11-year solar cycle in X- radiation. J. Atmos. Sol.-Terr. Phys. **67**, 553 (2005)

[191] Roldugin, V.C., Maltsev, Y.P., Vasiljev, A.N., Schokotov, A.Y., Belya- jev, G.G.: Schumann resonance frequency increase during solar X-ray bursts. J. Geophys. Res. **109**, A01216 (2004b)

[192] Dyrda, M., Kułak, A., Młynarczyk, J., Ostrowski, M.: Novel analysis of a sudden ionospheric disturbance using Schumann resonance measurements. J. Geophys. Res. **120**(3), 2255 (2015)

[193] Sátori, G., Mushtak, V., Williams, E.: Schumann resonance signatures of global lightning activity. In: Bets, H.D., et al. (eds.) Lightning: Principles, Instruments and Applications, pp. 347–386. Springer, New York (2009)

[194] Chand, R., Israil, M., Rai, J.: Schumann resonance frequency variations observed in magnetotelluric data recorded from Garhwal Himalayan region India. Ann. Geophys. **27**, 3497 (2009)

[195] Kirillov, V.V.: Parameters of the Earth-ionosphere waveguide at ELF. Prob. Diffr. Wave Propag. **25**, 35 (1993) (in Russian)

[196] Mushtak, V.C., Williams, E.R.: ELF propagation parameters for uniform models of the Earth-ionosphere waveguide. J. Atmos. Sol.- Terr. Phys. **64**(18), 1989 (2002)

[197] Held, I.M., Soden, B.J.: Water vapor feedback and global warming. Annu. Rev. Energy Environ. **25**, 441 (2000)

[198] Price, C.: Evidence for a link between global lightning activity and upper tropospheric water vapour. Nature **406**, 290 (2000)

[199] Chen, H. H. C. & Cheng. D. A: Solution of Electromagnetic Problems in anisotropic and Compressible Media, J. Appl. Phys., **36**, 3320, (1965)

[200] Tai, C. T: Ionospheric radio wave propagation. Radio Sci., 69D, 401, (1965)

[201] Liu, C. H: Effective dielectric tensor and propagation constant of plane waves in a Radio Anisotropic medium. Journal Mathematical Phys., **8** (1967), 2236

[202] Chen, H. H. C & Cheng, D.K: Concerning lossy, compressible, magnetic-ionic media- General formulatic and equation decoupling IEEE. Trans. Antennas Propagate, **14**, 497, (1966)

[203] De, S. S, Proc. Inst. Elect. Electronics Engrs, **38**, 765, (1969)

[204] De, S. S: Scattering of radio waves from the ionosphere in presence of time varying random irregularities, Pure & Appl. Geo Phys., **83**, 38, (1970)

[205] Dison, P. L & Newbery, S. N, J. Atmos., Terr. Phys., **44**, 363, (1982)

[206] Schumann, W. O, J. Naturforsch, **7**A, 149 (1952)

[207] E.A. Bering, III, A. A. Few and J. R. Benbrook: The global circuit, Physics Today, **51(10)**, 24-30, 1998.

[208] Nickolaenko, A. P, Journal of Atmospheric & Solar Terrestrial Physics, **59**, 805, (1997)

[209] A.V. Shvets, A. P. Nickolaenko,1 and V. N. Chebrov 2, Effect of solar flares on the Schumann-resonance frequencies, Radiophysics and Quantum Electronics, August 2017, Volume **60,** Issue 3, pp 186–199

[210] High-*Z* energetic particles at geosynchronous orbit during the Great Solar Proton Event Series of October 1989 R. D. Belian**,** G. R. Gisler**,** T. Cayton**,** R. Christensen**,** Volume **97**, Issue **A11,** 1 November 1992, Pages 16897-1690

[211] Middle atmospheric changes caused by the January and March 2012 solar proton events, C. H. Jackman[1], C. E. Randall, Volume **14**, issue 2, Page 1025-1038,

[212]. Impact of solar proton events on noctilucent clouds, by N Rahpoe - 2011 Impact of solar proton events on noctilucent clouds ... *Journal of Atmospheric and S*olar-Terrestrial Physics, Volume **73**, Issue 14-15, p. ... (c) *2011* Elsevier Ltd.

[213] Nitrate ions spikes in ice cores are not suitable proxies for solar proton events, The Astrophysical Journal, Volume 851, Number 1

[214] Atmospheric ionization by high-fluence, hard spectrum solar proton events and their probable appearance in the ice core archive, Adrian L. Melott, Brian C. Thomas, Claude M. Laird, Ben Neuenswander, Dimitra Atri, *(Submitted on 26 Feb 2016)*

[215] The Acceleration of High-energy Protons at Coronal Shocks: The Effect of Large-scale Streamer-like Magnetic Field Structures, Xiangliang Kong[1,2], Fan Guo[2,3], Joe Giacalone[4], Hui Li[2], and Yao Chen[1] , Published 2017 December 8 • © 2017. The American.

[216] SOHO/ERNE proton event catalog: Progress results under the SEP origin project R. Miteva and D. Danov Space Research and Technology Institute, Bulgarian Academy of Sciences, Sofia, Bulgaria.

[217] A summary of major solar proton events M. A. Shea, D. F. Smart, Solar Physics, June 1990, Volume 127, Issue 2, pp 297–320.

[218] Dependence of solar proton events on their associated activities: Coronal mass ejection parameters J. Park,1 Y.-J. Moon,1 and N. Gopalswamy2 Received 21 December 2011; revised 25 June 2012; accepted 30 June 2012; published 16 August 2012.

[219] Mesospheric ozone depletion during the Solar Proton Event of July 13, 1982 Part II. Comparison between theory and measurements, S. Solomon , G. C. Reid , D. W. Rusch , R. J. Thomas, Volume 10, Issue 4, April 1983, Pages 257-260

[220] A summary of major solar proton events M. A. Shea, D. F. Smart, Solar Physics, June 1990, Volume 127, Issue 2, pp 297–320.

[221] Solar proton events and their effect on space systems, C.Tranquille, Radiation Physics and Chemistry, Volume 43, Issues 1–2, January–February 1994, Pages 35-45.

[222] Bimal Pande, Seema Pande, Ramesh Chandra, Mahesh Chandra Mathpal, Solar flares, CMEs and solar energetic particle events during solar cycle 24, Advances in Space Research Volume 61, Issue 2, 15 January 2018, Pages 777-785.

[223] Statistical analysis of solar proton events, V. Kurt[1], A. Belov[2], H. Mavromichalaki[3], and M. Gerontidou[3], Volume 22, issue 6, 14 Jun 2004

[224] The Wind/EPACT proton event catalog (1996-2016), Rositsa Miteva etal, Solar Physics 293(2) · February 2018

[225] Combined Radio and Space-Based Solar Observations: From Techniques to New Results, Solar Physics 293(6) · June 2018

[226] Nowcasting Solar Energetic Particle (SEP) Events using Principal Components Analysis (PCA), June 2018, A Papaioannou etal

[227] Catalogue of 55-80 MeV solar proton events extending through solar cycles 23 and 24, Miikka Paassilta, Osku Raukunen,

[228] Middle atmospheric changes caused by the January and March 2012 solar proton events, C. H. Jackman[1], C. E. Randall**,** Volume **14**, issue 2, Page 1025-1038,

[229] Bernhardt, P. A. and Duncan, L. M., J. Atmos. Terr. Phys. **44**, 1061, (1982)

[230] Holt, O., Brekke, A, Hansen . T, Kopka. H. and Stubbe, P., J. Atmos. Terr. Phys. **47**, 537, (1982)

[231] Fejer, J. A., Gozales, C. A., Ieric, H. M., Sulzer, M. P., Templey, C.A., Duncan, L. M., Djuith, F. T., Ganguly, S. and Gordon, W.E., J. Atmos. Terr. Phys. **47**, 1165, (1985)

[232] Migulin, V. V. and Gurevich, A. V., J. Atmos. Terr. Phys. **47**, 1181, (1985)

[233] De, S. S., Bondyopadhyay, J., Adhikari, S. K. and Paul, S. N., Indian J. Radio and Space Phys., **16**, 286, (1987)

[234] Chen, H. H. C. and Cheng, D. K., Proc. IEEE., **55**, 705, (1967)

[235] Gray, K. G. and Bowhill, S. A., Radio Sci., 9, 63, (1974)

[236] Fejer, J. A.: Ionospheric modification and parametric instabilities Geophys. Space Phys., 17, 135, (1979)

[237] Mantas, G. P., Carlos, H.C. and Latloz, C. A., J. Geophys. Res., **86**, 561, (1981)

[238] Duncan, L. M. and Gorgon, W. E., J. Atmos. Terr. Phys. **44,** 1009, (1982)

[239] Bernhardt, P. A. and Duncan, L. M., J. Atmos. Terr. Phys**. 44,** 1061, (1982)

[240] Holt, O., Brekke, A, Hansen . T, Kopka. H. and Stubbe, P: Ionospheric modification experiments in northern Scandinavia, J. Atmos. Terr. Phys. **47**, 537, (1982)

[241] Schumann Resonance Mode Variation during Seismic Activity: A Review Pranab Hazra1, Shreya Chatterjee2 , Moumita Banerjee. 2017

[242] A new deep generative network for unsupervised remote sensing single-image super-resolution JM Haut, R Fernandez- Beltran… - … and Remote sensing, 2018

[243] Innovative technical implementation of the Schumann resonances and its influence on organisms and biological cells To cite this article: S Danho et al 2019 IOP Conf. Ser.: Mater. Sci. Eng. 564 012081

[244] Schumann Resonances, a plausible biophysical mechanism for the human health effects of Solar N Cherry - Natural hazards, 2002

[245] Schumann Resonance and Brain Waves: A Quantum Description May 2015 Neuro Quantology 13(2)

[246] Disrupting the blood–brain barrier by focused ultrasound induces sterile inflammation BK Lewis, M Bresler, SR Burks - Proceedings of the …, 2017

[247] Schlegel, K. and M. Füllekrug, 1999: Schumann resonance parameter changes during high-energy particle pre- cipitation. J. Geophys. Res., **104**, 10111-10118,

CHAPTER - II

Theoritical Background and Experimental

2.1 Introduction:

The space between the two spherical conducting shells, Earth surface and the lower boundary of the ionosphere, behaves as a spherical cavity in which some electromagnetic signals can propagate a long distance and is called Earth-ionosphere waveguide. Through this waveguide ultra low frequency (ULF), extremely low frequency (ELF) and very low frequency (VLF) signals can propagate efficiently with low attenuation. Resonances which occur for ELF waves due to round-the-world propagation interfering with $2n\pi$ phase difference are called Schumann resonances.

The resonance occurs when the wavelength is of the order of dimension of the resonator. The observed discrete peak frequencies are 8, 14, 20, 26 . . . Hz in the ELF range. Winfried Otto Schumann first theoretically predicted this electromagnetic resonance phenomenon in 1952 and calculated their eigen frequencies in the spherical earth-ionosphere cavity as 10.6, 18.4, etc . . . Hz [1,2].

The experimental evidences of this phenomenon came later, with subsequently developed more realistic analytical models taking into account the inhomogeneities due to asymmetry of the day- and night-time ionospheres, variations of conductivity of the ionosphere, the distribution of sources etc.

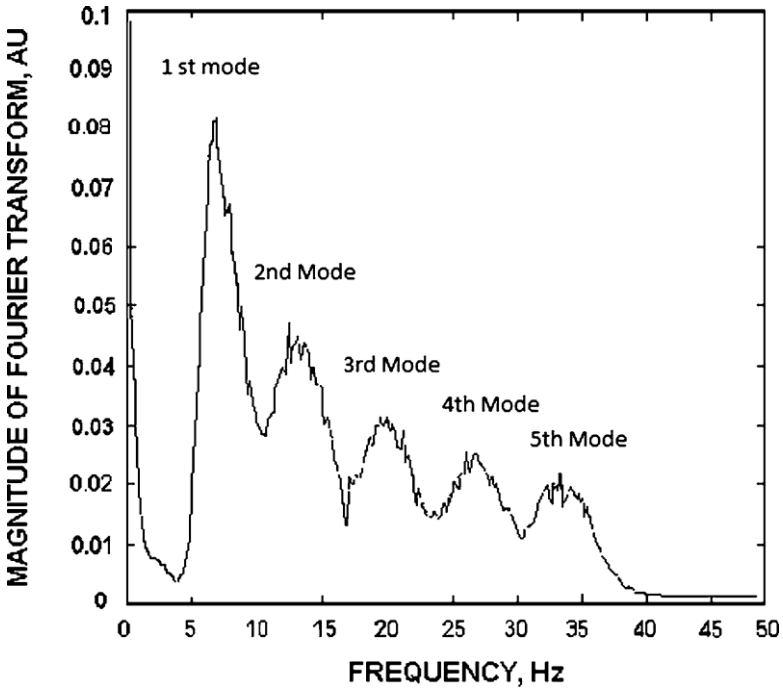

Fig. 2.1 : Frequency response of Schumann resonance signal

recorded at Kolkata on April 2, 2000 [3]

The first mode Schumann Resonance frequencies are influenced by different geophysical and extra-terrestrial events like lightning, earthquakes, Leonid meteor shower, solar flares, solar eclipse, geomagnetic storms, Solar Proton Event etc. [4 - 8]. Also Schumann Resonance frequencies are influenced by γ - ray flares [9, 10].

Due to Solar Proton Event the variation of frequency of first mode Schumann Resonance spectra was recorded by many reputed scientists and reported in different national and international journals. The first mode frequency enhanced (~8.14 Hz, 3.85%) during the solar X-ray bursts and immediately after its value decreased (~7.44 Hz, 5.13%) during the proton event. The observation was recorded experimentally. Square loop antenna, a vertical cable of 50 meter length, a receiver circuit and a Data Acquisition Card (DAC) and computer were used in this experiment.

2.2 Theory. Rudimentary concepts:

Inhomogeneity can arise due to unequal extra ionization in different layers during solar X-ray flares (SF) and solar proton events (SPE) [4]. The variation in the first and second mode Schumann resonance frequencies occurred during the intense solar X-ray burst by 0.2 Hz and 0.3 Hz, respectively [11]. The observed maximum of first, second and third SR mode frequencies during sudden ionospheric disturbance were 8.51 Hz, 14.71 Hz and 21.22 Hz respectively [4].

During solar activity, there may be two kinds of changes to the lower boundary of the Earth-ionosphere waveguide:

(i) ionization enhancement at the normal *D*-region reflection heights, and (ii) the variation of *D*-region's lower edge [11]. According to the simplest vacuum model [4] the variation of the first SR frequency can be written as [11].

$$\nabla \mathrm{f}_1 / \mathbf{f}_1 \approx 0.36(\nabla \mathrm{N} / 2\mathrm{N} + \nabla \mathrm{h} / \mathrm{h}) \ldots\ldots\ldots\ldots\ldots\ldots (1)$$

where f_1 is the first mode frequency, Δf_1 change in first mode frequency, N is the ion density and ΔN change in ion density, h is the ionospheric reflection height and Δh change in reflection height.

It is established that solar X-ray radiation causes extra ionization mainly in the height range of 70–80 km, whereas SPE can cause extra ionization up to the depth of 40– 50 km. To explain the effect of this kind of inhomogeneity on SR, the two-layer waveguide model has been proposed by Greifinger et.al [12]. For the lower layer $\sigma = \varepsilon_0 \omega$, i.e., where displacement and conduction currents are equal to each other and relatively upper layer is that at which $\mu_0 \omega \sigma \zeta^2 > 1$ where ζ is the conductivity scale height at the altitude for reflection of ELF wave. The unequal ionization of these two layers by solar extra radiation, i.e., by both x-ray and γ-rays can give rise to vertical inhomogeneity which modifies the SR

frequency. The SR frequencies was expressed by Satori et.al and Sentman et.al respectively [4,13].

$$f_n = \frac{1}{\sqrt{2\pi}} \frac{c}{r_e} \sqrt{n\,(n+1)} \sqrt{\frac{h_1}{h_2}} \quad \ldots\ldots\ldots\ldots\ldots\ldots (2)$$

where n is the mode number, c, the velocity of light; r_e, mean radius of the earth; h_1 and h_2 are the two characteristic heights in the D-region. For $n = 1$,

$$f_1 = \frac{1}{\sqrt{\pi}} \frac{c}{r_e} \sqrt{\frac{h_1}{h_2}} \quad \ldots\ldots\ldots\ldots\ldots\ldots (3)$$

During solar flare, the lower height h_1 is almost unaffected because it causes extra-ionization mainly around 70 km, i.e., the reduced upper reflection height δ_2 or h_2 modified the first SR frequency as:

$$(f_1)_{SR} = \frac{1}{\sqrt{2\pi}} \frac{c}{r_e} \sqrt{\frac{h_1}{h_{2-\delta 2}}} \quad \ldots\ldots\ldots\ldots\ldots\ldots (4)$$

and thus the first mode SR frequency increases. During solar proton events, energetic protons can penetrate deeply into the ionosphere upto 50 km and possibly even deeper and can ionize regions lower than the normal D-region [11]. Thus, the δ_1 decrement over h_1 lower reflection height modifies the first mode SR frequency resulting in a diminishment of SR frequency.

2.3 Experimental Setup & Recording System:

2.3.1 Square Loop Antenna:

Fig. 2.2 : A standard square loop antenna

A square loop antenna is supposed, to radiate a conical beam, using the moment method. The loop has a single feed and two corners are truncated for circularly polarized (CP) radiation. It is revealed that the antenna shows a gain of approx. 9 dB, which is higher than that of a conventional loop by 2 dB. However there are square loop antenna with differnet structures and gains.

A square loop antenna under even-mode operation is analysed and an approximate model based on equivalent multiple sources is developed to describe its radiation characteristics. The calculated results of the proposed model are validated by a few classical analytical models at first. The proposed model is then applied to analyse traditional linearly polarised (LP) and circularly polarised (CP) loop antennas. [14].

2.3.2 Co Axial Cable:

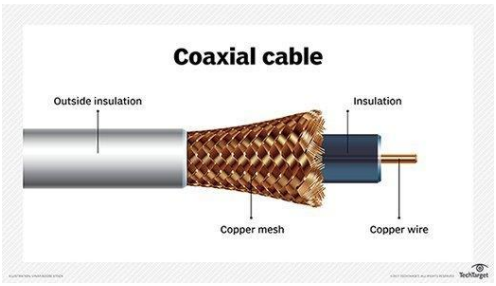

Fig. 2.3 : Structure of a Co-axial Cable

Coaxial cable is a type of transmission line, used to carry high-frequency electrical signals with low losses. It is used in such applications as telephone trunk lines, broadband internet networking cables, high-speed computer data busses, cable television signals, and connecting radio transmitters and receivers to their antennas. It differs from other shielded cables because the dimensions of the cable and connectors are designed to give a precise, constant conductor spacing, which is needed for it to function efficiently as a transmission line [15].

Coaxial cable was used in the first (1858) and following transatlantic cable installations, but its theory was not described until 1880 by English physicist, engineer, and mathematician Oliver Heaviside, who patented the design in that year (British patent No. 1,407). Co-axial cable is used as a transmission line for radio frequency signals. Its applications include feedlines connecting radio transmitters and receivers to their antennas, computer network (e.g., Ethernet) connections, digital audio (S/PDIF), and distribution of cable television signals. One advantage of coaxial cable over other types of radio transmission line is that in an ideal coaxial cable the electromagnetic field carrying the signal exists only in the space between the inner and outer conductors. This allows coaxial cable to be installed next to metal objects such as gutters without the power losses that occur in other types of transmission lines. Coaxial cable also provides protection of the signal from external electromagnetic interferences.

2.3.3 The Receiver Circuit:

The Receiver Circuit consists of protective circuit, buffer amplifier circuit, notch filter circuit, differential amplifier circuit, tuning circuit, detector stage [16].

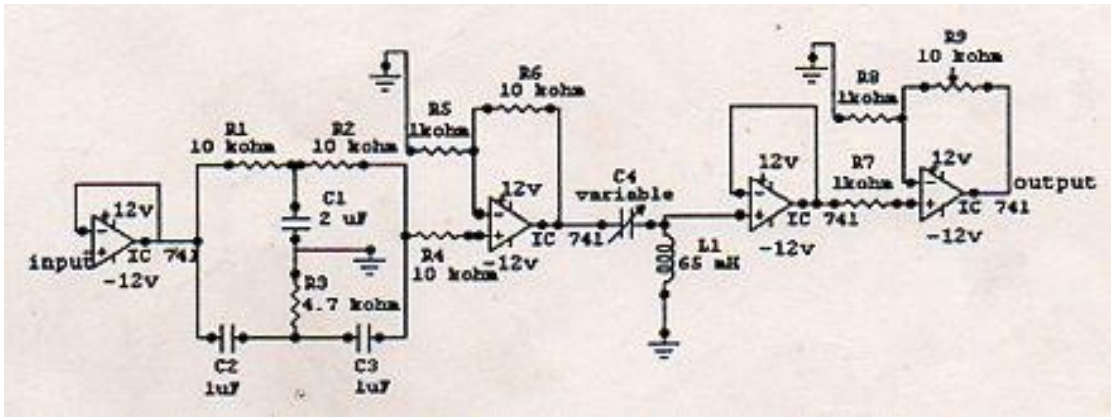

Fig. 2.4 : A receiver circuit used in our measurement

2.3.3.1 Protective Circuit:

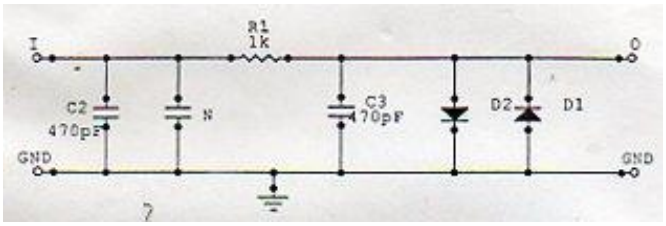

Fig. 2.5 : A protective circuit used in our measurement

As the name suggests protective circuit protects the receiver circuit from the high voltage. 2 LED diodes are connected parallelly.

2.3.3.2 Notch Filter Circuit:

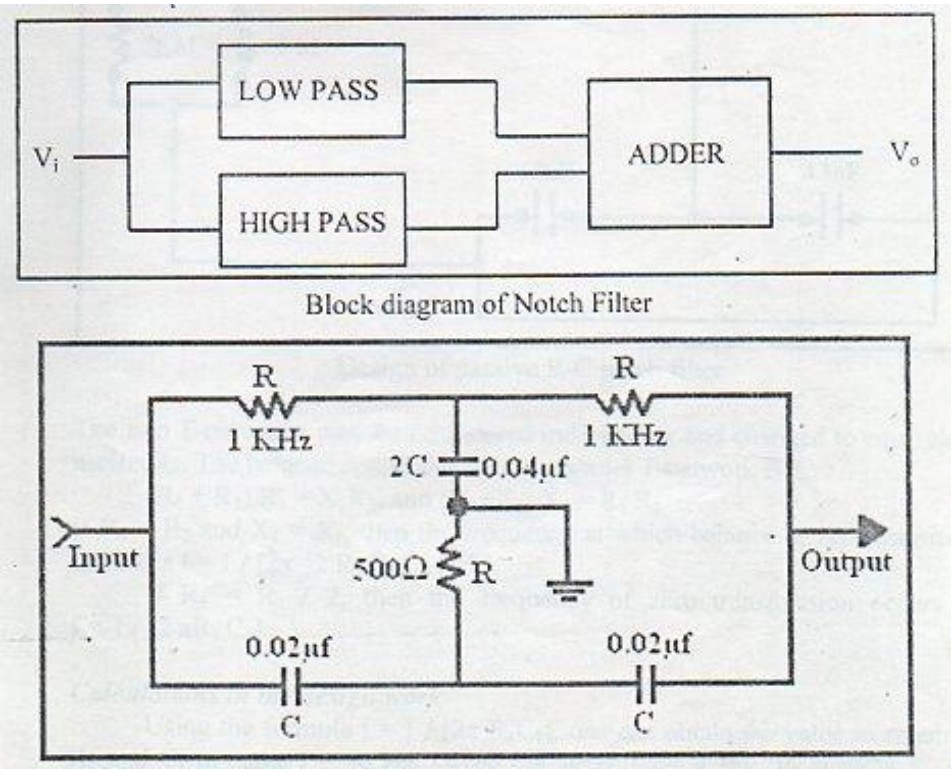

Fig. 2.6 : An ideal Notch filter circuit which rejects 50 Hz signal.

The design and fabrication of a 50 Hz notch filter is presented here. It is designed mainly by using passive components. The circuit of passive notch filter is given in figure above. The frequency response is presented in fig 2.7 and 2.8 [16].

The notch filter may be used to remove the effect of line frequency (50 Hz) components. Active 50 Hz notch filter can be designed in two different ways.

1. Passive RC components followed by active device.
2. The Active filter chip UAF42 (Universal Active Filter)

A reactive network that freely passes low bands of frequencies while almost totally suppressing other high bands of frequencies is called low pass filter. Similarly reactive network that freely passes high bands of frequencies while reject low bands of frequencies is called high pass filter. An RC circuit can be used as a notch or band reject filter when the low

pass and high pass filters are connected in parallel with each other.

If the reactances and resistances are properly chosen this network may be used to balance out or reject a particular frequency.

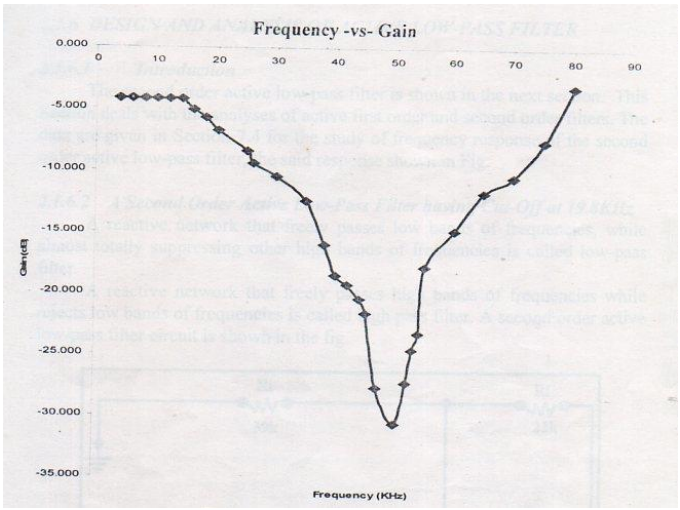

Fig. 2.7 : Variation of frequency and gain of 50 Hz notch filter

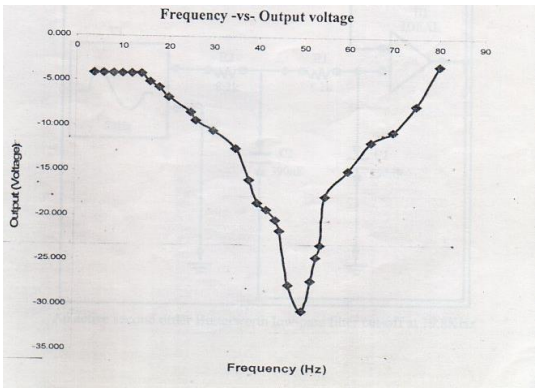

Fig. 2.8 : Variation of frequency and output voltage of 50 Hz notch filter.

2.3.3.3 Differential Amplifier:

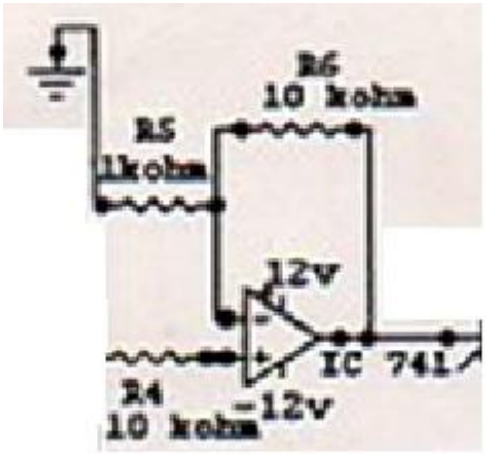

Fig. 2.9 : An non- inverting amplifier circuit

The OP-AMP can also the used as an non–inverting amplifier. Such a configuration is shown in above figure. The overall voltage gain greater than or equal to unity and almost infinite input impedence.

2.3.3.4 Tuning Circuit:

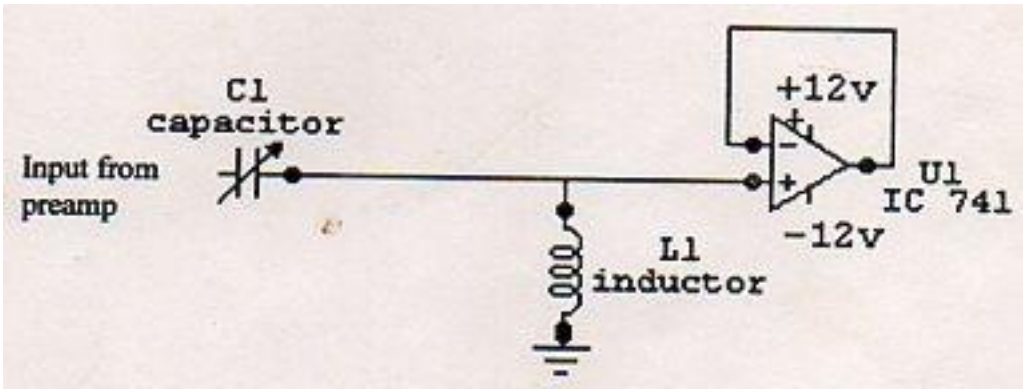

Fig. 2.10 : A typical tuning circuit used in our measurement

The signals are often contaminated with various types of noises (manmade or environmental). The signal received by the antenna after passing to the buffer stage is fed to the tuning circuit which is basically an LC circuit. It is designed so that it selects the required signal rejecting the noise signal.

2.3.3.5 Buffer Amplifier Circuit:

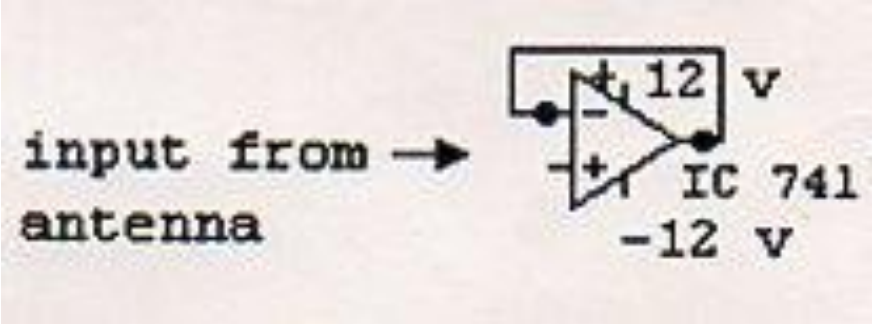

Fig. 2.11 : Ideal buffer circuit used in our measurement

If the signal is applied to the non-inverting input terminal and feedback is given, the circuit amplifies without inverting the input signal and such a circuit is called non-inverting amplifier. It is a negative fed back system, as output is being fed back to the inverting input terminal. This non-inverting amplifies can be used as a unity gain buffer which acts as an impedance matching device. The output voltage follows the input voltage exactly. Hence the circuit is called voltage follower. Its input impedance is very high and output impedance is almost zero. Therefore it draws negligible current from the source. Hence this circuit is used as an impedance matching device between any two stage of an electronic circuit whose impedances are not properly matched. The voltage follower may be used as a buffer to connect a high impedance source to a low impedance source.

2.3.3.6 Attenuator:

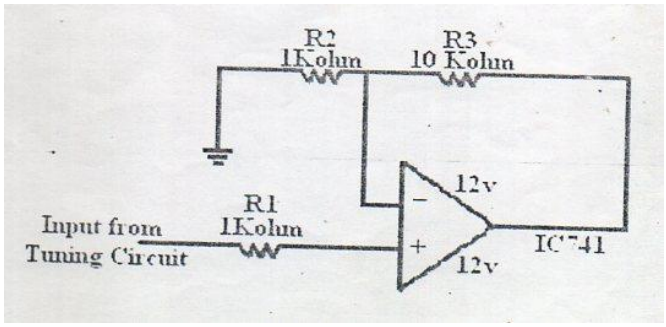

Fig. 2.12 : Ideal attenuator circuit used in our measurement

The Data Acquisition Card used in the above case could not handle voltages having a value above two volts, peak to peak. The signal fed from the antenna fluctuates due to various reasons and so attenuator is applied so that the acquired signal has a safe value and there will be no clipping of the signal. The attenuator is constructed using OP-AMP IC741 in the non-inverting mode. Where the feedback resistance used is a variable one. The gain is <1.

2.3.3.7 Diagram of OP-AMP 741 and its Pin Connection

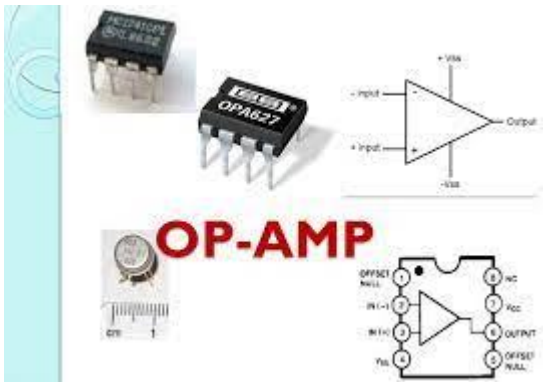

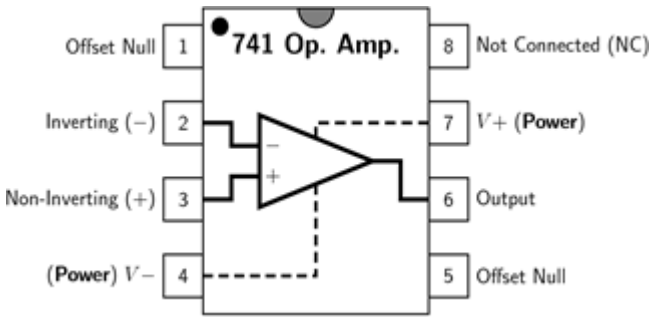

Fig. 2.13 : Pin connection of OP-AMP 741 used in our measurement

2.3.3.8 Features of OP – AMP IC741:

Parameters	Value
Input offset valtage	5.0 mV Max
Slew Rate	0.5 V/μs
Common Mode Rejection Ratio	70 Min
Drift with Temperature	15 μV/^{0}C
Voltage Gain	2 Million Min

2.3.3.9 Detector Stage

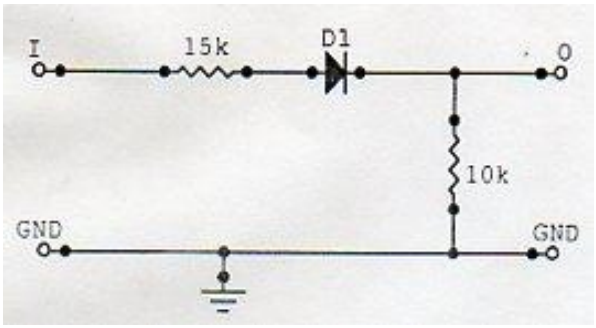

Fig. 2.14 : Ideal detector circuit used in our measurement.

The detector stage is fed to the attenuator. It detects the output tuning signal. Here the diode used is IN4007.

2.4 Recording of Data:

2.4.1 Data Acquisition Card & Computer:

After a reasonable gain has been achieved the desired signal has to be processed for further studies. But the signal being in the analog domain cannot be processed by digital computer. So at first it is converted into digital form and then the acquired data is stored into a computer. The data acquisition card basically consists of a Digital to Analog Converter (DAC) card which is made up of a sample, hold circuit and a coder. The sample and hold

circuit samples the analog value at an instant and feeds it to the coder which converts it into digital form. Thus taking numerous samples of the input signal, the original waveform can be retraced later on. The data acquisition card used here is a sound card. Radio Sky-Pipe software is used here.

The detected signal is sampled 44100 times per second and the analog voltage is converted into 12 bit digital signal. So the numbers of levels in corresponding PCM is 4095. Since the highest frequency encountered in the experiment is 8 Hz, the choice of the sampling frequency is alright. The data acquisition system used is the computer sound card. The typical data acquisition system is shown below.

In general, the model accepts a number if analog input, called channel. Typically a system may have 8 different input channels or 16 single input channels. The computer can select any one of the channels for input data through the channel.

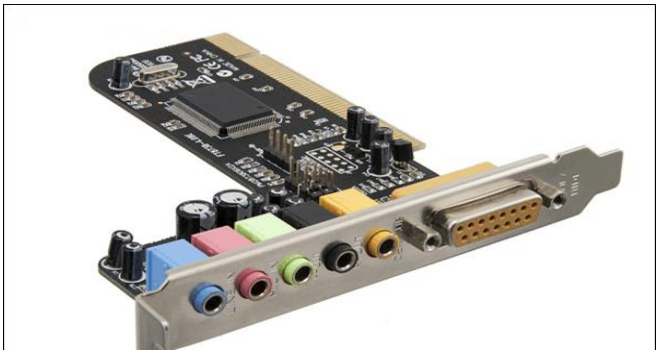

Computer Sound Card

Fig.2.15 : Computer Sound Card used in our measurement

2.4.2 Data Acquisition System:

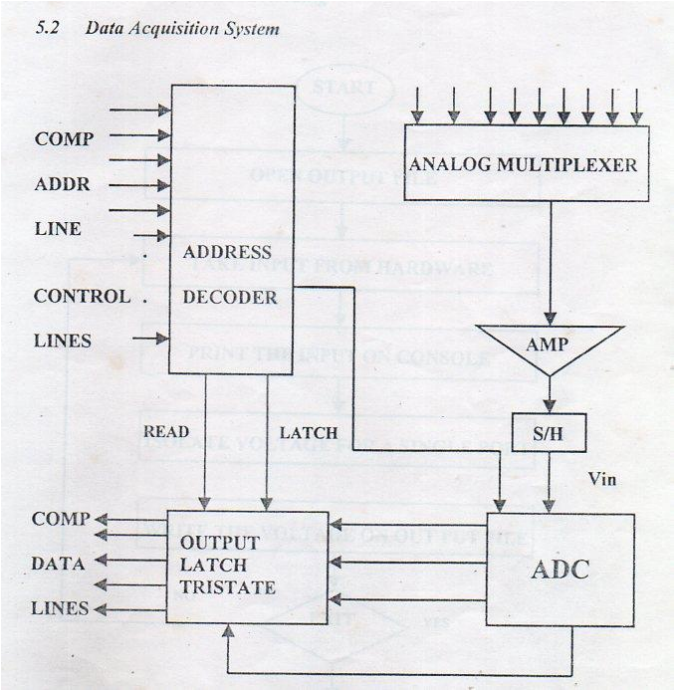

Fig. 2.16 : A standard DAC system

2.4.2.1 Flow Chart of Data Acquisition System:

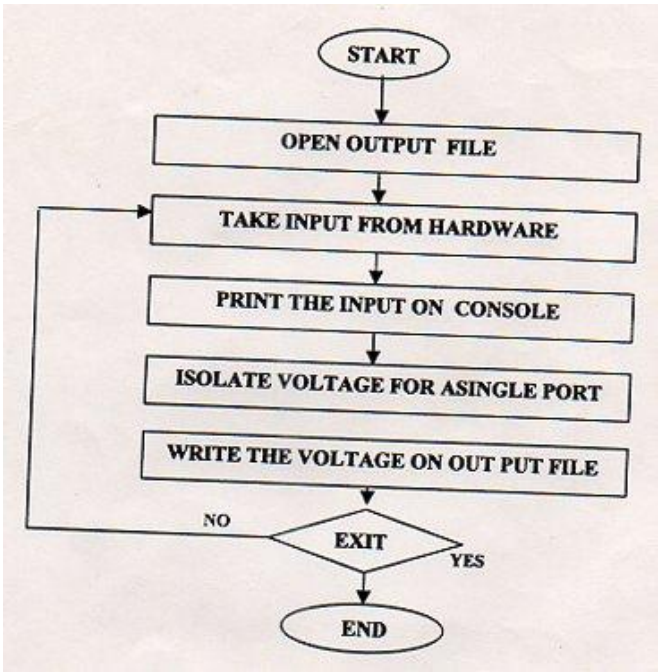

Fig .2.17 : A standard flow chart of DAC system

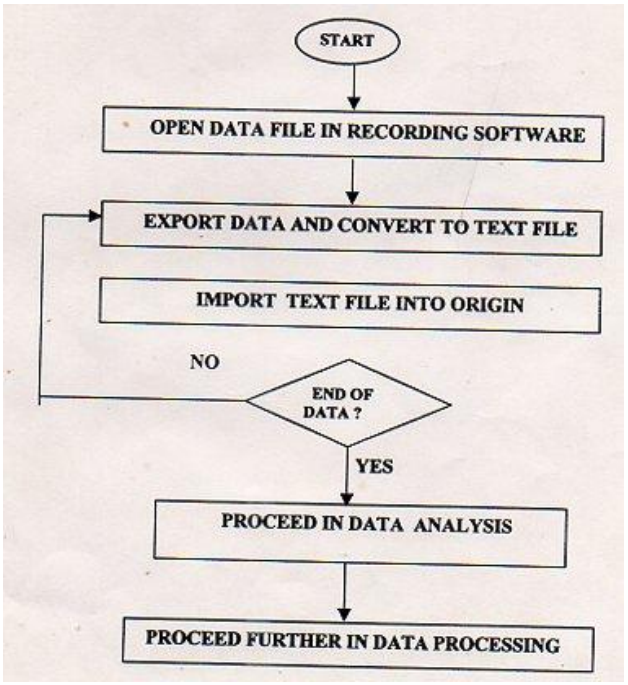

Fig.2.18 : A standard flow chart of DAC system

2.4.3 Calculation of the Resolution of the system:

Percentage resolution = (step size) * FSV *100%

(2/4096)*2*100=0.0976%

FSV = Full Scale Value

The real time data was recorded with the help of a software specially designed for this purpose, named Radio-Sky-Pipe. It records the incoming signal form antenna with the help of sound card. The amplitude of the signal is obtained by multiplying the record signal with 10^{-2} in the unit of millivolt.

2.5 Design & Fabrication of ELF Receiver:

The cut-off frequency of the RC Low pass filter is given by $f_o = 1/2\pi RC$ and closed loop gain $A_v = [1+R_f/R_1]$. Therefore for an active low pass filter

i. A very low frequency ($f << f_o$) closed loop gain nearly A_v

ii. At $f = f_o$ closed loop gain nearly $0.707\ A_v$

iii. At very high frequency ($f >> f_o$) closed loop gain nearly o.

The tuning frequency for L-C circuit is =1/2π $\sqrt{LC}$.

The tuning circuit selects the required signal rejecting the noise signal. But the noises at the resonant frequencies are not available.

2.6 Block Diagram of the ELF/VLF Receiving System:

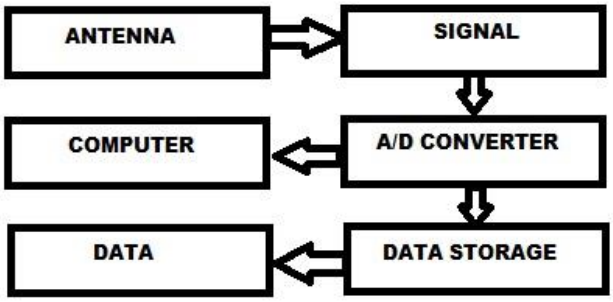

Fig.2.19 : A standard block diagram of ELF/VLF receiving system

2.6.1 Block diagram of ELF measurement system:

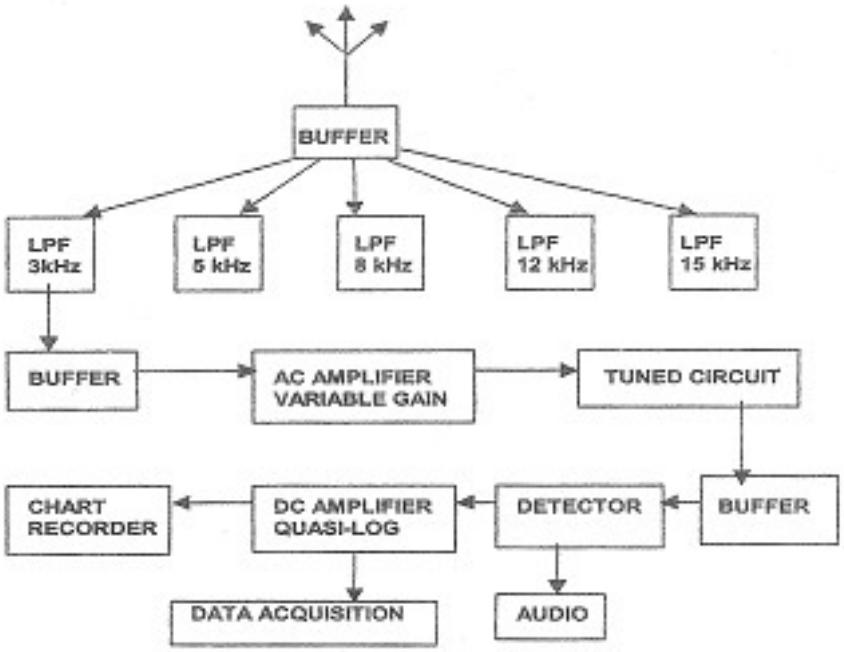

Fig. 2.20: A standard block diagram of ELF measurement system

2.7 Mathematical Explanation:

According to the two layer SR theory frequencies can be expressed as [13]

$$f_n=\sqrt{\frac{n(n+1)}{2\pi}}\,\frac{c}{r_e}\,\sqrt{\frac{h_1}{h_2}} \quad \ldots\ldots\ldots\ldots\ldots\ldots (5)$$

where n is the mode number (n = 1, the first harmonic is regarded here), c the velocity of light, r_e the mean radius of the earth and h_1 and h_2 the two characteristic heights in the D-region.

$$\text{For } n = 1,\ f_1 = \sqrt{\frac{1}{\pi}}\,\frac{c}{r_e}\,\sqrt{\frac{h_1}{h_2}} \quad \ldots\ldots\ldots\ldots\ldots\ldots (6)$$

During an X-ray flare the lower height h_1 is almost unaffected because it causes extra-ionization mainly around 70 km, i.e., the height of reflection h_2 is slightly reduced by the value δ_2 so that the modified first SR frequency becomes

$$(f_1)_{SR} = \sqrt{1/\pi}\ (c/r_e)\ \sqrt{h_1/(h_2-\delta_2)} \ldots\ldots\ldots\ldots\ldots\ldots (7)$$

During an SPE energetic protons can penetrate deeply into the ionosphere up to 50 km and can ionize regions lower than the normal D-region [11, 17]. In this case h_1 changes by the value δ_1. If the effect on h_2 is neglected the modified first SR frequency will be

$$(f_1)_{SRP} = \sqrt{1/\pi}\ (c/r_e)\ \sqrt{(h_1-\delta_1)/h_2} \ldots\ldots\ldots\ldots\ldots\ldots (8)$$

2.8 Summary and Conclusion:

The concept of Schumann Resonance have been discussed in details. The mathematical formula of Schumann Resonance Spectra also have been discussed due to solar proton event. The co-relation between solar activity and SR parameters might be used for many studies like the study of sun and extra-terrestrial sources. To detect the Schumann Resonance frequencies an experimental setup have been designed which are discussed in detail in this chapter.

2.9 REFERENCE:

[1] Schumann, W. O. (1952), Uber die strahlungslosen Eigenschwingungen einer leitenden Kugel, die von einer Luftschicht und einer Ionospha¨renhu¨ lle umgeben ist, Z. Naturforsch A, 7, 149–154.

[2] Madden, T. and W. Thompson, 1965: Low-frequency electromagnetic oscillations of the Earth-ionosphere cavity. Rev. Geophys., **3**, 211-254,

[3] De, S.S., De, B.K., Sarkar, B.K., Bandyopadhyay, B., Haldar, D.K., Paul, S., Barui, S.: Analyses of Schumann resonance spectra from Kolkata and their possible interpretations. Indian J. Radio Space Phys. **38**(4), 208 (2009)

[4] Sátori, G., Williams, E., Mushtak, V.: Response of the earth-ionosphere cavity resonator to the 11-year solar cycle in X- radiation. J. Atmos. Sol.-Terr. Phys. **67**, 553 (2005)

[5] Roldugin, V.C., Maltsev, Y.P., Vasiljev, A.N., Schokotov, A.Y., Belyajev, G.G.: Schumann resonance frequency increase during solar X-ray bursts. J. Geophys. Res. **109**, A01216 (2004b)

[6] A.V. Shvets,1∗ A. P. Nickolaenko,1 and V. N. Chebrov 2, Effect of solar flares on the schumann-resonance frequencies, Radiophysics and Quantum Electronics, August 2017, Volume **60**, pp 186–199

[7] Price, C., Mushtak, V.: The impact of the August 27, 1998, γ -ray burst on the Schumann resonances. J. Atmos. Sol.-Terr. Phys. **63**(10), 1043 (2001)

[8] Price, C., Pechony, O., Greenberg, E.: Schumann resonances in lightning research. J. Lightning Res. **1**, 1 (2007)

[9] Nickolaenko, A.P., Kudintseva, I.G., Pechony, O., Hayakawa, M., Hobara, Y., Tanaka, Y.T.: The effect of a gamma ray flare on Schumann resonances. Ann. Geophys. **30**, 1321 (2012)

[10] Nickolaenko, A.P., Hayakawa, M.: Model disturbance of Schumann resonance by the SGR l806-20 γ -ray flare on December 27, 2004. J. Atmos. Electr. **30**(1), 1 (2010)

[11] Roldugin, V. C., Y. P. Maltsev, A. N. Vasiljev, and E. V. Vashenyuk, 1999:Changes of the first Schumann resonance frequency during relativistic solar proton precipitation in the 6 November 1997 event. Ann. Geophys., **17**, 1293-1297,

[12] Greifinger, C., Greifinger, P.: Approximate method for determining ELF eigenvalues in the earth-ionosphere waveguide. Radio Sci. **13**(5), 831 (1978)

[13] Sentman, D.D.: Approximate Schumann resonance parameters for a two-scale-height ionosphere. J. Atmos. Terr. Phys. **52**(1), 35 (1990)

[14] Chen, Ying ; Lu, Wen-Jun ; Zhu, Lei ; Zhu, Hong-Bo. International Journal of Electronics, Volume **104**, Issue 2, p.271-285, February 2017

[15] Baydaa Hadi Saoudi Analysis and Study the Performance of Coaxial Cable Passed On Different Dielectrics. International Journal of Applied Engineering Research ISSN 0973-4562 Volume **13**, Number 3 (2018) pp. 1664-1669

[16] Paul Malvino. Electronic Principles (SIE) | 7th Edition

[17] Clilverd, M. A., A. Seppälä, C. J. Rodger, N. R. Thom- son, P. T. Verronen, E. Turunen, T. Ulich, J. Lich- tenberger, and P. Steinbach, 2006: Modeling polar ionospheric effects during the October-November 2003 solar proton events. Radio Sci., **41**, RS2001,

CHAPTER - III

First Mode Schumann Resonance Frequency Variation During a Solar Proton Event

3.1 Introduction:

The Schumann resonance (SR) is the electromagnetic resonance phenomenon generated by global lightning discharges within the resonator formed between the Earth and the ionosphere. The various aspects of SR phenomena are being explored [1-17] over the years. The inhomogeneities originate from the asymmetry of the day and night time ionosphere. Another class of inhomogeneity may arise due to unequal extra ionization in different layers during solar X-ray flares (SF) and solar proton events (SPE). SF cause extra ionization mainly in the 70 - 80 km height range, whereas SPE can cause extra ionization up to a depth of 40 - 50 km. The effect of this kind of inhomogeneity on SR can be explained using the two-layer waveguide model by Greifinger et.al [18]. The geomagnetic field, the anisotropic conductivity of the cavity influence the wave propagation in the Earth-ionosphere cavity. Within the cavity disturbances like random fluctuations of irregularities are occurring regularly along with other causalities, such as Polar-Cap absorption, X-ray bursts, etc.

Protons with energy up to 100 MeV are most often emitted from the Sun in conjunction with solar flares, which can penetrate deeply into the D-region and cause additional ionization leading to the conductivity changes thereby modifying the SR parameters explained by Roldugin [19-21]. High solar proton fluxes cause serious radiation hazards in the solar system by Reddy [22]. The spectra of the signals in the realistic and idealistic earth-ionosphere cavities have been computed in the frequency and time domains and the features pertinent to the Earth-ionosphere cavity with exclusively low losses implying a special

atmospheric conductivity model are discussed by Nickolaenko and Hayakawa [23].

The variation in frequency of the first SR spectra mode during SPE from 06 - 07 March 2012 is presented in this work from the observed data recorded over Kolkata. The result shows the decrease in frequency during SPE occurrence and enhancement of the first mode frequency during the severe solar X-ray bursts occurring just before the proton event. The influences of SPE and X-ray bursts upon the SR frequency fluctuation are explained in terms of changes in ionization produced by the events and corresponding modification in the Earth-ionosphere waveguide.

3.2 Experimental:

The antenna system for these experiments were erected on the ground at a vast bare land area near Kolkata having the geographic coordinates (Lat: 22.56°N, Long: 88.5°E).

Square-loop antennas were made for the detection of extremely low frequency (ELF) signals. Two such loops were mounted onto wooden structures connected in series and thus their effective gain was increased beyond 5 dB. The length of each side of the square loops was 1 m with a total of 75 turns and the other with 90 turns has the length of 1.3 m for each side. A coaxial cable of 50m in length is used to transfer the signal from the antenna into the receiver input where it is pre-amplified. A stereo-preamplifier-integrated circuit with LA3161 chip is chosen whose low frequency response starts below 5 Hz and extends up to a few kHz. This chip is superior to others in handling input voltage in the range of few microvolts to millivolts. The frequency selective stages were designed with active circuit elements. A wideband amplifier whose output is taken through an active low-pass filter having cut-off frequency nearly 35 Hz further amplified it. A wideband, very low input voltage sensitive and low frequency sensitive receiver was fabricated to detect input signals in the range of 100 - 500 mV.

The detected ELF signal is sampled at a rate of 40000 times per second and the voltage is then converted into a 12-bit digital signal using a computerized data acquisition system through a PCI 1050, 16 channel 12 bit DAS card. These signals are further processed and stored in a computer. Because of the choice of sampling frequencies, no information is lost in the sampling process, except for the quantization error. The loop antennae are vertically mounted in series with their planes kept parallel to each other along a fixed E-W or N-S direction. The recorded data were analyzed through Origin software.

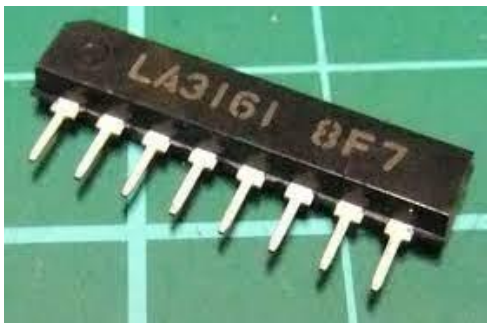

Fig. 3.1 A standard IC LA3161

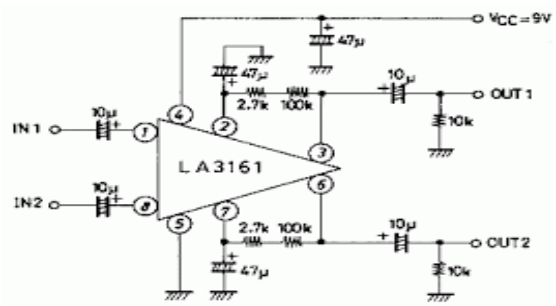

Fig.3.2 : Pin connection of LA3161

LA3161 Monolithic Linear IC 2-Channel Pre-amplifier Features

- On-chip 2 preamplifiers
- Good ripple rejection owing to on-chip voltage regulator
- Minimum number of external parts required
- Low noise
- 8-pin SIP package facilitating easy mounting
- Pin-compatible with LA3160 specifications.
- Absolute Maximum Ratings at Temparature = 25°C.
- Parameter Maximum Supply Voltage 18 Volt
- Allowable Power Dissipation 200 mW
- Operating Temperature –20 to +75 ^{0}C

- Storage Temperature –40 to +125 ^{0}C

Fig. 3.3 : A standard inductance used in our measurement

The Inductance used in this experiment was made by my own hand.

3.3 Results & Discussion:

High energy solar proton flux of 07 March 2012 was detected using the GOES 13 satellite at 0010 UT which showed solar proton maxima at 1500 UT. It was preceded by the solar X-ray bursts. Its onset occurred at about 0000 UT and the maximum took place at 0010 UT. The variations in proton flux at energy (E) ≥ 100 MeV and X-ray at wavelength (λ) at $0.1 < \lambda < 0.8$ nm are shown in Fig. 3.4 by a continuous line curve and dashed line curve, respectively.

The changes in the first SR frequency on 07 March 2012 over Kolkata are shown by the continuous line graph joining the square blocks in Fig. 3.5. The values of the first SR frequency are averaged over five days adjacent to the day of occurrence for these two events. The frequencies are plotted by a dot-dashed curve. The SR frequency started enhancing from 2300 UT March 6 and reaches the highest value ~8.14 Hz (3.85%) at 0010 UT during solar bursts. Immediately after the solar proton flare, it approached a lower value showing the minima at ~7.44 Hz (5.13%) because of the instantaneous high energy SPE. The decrease in the first mode SR frequency continued up to around 1500 UT and returned to its normal value at 2000 UT of March 7.

The earliest ELF propagation parameter models in the Earth-ionosphere waveguide were based on the supposition that the lower ionosphere conductivity profile is horizontally

homogeneous and varies exponentially in the vertical direction. During solar activity there may be two kinds of changes:

(1) increase in ionization level at the normal D-region reflection heights, and (2) the variation of D-region's lower edge [12]. According to this model the variation in the first SR frequency is given by [22]

$$\nabla f_1 / f_1 \approx 0.36(\nabla N / 2N + \nabla h / h) \ldots\ldots\ldots\ldots\ldots\ldots\ldots\ldots (1)$$

where f_1 is the first mode frequency, Δf_1 change in first mode frequency, N is the ion density and ΔN change in ion density, h is the ionospheric reflection height and Δh change in reflection height.

This expression shows that the frequency can change due to both electron density variations in the ionospheric D-region and the change in D-region lower boundary height. X-ray flux growth enhances the electron density without a significant change in the ionospheric altitude, causing the first SR frequency increase. Solar protons penetrating deep into the atmosphere caused a decrease in D-region altitude.

This gives rise to a decrease in the first SR frequency. SPE can also affect the ionization. Thus, the two terms compete with each other and their relative magnitudes are the decisive factors, i.e., whether there will be an increase or decrease in the first SR frequency. If the two terms are comparable there may be no change in the first SR frequency. Apart from this, the two terms are inter-linked. This model will not be efficient in estimating the magnitude of variation in the first SR frequency. Later on, two characteristic layers were identified within the lower ionosphere by Madden et.al [2] to be responsible for vertical electric field height variation and horizontal magnetic field components. Another kind of inhomogeneity can arise during solar X- ray or proton flux enhancement. In this method the eigenvalue depends on the conductivity of the atmosphere in the two height-independent characteristic layers: h_1 and h_2. One layer is

defined as the height h_1 where displacement and conduction currents are equal (typically 40 - 55 km for $f < 50$ Hz). The other is at a height of 60 - 70 km, where $4n_0 \sim vg^2 = 1$, g being the conductivity scale height at the altitude responsible for ELF wave reflection. The unequal ionization of these two layers by solar extra radiation can give rise to vertical inhomogeneity affecting the SR frequency. An approximate variation in medium conductivity around 30 - 80 km is shown in Fig. 3.6. A modeled altitude profile of conductivity using an exponential equation under perturbation due to extra ionization of the medium can be expressed as [15].

$$\sigma(z) = 10^{-16} \exp\left[\frac{z}{3.1} + 2.303\beta \exp -\left(\frac{z-zo}{a}\right)^2\right] \quad \text{.....(2)}$$

where $\sigma(z)$ is the conductivity profile, the perturbation parameter β is the perturbation amplitude in powers of ten about its undisturbed value, z is the altitude and z_0 is a particular altitude, and a is the width of perturbation.

According to the two layer theory SR frequencies can be expressed by Sentman [5]

$$f_n = \sqrt{\frac{n(n+1)}{2\pi}}\,\frac{c}{r_e}\sqrt{\frac{h_1}{h_2}} \quad \text{..... (3)}$$

where n is the mode number ($n = 1$, the first harmonic is regarded here), c the velocity of light, r_e the mean radius of the earth and h_1 and h_2 the two characteristic heights in the D-region.

$$\text{For } n = 1,\ f_1 = \sqrt{\frac{1}{\pi}}\,\frac{c}{r_e}\sqrt{\frac{h_1}{h_2}} \quad \text{..... (4)}$$

During an X-ray flare the lower height h_1 is almost unaffected because it causes extra ionization mainly around 70 km, i.e., the height of reflection h_2 is slightly reduced by the value δ_2 so that the modified first SR frequency becomes

$$(f_1)_{SR} = \sqrt{1/\pi}\,(c/r_e)\,\sqrt{h_1/(h_2 - \delta_2)} \ldots\ldots\ldots\ldots\ldots\ldots (5)$$

The first SR frequency, therefore, increases. In our observation the proton event was preceded by a flare during which we observed an increase in the first SR frequency. During the solar flare the reflectivity of the upper height is also increased. This fact contributes additionally to the increase in the first SR frequency. During an SPE energetic protons can penetrate deeply into the ionosphere up to 50 km and can ionize regions lower than the normal D-region [24]. In this case h_1 changes by the value δ_1 . If the effect on h_2 is neglected the modified first SR frequency will be

$$(f_1)_{SRP} = \sqrt{1/\pi}\,(c/r_e)\,\sqrt{(h_1 - \delta_1)/h_2} \ldots\ldots\ldots\ldots\ldots\ldots (6)$$

As a result, the first SR frequency decreases. The altitude profile in perturbation of the first SR frequency, using the perturbation parameter β = 3 and the width parameter a = 6 is shown in Fig. 3.7 along with its unperturbed profile (β = 0). The dashed curve in this figure depicts the first resonance frequency altitude profile using the FDTD / prony result [5]. The geomagnetic storm is also an important agent that produces ionospheric disturbances and hence may also be responsible for generating transient electromagnetic pulses which in turn may enhance the SR signal levels when superposed in this frequency band. The geomagnetic storm observed during that period is evident from Fig. 3.8. Thus the observed signal variation, i.e., the SR frequency restoration almost to the undisturbed value may be due to the geomagnetic storm.

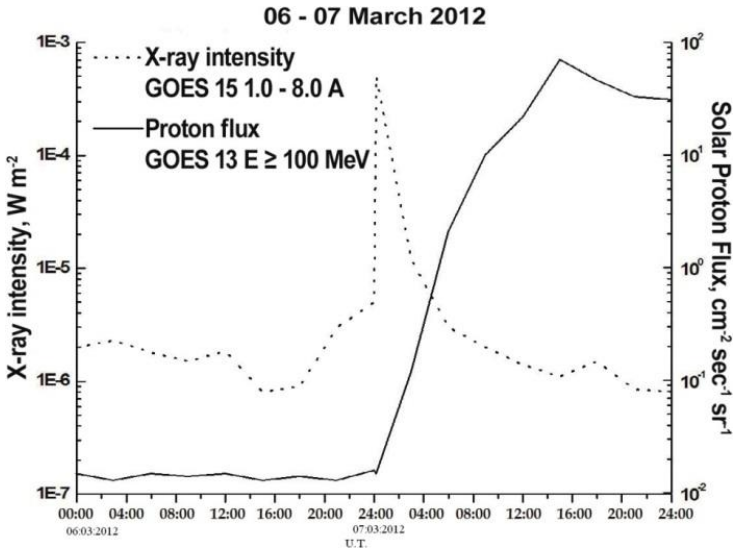

Fig. 3.4 Energetic solar proton flux and X-ray bursts as recorded onboard GOES 13 satellite during the solar proton event (SPE) of 06 - 07 March 2012. The continuous line curve is for the proton flux while the dashed line curve represents X-ray bursts.

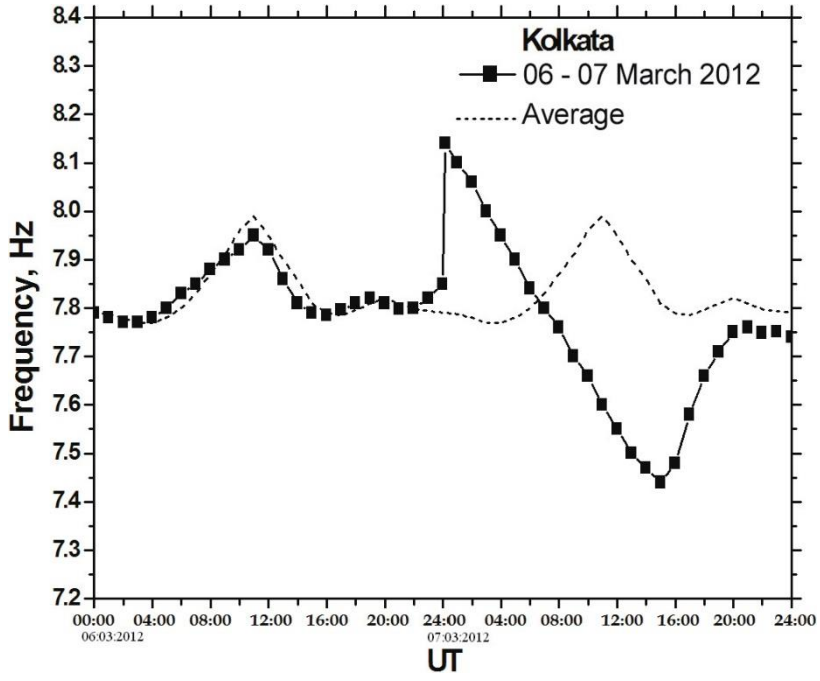

Fig. 3.5. Variation of the first mode SR frequency over Kolkata (22.56°N, 88.5°E) on 06 - 07 March 2012 depicted by the continuous line curve joining the square blocks. SR frequencies averaged over five days adjacent to the day of occurrence are shown.

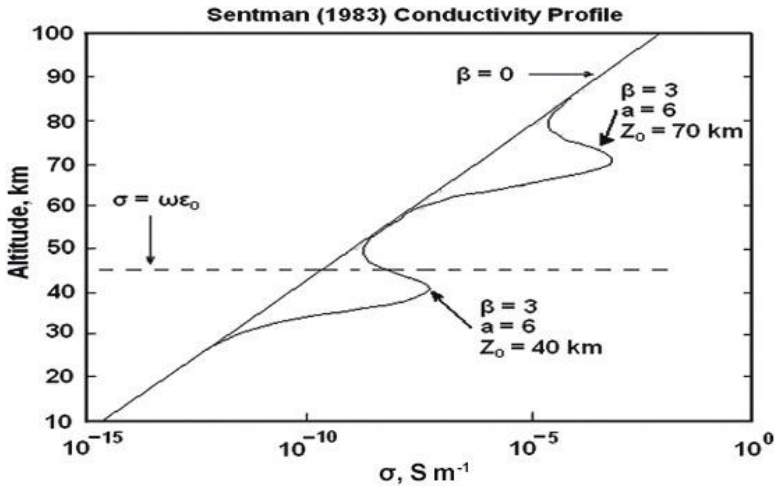

Fig. 3.6 Conductivity model according to Sentman [5] using the exponential equation with perturbation parameter b . The line $\nu = \sim f_0$ signifies the altitude in which ionosphere becomes conductive.

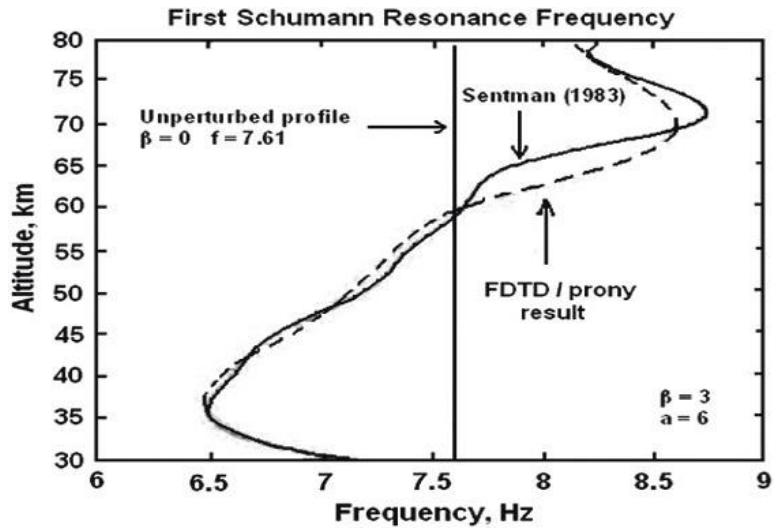

Fig. 3.7. Perturbed profile of first SR frequency according to Sentman [5].

Fig. 3.8. Variations in Dst-index during the month of March, 2012 (http://wdc.kugi.kyoto-u.ac.jp/dst_provisional/).

3.4 Conclusion:

The variation in frequency of the first SR spectra mode is not dependent on source-ionosphere geometry but depends on the waveguide characteristics. This kind of variation is to be explained by the two-characteristic-layer-model of two different heights. For the purpose of modeling the variation in the first SR frequency associated with SPE and solar X-ray bursts preliminary electron density data at the two characteristic heights are to be known during respective solar events. Further, very low frequency (VLF) phase and amplitude observations could be used to determine the ionospheric electron density variation. Very low frequency signals are known to be seriously affected during SPEs propagating through the earth-ionosphere cavity at about 50 - 60 km altitude by Clilverd et.al [24]. The D-region electron density and ionization change during high energy particle precipitation down to this altitude depend upon the particle energy at this altitude. The correlation between solar activity and SR parameters might be used for many studies like the study of the Sun and extra-terrestrial sources. Thus, it can be concluded that as the D-region and nearby layers are perturbed due to solar flares mainly by SPE and X-ray bursts, and the corresponding modification of dielectric property and reflection height change the SR mode frequency. In this way we can detect these kinds of extra-terrestrial events comparing the continuous time series spectra of the SR frequencies with some specific previous signatures.

3.5 REFERENCE:

[1] Balser, M. and C. A. Wagner, 1960: Observations of earth-ionosphere cavity resonances. *Nature*, **188**, 638-641,

[2] Madden, T. and W. Thompson, 1965: Low-frequency electromagnetic oscillations of the Earth-ionosphere cavity. *Rev. Geophys*., **3**, 211-254,

[3] Sao, K., M. Yamashita, S. Tanahashi, H. Jindoh, and K. Ohta, 1973: Experimental investigations of Schumann resonance frequencies. *J. Atmos. Terr. Phys*., **35**, 2047-2053,

[4] Tanahashi, S., 1976: Detection of line splitting of Schumann resonances from ordinary data. *J. Atmos. Terr. Phys*., **38**, 135-142,

[5] Sentman, D. D., 1983: Schumann resonance effects of electrical conductivity perturbations in an exponential atmospheric/ionospheric profile. *J. Atmos. Terr. Phys*., **45**, 55-65,

[6] Williams, E. R., 1992: The Schumann resonance: A global tropical thermometer. *Science*, **256**, 1184-1187,

[7] Füllekrug, M., 1995: Schumann resonances in magnetic field components. *J. Atmos. Terr. Phys.*, **57**, 479-484,

[8] Füllekrug, M. and A. C. Fraser-Smith, 1996: Further evidence for a global correlation of the Earth-ionosphere cavity resonances. *Geophys. Res. Lett*., **23**, 2773-2776,

[9] Yampolski, Y. M., P. V. Bliokh, V. S. Beley, V. G. Galushko, and S. B. Kascheev, 1997: Non-linear interaction between Schumann resonances and HF signals. *J. Atmos. Sol.-Terr. Phys*., **59**, 335-342,

[10] Heckman, S. J., E. Williams, and B. Boldi, 1998: Total global lightning inferred from Schumann resonance measurements. *J. Geophys. Res*., **103**, 31775-31779,

[11] Balling, R. C. and M. Hildebrandt, 2000: Evaluation of the linkage between Schumann Resonance peak frequency values and global and regional temperatures. *Clim. Res.*, **16**, 31-36,

[12] Hobara, Y., N. Iwasaki, T. Hayashida, N. Tsuchiya, E. R. Williams, M. Sera, Y. Ikegami, and M. Hayakawa, 2000: New ELF observation site in Moshiri, Hokkaido Japan and the results of preliminary data analysis. *J. Atmos. Electr.*, **20**, 99-109.

[13] Shvets, A. V., 2001: A technique for reconstruction of global lightning distance profile from background Schumann resonance signal. *J. Atmos. Sol.-Terr. Phys*., **63**, 1061-1074,

[14] Nickolaenko, A. P. and M. Hayakawa, 2002: Resonances in the Earth-Ionosphere Cavity, Modern Approaches in Geophysics, Vol. **19**, Springer Science & Business Media, New York, 380 pp

[15] Nickolaenko, A. P. and M. Hayakawa, 2007: Recent studies of Schumann resonance and ELF transients. J. Atmos. Electr., **27**, 19-39.

[16] Nickolaenko, A. P. and M. Hayakawa, 2014: Spectra and waveforms of ELF transients in the Earth-ionosphere cavity with small losses. Radio Sci., **49**, 118-130,

[17] Sekiguchi, M., M. Hayakawa, A. P. Nickolaenko, and Y. Hobara, 2006: Evidence on a link between the intensity of Schumann resonance and global surface temperature. Ann. Geophys., **24**, 1809-1817,

[18] Greifinger, C. and P. Greifinger, 1978: Approximate method for determining ELF eigenvalues in the earth- ionosphere waveguide. *Radio Sci.*, **13**, 831-837,

[19] Roldugin, V. C., Y. P. Maltsev, A. N. Vasiljev, and E. V. Vashenyuk, 1999: Changes of the first Schumann resonance frequency during relativistic solar proton precipitation in the 6 November 1997 event. *Ann. Geophys*., **17**, 1293-1297,

[20] Roldugin, V. C., Y. P. Maltsev, G. A. Petrova, and A. N. Vasiljev, 2001: Decrease of the first Schumann resonance frequency during solar proton events. *J. Geophys. Res*., **106**, 18555-18562,

[21] Roldugin, V. C., Y. P. Maltsev, A. N. Vasiljev, A. V. Shvets, and A. P. Nikolaenko, 2003: Changes of Schumann resonance parameters during the solar proton event of 14 July 2000. J. Geophys. *Res*., **108**, 1103,

[22] Reddy, R. C, 2006 : Solar Proton event integrated fluences during the current solar cycle. 37th Annual Lunar and Planetry Science Conference, March, 13-17, 2006, League City, Texas, abstract no. 1419

[23] Nickolaenko, A.P., Hayakawa, M.: Spectra and waveforms of ELF transients in the Earth-ionosphere cavity with small losses. Radio Sci. **49**, 118 (2014)

[24] Clilverd, M. A., A. Seppälä, C. J. Rodger, N. R. Thomson, P. T. Verronen, E. Turunen, T. Ulich, J. Lichtenberger, and P. Steinbach, 2006: Modeling polar ionospheric effects during the October-November 2003 solar proton events. *Radio Sci.*, **41**, RS2001,

CHAPTER – IV

STUDIES ON DIFFERENT GEOPHYSICAL AND EXTRA-TERRESTRIAL EVENTS WITHIN THE EARTH – IONOSPHERE CAVITY IN TERMS OF ULF/ELF/VLF RADIO WAVES

4.1 Introduction:

The scientific community invested many efforts by using satellite-based as well as various ground-based observational techniques to forecast natural calamities like earthquake, severe cyclone, tsunami, meteor shower, and solar flares etc. The outcome of these efforts, however, is not satisfactory enough except some meteorological predictions. ULF, ELF and VLF signals within the natural earth-ionosphere cavity can tell us this information, but we must have the ability to find out the signature of any particular natural event in these geophysical speakers. Thus we need in-depth study of these signals to realize specific signatures for the corresponding natural events.

A powerful radio noise burst radiating over a wide frequency ranging from a few Hz to several MHz during lightning discharges within the thunderclouds can propagate a long distance through the earth-ionosphere waveguide. Attenuation of the EM waves with frequencies <50 Hz is extremely low [1] and these waves can encircle the globe a few times through the earth-ionosphere cavity. When resonances occur these waves interfere with 2π phase difference, the wave path being the integral multiple of the wavelength, i.e., the wavelength is of the order of dimension of the cavity, around 40 Mm. This phenomenon is known as the Schumann resonance (SR) [2]. Some other electrical noises generated from different sources, e.g., electric railways, mechanical vibrations of the antennas, surrounding vegetation, drifting electrically charged clouds and power line transients, EM signals from

earthquake etc., also interfere with these resonance phenomena and perturb the signal intensity. Interest on these global electromagnetic resonances has continued to grow since early 1960's following their experimental detection [3]. A systematic description of theoretical and experimental research of this geophysical phenomenon, e.g., calculation of natural frequency of the cavity resonator based on different modes of ionosphere, study of excitation of the resonator by terrestrial and cosmic sources, lightning discharges, magnetospheric phenomena has been presented by Bliokh and co-workers [4]. They also discussed about location of lightning discharge, properties of the lower ionosphere, connection between resonances and magnetic disturbances, solar activity etc. in detail in connection with ELF signals. Presently Schumann resonances are being used to monitor global lightning activity [5-8], in characterizing the main African thunderstorm center [9], global variability of lightning activity [10] and sprite activity [6, 11]. A characteristic customary outline of the amplitude spectra has been exploited for evaluating the source-observer distance [12]. The relations between lightning and ELF noise levels on the global basis have been used to study the space-time dynamics of worldwide lightning activity [13]. ELF measurements can be used in the studies of TLEs (Two line element set) [14 - 16]. The field decomposition method was used in a spherical cavity by Kulak et.al [17] to determine the source observer distance, by separating the resonant field from the traveling waves. Dyrda et.al [18] studied the African thunderstorms by solving the inverse problem and by using the SR power spectrum templates derived analytically. They calculated the distances to the most powerful thunderstorm centers and presented the simplified 1-D thunderstorm lightning activity 'maps' in absolute units C^2m^2/s. Schlegel et.al [19] showed the influence of solar proton events as an increment in frequency, Q-factor and amplitude of the SR modes. SR has also been used for the earthquake precursory studies [20 - 22]. Nickolaenko and coworkers computed the idealistic and realistic radio signals in the frequency and time domains and

discussed features significant to the Earth-ionosphere cavity with low losses for the discrete ELF transients (Q-bursts) considering the special model of atmospheric conductivity [23 - 24].

The waves in the range of 3–30 kHz, called Very Low Frequency (VLF), can propagate throughout the globe at a large distance. VLF signals generated over the globe from different natural sources (mainly due to lightning) are known as sferics. Some VLF waves can penetrate into the ionosphere from the thundercloud top when the incident angle becomes less than the critical angle. This mode of propagation is termed as whistler. Lightning whistlers are originated from lightning discharges and propagating along the geomagnetic field lines without appreciable attenuation reach the opposite hemisphere and whistler-mode waves are generally from the magnetospheric origin. The whistler waves achieve energy coupling between the lower atmo- sphere (troposphere) and the magnetospheric altitude, initiated by thunderstorm and lightning discharges. Very large amplification (40 to 60 dB) of the primary whistler wave occurs during the process of cyclotron interaction with energetic electrons in the Earth's magnetosphere [25 - 27]. As the wave propagates through the ionized medium embedded in the geomagnetic field, it is dispersed and a particular form of whistler spectrogram is obtained in the time-frequency domain. VLF whistlers having spectra of different shapes are also observed; these are broadly classified as hiss or unstructured emissions characterized by continuous band-limited signal producing a hissing sound, or chorus of structured emissions exhibiting coherent discrete spectra including periodic emissions, quasi-periodic emissions and triggered emissions [28, 29]. As the main energy source of whistlers are lightning discharges during thunderstorm, it can provide us with information regarding the occurrence of thunderstorm and lightning in the conjugate hemisphere of a particular longitude as well as the disturbance in the geomagnetic field lines at the magnetospheric altitude, i.e., geomagnetic storm. The impacts of extra-terrestrial

activities like solar flares, CMEs, Sunspot number variation and meteor showers can be investigated through the study of whistlers. Anomalous detection of whistler signals at low latitudes during the occurrence of earthquakes shows significant interest for the precursory study [30] .

Some fixed frequency man-made VLF signals are also transmitted from different stations like Alpha, VTX, NWC, NPM etc. for the global navigation system, detection of ionospheric irregularities and various other purposes. The intensity and phase of these signals are modulated by the waveguide characteristics, i.e., reflection height variation, dielectric constant of the medium etc. [31]. Different geophysical events, e.g., earthquake, thunderstorms and lightning, meteor showers etc. modify the earth-ionosphere cavity by introducing huge energy which contributes additional ionization in the lower-ionospheric region. Thus the waveguide characteristics like reflection height, dielectric permeability etc. are changed by different natural sources. During the lithosphere ionosphere atmosphere (LIA) coupling, through the simultaneous effects of (1) chemical channel, (2) wave channel and (3) electric field channel, the seismic energy transport to the ionospheric height can modify the waveguide characteristics by extra ionization [32]. The lithosphere ionosphere atmosphere coupling will be discussed in detail in Sect. 4.5.5 later. It produces the seismo-induced ionospheric instabilities and modifies the charge density distribution which changes the reflection height and perturbs the over-horizon radio wave propagation within the earth-ionosphere waveguide [33, 34].

Solar X-rays ionize the ionospheric layers on a regular basis and over the solar cycle but a kind of inhomogeneity can arise due to unequal extra ionization in different layers during solar X-ray flares (SXF) and solar proton events (SPE). Thus the flares and astronomical events like gamma ray flare modify the ionosphere and are detected by the sub-ionospheric VLF propagation and ELF waves [35,36]. Protons with energy up to 100

MeV are most often emitted from the Sun in conjunction with solar flares which can penetrate deeply into the *D*-region nearly 40 km and can cause additional ionization leading to conductivity changes thereby modifying the SR parameters [37 - 42]. Meteor showers also introduce perturbations in ion composition, temperature and other physical parameters within the ionospheric medium at different altitudes extending from the *D*-region to the ionospheric altitude [43 - 46].

In this work, we discussed about different sources of noises regarding different geophysical and extra-terrestrial events, which introduce some perturbations in the waveguide characteristics and generate some anomalous signals, such that we can identify the nature of perturbation for a particular event. In Section 4.5, we studied the effects of different events on the Schumann resonance signals with the historical point of view along with remarkable findings of some reputed researchers. Section 4.6 discusses the similar approach for the VLF radio wave for the natural as well as man-made transmitted signals in terms of the variation of waveguide characteristic and noise generation. A conclusion regarding this study has been presented in Sec 4.7. Unique signatures of some specific events may also be identified through regular monitoring of these signals associated with simultaneous events and their cross-correlation.

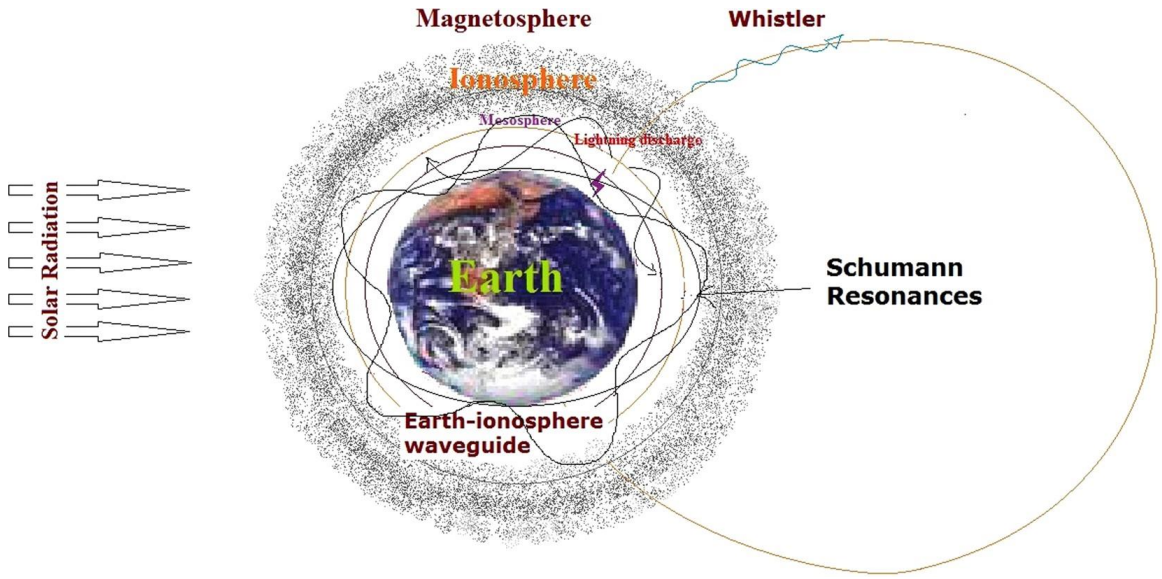

Fig. 4.1 Model diagram of the Earth-ionosphere waveguide

4.2 Atmospheric layers and waveguide:

A brief overview of atmospheric layers and the earth-ionosphere waveguide with a model diagram is given in Fig. 4.1. The troposphere extends up to 12 km on average from the ground surface, 9 km at pole and 17 km at Equator with some variations. All kind of meteorological phenomena, e.g., thunderstorms and lightning, wind and rainfall occur in this spherical shell. 80 % of the total atmospheric mass 5.1480 x 10^{18} kg is present in this zone. Upper boundary of the troposphere, where an abrupt change in lapse rate usually decreases to 2 °C/km or less is called tropopause. Stratosphere starts from the top of the troposphere, i.e., tropopause and extends up to 50 km altitude. The altitude span of the mesosphere 50–85 km is basically the *D*-region of ionosphere. Different transient luminous events (e.g., elves, red sprites etc.) predominantly occur in this altitude during severe thunderstorm. All meteors of mass <50 kg break apart and dissipate energy in this zone. The spherical shell of the atmosphere ionized by the solar X-ray and γ -ray radiation in the range of 50–1000 km altitude is called the ionosphere. Below this altitude medium is ionized only by highly energetic galactic cosmic rays. The ionosphere consists of different layers, viz., D-layer (60–

90 km), E-layer (90–120 km), E_s-layer, F-layer (120–500 km) and above this is the topside ionosphere. The day side F-layer is sub-divided into F_1 and F_2 layers. The space above ionosphere around the planet, where magnetic field lines are dominant is called the magnetosphere which is controlled by the planet's magnetic field. The solar wind is primarily responsible for the teardrop shape of the earth's magnetosphere which prevents most of the particles from the Sun from reaching the earth. In the day side atmosphere the magnetosphere extends up to 10 R_E (Earth's radius) whereas for the night side it extends up to 100 R_E. Various literatures are available regarding the magnetosphere of the earth [47 - 49] and references there in. The medium confined within the spherical shell between the conductors, i.e., Earth surface and lower boundary of the ionosphere (50–60 km altitude) is dielectric in nature, and eventually becomes a spherical waveguide for the low frequency radio wave.

4.3 Thunderstorm and lightning:

The thunderstorm is the main process through which charge separation occurs in the troposphere under all circumstances which produces stratified charge distribution in the different layers and creates different charge centres. Electrical discharges occur between these opposite polarity charge centres in the form of lightning. Numerous processes operate synergistically within the environment of a mature convective cloud, and different processes with varying effectiveness and time-dependencies affect cloud electrification [50 - 55].

The charging of thunderstorms takes place via inductive or non-inductive process. An inductive charging process requires pre-existing electric fields to induce charges on a particle so that when it rebounds from another charged particle charge gets separated and the field is enhanced. The another electric field resulting from positive charges in the atmosphere and negative charges on the ground could be considered as the pre-existing field which has been verified by laboratory experiments [56].

Non-inductive processes are independent of external electric field(s) and are based only on a collision mechanism between graupel with cloud-ice particles and the selective transfer of charge of a certain polarity to the larger particle. This mechanism is dominant in the charging of thunderstorms [57]. In an ordinary thundercloud, the smaller ice crystals are charged positively and move upward, whereas larger graupel particles charged negatively descend down relative to the smaller particles. Depending on the prevailing conditions of temperature, liquid water content and mixing in the thunderstorm this is the normal situation. A variant of this situation may lead to the reverse condition. Charging of solid particles can engage triboelectric charging by fractoemission and photoelectric charging, as discussed in detail in this article [59]. The presence of soluble ionic substances in the liquid and ice phases have a significant effect on the charging processes and may significantly alter the outcome of particle interaction and the charging processes. In the non-inductive mechanism, Saunders [59] has discussed drop break up, ion charging (atmospheric ions produced by cosmic rays, or radioactivity) and convective mechanisms, etc. Macgorman and co-workers [60 - 62] recommended in other cases that the small fraction of flashes striking ground was caused by a severe storm's very strong updraft. The strong updraft lifts the formation and growth of the frozen hydrometeor charge carriers to higher altitudes than usual height of storms, and causes the resulting charge to remain relatively high for a substantial period. It has also been noted that cloud-to-ground lightning creation may be inverted in severe storms by the time required to form and bring downward the precipitation carrying the low-level charge region that is needed to initiate lightning from the mid-level oppositely charged region [60 - 62].

Additional electrification due to tall updraft pulse which modifies the timing of major inflections, peaks or minima in lightning flash rates of the storm in general can depend on the competing affinity from the co-evolving updraft and downdraft formations in different regions of the storm. Eventually the tendency of increasing electrification during precipitation growth in the mixed phase region appears to be the circumstances in which the

surface of frozen precipitation becomes wet. Thus, while a large and rapid increase in lightning flash rates reliably indicates the growth of a storm through and above the mixed phase region whereas decreasing storm flash rates do not necessarily imply that updrafts or storms are in steady state or weakening [63].

4.4 ULF waves:

EM waves with frequency <3 Hz is the ultra low frequency (ULF), predominantly radiated by CG lightning discharges and propagate to a long distance due to huge charge transfer. Attenuation of this signal in the waveguide is very low. They can be recorded from remote places by any receiver with very low cut-off frequency, e.g., Fluxgate magnetometer, Induction coil magnetometer, Pulsation magnetometer etc. As the attenuation is the lowest for this signal frequency, more promising result may be obtained from the above scientific research.

4.4.1 Ionospheric Alfvén Resonator (IAR) and Spectral Resonance Structure (SRS):

The electron density fluctuation with altitude in the upper ionosphere is appropriate for establishing a resonator for the shear Alfvén waves in the range of 0.1–10 Hz [64]. The 'walls' of the ionospheric Alfvén resonator (IAR) can be the *E*-layer and the electron density gradient above the maximum of the F-layer. The lower boundary of the ionospheric Alfvén Resonator (IAR) coincides with the lower ionospheric boundary, whereas the upper boundary extends up to the altitude of a few thousand of km due to partial reflection of Alfvén waves from a steep gradient of the vertical Alfvén velocity profile $V_A(z)$ above the maximum of F-layer. The ionospheric cavity with minimum of $V_A(z)$ works not only as a resonator for Alfvén waves, but also as a waveguide for the magnetosonic mode. The idea about this resonator referred to as the ionospheric Alfvén resonator (IAR) was first suggested by Belyaev et.al [65] and developed afterwards by Polyakov et.al [66]. Alfvén velocities are several orders of magnitude smaller than the velocity of light and at a height of typically 3000

km (where an Alfvén velocity maximum exists) this velocity changes with height and enough reflection of the wave takes place. The Spectral Resonance Structures (SRS) are the comb-shaped spectra which are frequency domain representation of IAR oscillations on the ground surface generated under the lightning discharge. SRS, the unique signature of IAR spectra, are the background electromagnetic noise in the frequency range of 0.1–4.0 Hz. Detection of SRS in the spectrogram of ULF signals up to 4 Hz recorded at Sodankylä Geophysical Observatory (SGO) for two successive days indicated by the black bar are shown in Fig 4.2 [67]. The large Alfvén velocity gradient performs as the upper boundary of a cavity at this height region; whereas the lower boundary is formed in a similar way at the lower side of the F-region. The Alfvén velocity again shows a large gradient at the electron density peak at the F-layer as Shear Alfvén waves and may get trapped within the cavity in the form of standing waves. Thus the idea about this resonator subsequently referred to as the Ionospheric Alfvén resonator (IAR). Nowadays, geophysical importance of this phenomenon goes far beyond the primary effect. We already have many applications of IAR and it plays an important role in large collection of phenomena where the ionosphere-magnetosphere coupling is significant [68 - 73]. The waveguide magnetosonic modes excited by the

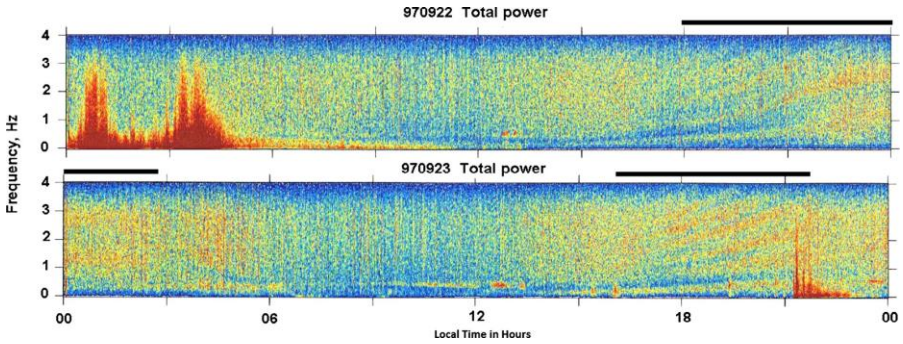

Fig. 4.2 Detection of Spectral Resonance Structure in the time interval indicated by *black bars above* the spectrograms recorded at Geophysical Observatory Sodankylä (SGO) for two successive days (Yahnin etal. 2003) [67].

magnetospheric [74] or atmospheric sources [75] can propagate to large distances (up to a few thousand of km) through the ionosphere. The ionospheric wave guidance manifests itself as an occurrence of low-frequency cut-off corresponding to the waveguide critical frequency (lower than the IAR fundamental frequency). The damping rates and Q-factors of the IAR modes depend strongly on the Alfvén velocity differential in the upper ionosphere (120–400 km) as well as on the lower ionospheric (nearly 40–100 km) conductivity. This concept was accepted theoretically [64 – 66,76,77] and it motivated experimental investigations of the resonator effects. The experimental efforts give way the finding of the resonance structures in the spectra of the electromagnetic noise of ground-based observations in the ULF range [78]. ULF noise enhancement (ULF-burst) associated with local lightning transients in the frequency range of few Hz to several Hz in the thunderstorm proximity was observed [79]. A fundamental night time feature (observed between 1900 and 0500 LT) of the geomagnetic field variations in the ULF band just below the first SR mode is the occurrence of Spectral Resonant Structure (SRS), observed at low [80], middle [76] and high latitudes [67]. The occurrence of SRS was commonly attributed to the Ionospheric Alfvén Resonator (IAR) in the upper ionosphere [81]. The lowest frequency of the SRS was about fraction of Hz, and the difference between the equidistant spectral harmonics was about 0.3–0.5 Hz. A prominent seasonal fluctuation is observed in the SRS modes, which was the maximum during the period of September–January and was almost completely absent during spring-early summer time [82, 83].

The world thunderstorm centres were suggested to be the primary sources of the IAR excitations [84]. However, it's been theoretically estimated that the electromagnetic field intensity in the IAR band is about one-two orders of magnitude less than the observed value at the mid latitude. This is due to the contribution of typical charge moments of negative CG flashes of the distant world thunderstorm centres [85]. It was suggested that thunderstorms

are able to excite the IAR with sufficient intensities [86]. Another possible source for IAR excitation is the generation of the ionospheric turbulence and currents by the neutral wind in the lower ionosphere where some part of neutral gas kinetic energy can be transferred into the electric current in the conductive ionosphere and converted into the energy of Alfvén and fast compression MHD modes [87]. The IAR resonance cavity occupies a space bounded from below by E-layer at 100 km and from above by a zone located at an altitude of about 500–2000 km in the F-layer, where the plasma density and Alfvén velocity change abruptly. It is the excitation due to electromagnetic emission stemming from global thunderstorm activity. The spectral resonance structure (SRS) due to IAR formation has been identified in the ground-based observation in low latitudes [84, 88]. The radiation energy from the lightning excitation introduces into the IAR and modifies the SRS. The mechanism of the SRS formation is not related to the oscillatory response of the IAR, but the specific multi-phase structure of geomagnetic disturbances during lightning activity [89]. A theoretical investigation is described by using numerical approach during the presence of main magnetic inclination signatures in the spectral resonance structure (SRS) of IAR [90].

4.4.2 ULF signal and earthquake research:

It has been found that emissions in the ULF band are more convincing precursors of earthquakes in comparison with higher frequency band owing to its inherent characteristics of large skin depth, less contamination, and low attenuation involved [91]. One to two hours before the occurrence of Great Alaska earthquake (*M* 9.2) on 27th March, 1964, strong ULF electromagnetic field disturbances at Kodiak observatory had been observed [92]. Remarkable change in the ULF signals was detected which started about 14 days before the vast Loma Prieta earthquake in the year of 1989 (*Ms* 7.1) in the USA. They also observed a prominent increase around 4 o'clock prior to the main shock which continued even after the event. Simultaneously, seismo-electromagnetic phenomena are also observed in different

frequencies ULF-ELF-VLF by many workers [40,41,93 – 97, 98 - 100].

The ULF resonances in the H-component in the narrow frequency bands f_{R2} 10.2–11.1 mHz and f_{R2} = 13.6–14.5 mHz have been observed at the Teoloyucan magnetic station two weeks to one month prior to some earthquakes during 1999– 2001 and also for the volcanic activity at Tlamacas station during March–July, 2005 [101].

Discrete packets of ion cyclotron waves are generated in the equatorial region of the magnetosphere and bounce between conjugate ionospheres; penetrating partially into the lower atmosphere to be observed on the ground, known as Pc1 pulsations. Changes in the resonance properties due to the earthquake of two complex processes (Pc1 and SRS oscillations) are the main reasons for the signal anomaly during the seismic hazards [102 - 104]. Different types of IAR response to seismic effects have been found for remote earthquakes [103]. According to the Geophysical Observatory Borok (58.0°N, 38.2°E) data, it has been discovered that ionospheric Alfvén resonances (IARs) observed as geomagnetic pulsations at frequencies of a few Hz arise in response to seismic events. The different ways of affecting the IAR regime by seismic waves and corresponding possible mechanisms of this effect are discussed elsewhere [102].

Hayakawa et.al [105] observed ULF magnetic field variations before great earthquake at Guam, 1993 (M*s* 8.0) at an epicentral distance of 65 km and suggested to analyze the polarization ratio R Z/H (Z and H are vertical and horizontal field components respectively) in frequency band 0.01–0.05 Hz. They also found that polarization ratio increased about 1 month before that earthquake but returned to the normal level after the event. Later they analyzed the data once again and showed that the slope of the ULF spectrum (fractal number) also changed before the earthquake. Hayakawa, Hattori et.al [106, 107] reported their observations of ULF magnetic variations around the date of two large events at Kagoshima in 1997 (M 6.5 and M 6.3) at a distance of about 60 km from both the

epicentres and also found the polarization ratio to increase about 1 month prior to the date of events. Hobara et.al [108] applied the same data analysis technique (polarization method) to ULF magnetic data for three different earthquakes and compared the results. Then simple current models were suggested for each earthquake [108]. Kopytenko along with his co-workers observed ULF magnetic field variations related to the earthquake swarm during June–July 2000 with strongest earthquake of magnitude 6.4 (in the middle of the swarm) where epicentral distances were around 70 to 150 km from the network of stations situated in the Izu and Chiba area of Japan [307]. They paid main attention to the polarization ratio near frequencies F_1 = 0.1 Hz ± 0.005 Hz, F_2 = 0.01 Hz ± 0.005 Hz and F_3 = 0.005 Hz ± 0.003 Hz and observed Z/G ratio anomaly in a frequency range F_2 for the night time intervals (00:00– 06:00 LT) began to increase one and half months before the period of the seismic activity. Interestingly they detected sharp increment in $R(F_3)/R(F_1)$ ratio just before the onset of the strong seismic activity.

Some efforts have also been made to utilize ULF data for direction finding of the emitted signals from epicentre regions [104,109,110] detected signal enhancement in wavelet analysis around 2 Hz and 7–8 Hz for the large India-Pakistan border earthquake. Their polarization ratios also indicated the origin of signal was from beneath the ground. A sudden decrement (67 %) of the cross-correlation values of the amplitude between (0.1–0.01 Hz) and (0.01–0.001 Hz) frequencies, during some seismic events (M > 5) within the period of September, 2010 to March, 2011 has also been observed [111].

4.5 ELF waves and Schumann resonance:

The spherical cavity and lower ionosphere acts as a resonator in which the standing electromagnetic waves between the Earth's surface are generated due to excitation energy from lightning. The resonance occurs when the wavelength is of the order of the dimension of the resonator. The observed discrete peak frequencies are 8, 14, 20, 26 . . . Hz in the ELF

range. Winfried Otto Schumann first theoretically predicted this electromagnetic resonance phenomenon in 1952 and calculated their eigen frequencies in the spherical Earth-ionosphere cavity as 10.6, 18.4, etc . . . Hz [2]. The characteristic Schumann resonance spectra shown in Fig.

4.3 were recorded at Kolkata on April 2, 2000 [112]. A modified formula for eigen frequencies within the Earth-ionosphere cavity is given by $f_n = \frac{c}{2} n(n-1)$ according to Schumann's formula where *n* is the mode number [24] assuming the earth and the ionosphere to be perfect conductors and the space between them is vacuum.

The experimental evidences of this phenomenon came later, with subsequently developed more realistic analytical models taking into account the inhomogeneities due to asymmetry of the day-and night-time ionospheres, variations of conductivity of the ionosphere, the distribution of sources etc. However, these factors in the lower ionosphere

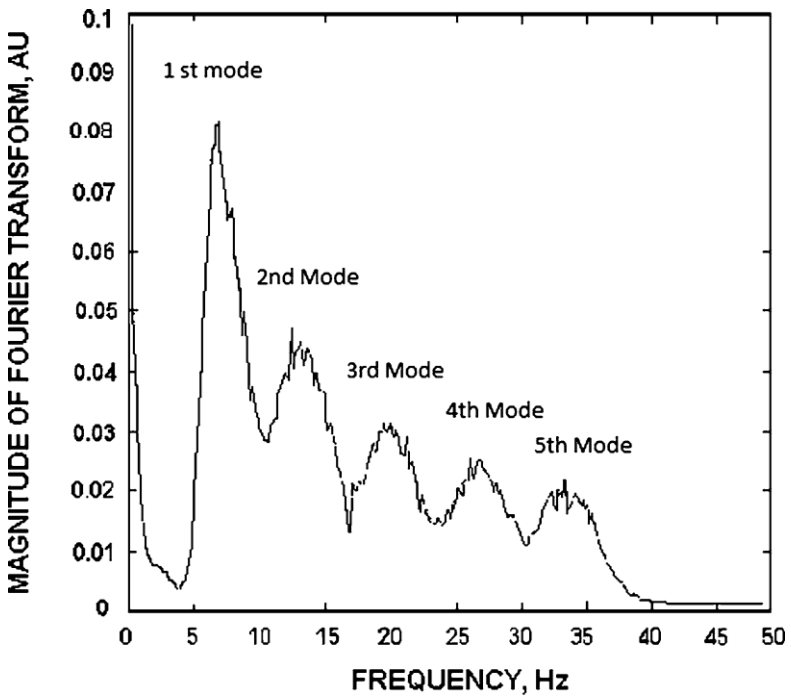

Fig. 4.3 Frequency response of Schumann resonance signal recorded at Kolkata on April 2, 2000 [112].

have relatively small influence over the resonance frequencies to decrease to the experimentally observed value. The fact that the observed frequencies are 8 Hz, 14 Hz etc. instead of 10.6 Hz, 18.4 Hz etc., is primarily due to the low propagation speed of radio waves in the Earth-ionosphere cavity compared to that of light in vacuum. Hence the observed peak frequencies are lower than the eigen frequencies for a perfect cavity. The ratio of velocity of propagation in vacuum and within the waveguide is (c/v) 1.36 at 10 Hz [1]. Considering this velocity ratio the calculated resonant frequency will be reduced to the observed SR peak frequency at the Earth surface. Different aspects of Schumann resonance phenomenon as well as their observation and measurement techniques are presented by different workers, e.g., SR signal as the global thermometer [16]; for the detection of upper tropospheric water vapor content [114]; detection of pre-seismic anomalies during large earthquakes [115, 116] etc. Some frequency changes about the peak values and some amplitude changes were found to be present in the observed spectra, which may be attributed to the uncertainties arising from spatial distribution of lightning sources exciting the SR modes [117].

The diurnal variation of peak frequencies and amplitudes of different modes were utilized to know (i) the characteristics of global thunderstorm activities, and (ii) the electron number density of the ionosphere. The seasonal and day-to-day variability of SR intensities, frequencies, line splitting and quality factors have been reported by many authors along with the possible explanations for such changes [3,12,118,120,121,177,178]. Schumann resonance frequency variations have been established as an indicator of the thunderstorm distribution over the globe [123]. Both linear and non-linear combinations of average power spectra of electric and magnetic fields are used successfully in the solution of the inverse problem [8,124].

After 1990s the scenario with these sub-ionospheric ELF waves changed and several new applications of SR emerged.

4.5.1 Global thunderstorms and lightning activity:

The SR intensity records are used to estimate the level of global thunderstorm activity. Balser et.al [125] suggested the variations of SR frequency to be related to the global thunderstorm distribution. From the records of SR background, the diurnal, seasonal and annual variations of the global lightning activity may be estimated [126,127]. A new ELF observation station is setup in Kagoshima, Japan in addition to the existing one in Moshiri Hokkaido, to establish the network observations of ELF transients and to deduce the detailed spatiotemporal lightning distribution with Charge Moment Change (CMC) around Japan and Asian region [128]. This was the first attempt to use an ELF network observation with separation distance of few thousand km scale applied to a rather small area to deduce more precise determination of both location and Qds of lightning discharges in comparison to the previous works for worldwide detection of very energetic lightning with a large locating error (500 km) [128]. Intensive lightning locations with CMC information are very useful for the several new spacecraft missions to monitor TLE with intensive lightning discharges from the space by Japanese ISS (Inter- national space station), GLIMS and French Micro Satellite TARANIS [128].

4.5.2 Tropical surface temperature of the earth:

The power in the lower SR mode of 8 Hz has been noted to correlate with the global temperature changes [16]. It has been observed that the SR increases with temperature on a global tropical scale consistent with the observed sensitivity of lightning to temperature in local measurement. Specific linkage between SR peak frequency values with global and regional temperatures is well known. The variation of SR peak frequency has been proved to be useful to indicate the variations in the tropical and global temperature [129]. The seasonal

migration of tropical thunderstorms along the meridian triggered by tropical temperature changes has been investigated [130]. A comparison between SR intensity data and the ground surface temperature (GST) data has been studied in Japan at different latitudes during the period 1999–2002. Sekiguchi and Hayakawa and co-workers [131,132] have made a quantitative comparison of temperature and electromagnetic data for 43 months long and used cross-correlation coefficient to evaluate their linear connection. A satisfactory positive cross-correlation was also found for SR intensity with the ground surface temperature data for the low latitude region at Agra, India [133].

4.5.3 SR for climate research:

Large amount of water vapor is transported into the upper troposphere due to continental deep convection. This water vapor is the key element of Earth's climate. It has direct impact as a greenhouse gas as well as indirect effect through interaction with cloud, aerosols and tropospheric chemistry for the generation of the charge centres. The relatively small amount of water vapor in the upper troposphere has a large impact on climate variation [134]. The retrieval of upper tropospheric water vapor concentration can be achieved through the continuous magnetic intensity measurements of SR spectra. Due to the presence of water vapor with some Aitkin particles through the formation of graupel, there is more charge separation at the expense of thermal energy and thereby producing stratified charge centres. Instantaneous discharge processes between opposite charge centres will emit EM radiation during the process of recombination of charges. This excess EM energy from the tropospheric zone will influence the SR magnetic records in a varying manner depending upon the intensity of the charge separation process.

It is known that ELF data, NASA water vapor project and upper-tropospheric water-vapor (UTWV) data are in good agreement with each other (correlation coefficient, r 0.76) [114]. The sensitivity of this relationship implied that for every 0.25 mm increase in UTWV

(1% of total column), the ELF signal increases by approximately 25%. A relatively simple and inexpensive method for continuous observation of global lightning variability is the use of the Schumann resonances. Thus monitoring of SR signal may provide a tool for time-tracking of the upper-tropospheric water-vapor changes which will be made useful to the processes involving climate change. That is, SR data → water vapor content → climate forecasting.

4.5.4 Solar terminator effect:

Significant solar terminator effects are found in SR magnetic and electric field characteristics [135]. The larger the area coverage by the ionospheric disturbances, the greater is its influence on SR characteristics. Thus, from the nature of variation of SR characteristics, the vastness of the magnitude of disturbance of solar terminator time can be determined. Hence, lateral ionospheric gradients across the terminator region have sufficient influences on ELF wave propagation along with the diurnal-seasonal lightning sources [136]. Effects of the solar terminator time on the diurnal frequency variation of Schumann resonance frequency had been studied at Garhwal Himalayan region, India, during March 10–May 23 in 2006 [137].

A general approach suggested by Madden et.al [138] based on the analogy between ELF propagation within a waveguide and wave propagation in a transmission line with two dimensional telegraph equation (TDTE) technique, has been developed later on by Kirillov et.al [139] where TDTE allowed incorporation of any conductivity profile. Mushtak et.al [140] introduced the 'knee' approximation on the basis of the TDTE formalism to obtain both realistic resonance frequencies and quality factors which overcomes the shortcoming of the two-exponential approach.

Pechony and Price [143] combined both the partially uniform global model developed [141] for the day night asymmetry with the 'knee' model by [140] into a partially uniform knee (PUK) model [142]. Further, it has been extended to a 'multi-knee' approximation by introducing additional 'knees' to the profile, in order to allow assimilation of different ionospheric profiles for modeling SR on other planets. As a result very flexible model with an easy switch from 'uniform' to 'day-night' model has been developed, allowing incorporation of structured conductivity profiles and a convenient treatment of the day-night asymmetry [143].

4.5.5 Schumann resonance for earthquake research:

In contrast to the direct method, e.g., observation of ULF/ELF emission at Nakatsugawa in Japan (35°25′N, 137°32′E) in Gifu Prefecture near the foot of Mt. Ena, the anomalous excitation of the Schumann resonance possibly associated with the 1999 Chi-Chi earthquake in Taiwan [142], is the indirect method. After that, some anomalous excitations of Schumann resonances before large earthquakes like Mid-Niigata Prefecture earthquake (2004), Noto-Hantou earthquake (2007, M 6.9) in Japan have been reported by Ohta et.al [142]. Anomalous Schumann resonances appearing in the background noise of the observations have been found in the analysis of ULF/ELF electromagnetic radiation data recorded before earthquakes in Japan and this anomalous Schumann resonance has a good correlation with seismicity [144]. They made a statistical analysis for 13 earthquakes with M 5.0 occurring in the Taiwan region during the period of 1999–2004 and found that the corresponding Schumann resonance anomalies were observed prior to all land earthquakes. Using Schumann resonance observations recorded at Nakatsugawa station of Japan, Hayakawa also found prominent anomalous Schumann resonances prior to the 4 groups of earthquakes of $M \geq 5.0$ in Taiwan in 1999 [144,145]. The spectral analysis of Schumann resonances of 13 earthquakes with $Ms > 4.0$ occurring in Yunnan from August, 2010 to June,

2011, indicated some positive signatures of pre-earthquake SR anomalies [22]. Figure 4.4 depicts SR anomalies before the Yingjiang earthquake on March 10, 2011 of M = 5.8 recorded at Yongsheng station [22]. Primarily the mechanism of anomalies of SR signals are: i) change of ionospheric height, i.e., height of the upper layer of the earth-ionospheric waveguide and the dielectric property of the medium contained within and (ii) generation of ELF signals and its influence on the SR signals from other sources. Three main physical mechanisms are there to perturb the ionosphere, lithosphere atmosphere ionosphere coupling due to the simultaneous effects of :- (1) chemical channel, (2) wave channel and (3) electric field channel. A possible mechanism is the development of micro-cracks, fluid penetration and stress change etc. which release different kind of greenhouse gases: methane, radon, helium, hydrogen, and carbon dioxide. This leaking from the crust can serve as carrier gases for radon including underwater seismically active faults due to the relative movement of tectonic plates and blocks of different sizes. These greenhouse gases can produce thermal anomalies in the atmosphere [32]. This thermal anomaly produces atmospheric turbulence and instability which generate Atmospheric Gravity Waves (AGW) with periods in a range of 6–60 min. This seismo-induced AGW mainly modifies the ionospheric instabilities and charge density distribution which changes the reflection height and thereby perturb the over-horizon radio wave propagation within the earth-ionosphere waveguide [32, 145-148]. Due to the friction and the attraction forces of small ions to the dust and aerosol particles during its breaking before the occurrence of seismic activity, the dusty aerosol particles become charged. Emanation of energetic radioactive radon during the seismic activity ionizes the lower atmospheric particles which enhances the lower atmospheric conductivity and modifies the atmospheric ion density. Thus it behaves like an electric channel in the Lithosphere-Atmosphere-Ionosphere coupling [32, 149]. Thus the reflection height as well as dielectric constant of the waveguide is changed due to pre-earthquake anomaly.

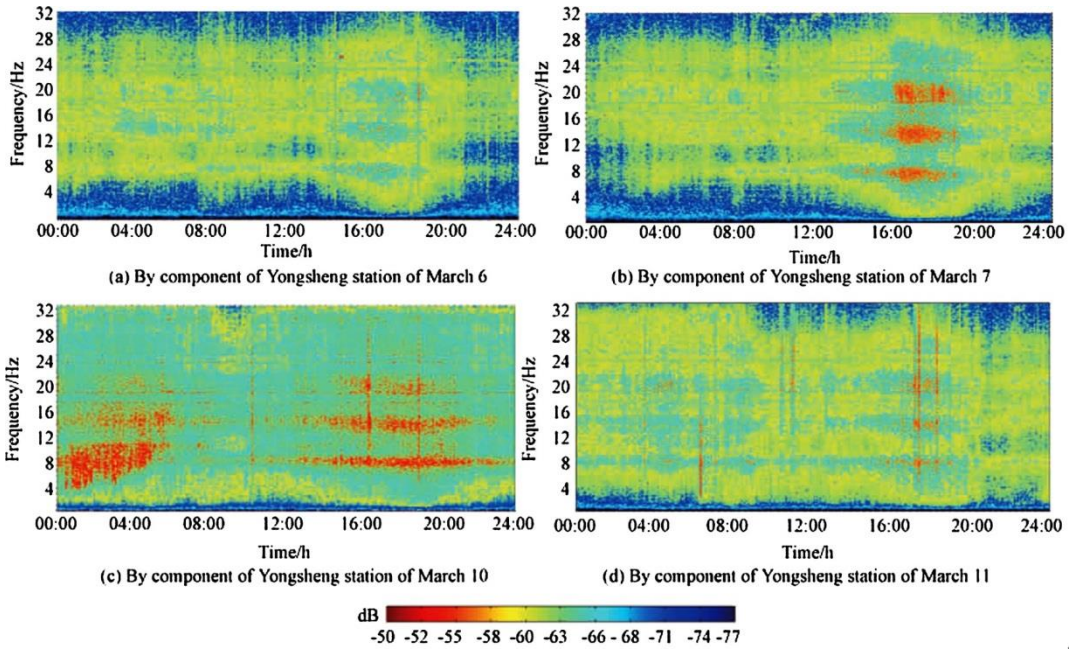

Fig. 4.4 Fig. 4.4 : Detection of pre-seismic ELF EM anomalies in the *By* component of Schumann resonance modes before the Yingjiang earthquake on March 10, 2011 of M = 5.8 recorded at Yongsheng station [22].

4.5.6 Solar Proton Events:

Schumann resonance frequencies are modified by the interaction of energetic precipitating particles within the lower ionosphere due to extra ionization. Solar proton precipitations cause the lower ionospheric boundary to move downward, e.g., lower ionospheric refection height decreases that manifests a change in the frequency of the first SR mode to lower values [150, 151]. A noticeable change, approximately 50 % of the mean on short time scale, in amplitude as well as in peak frequencies of the first two modes during the 30-min period γ-ray burst was observed. The normal variability of the peak frequency is about 0.5 Hz for the first mode and approximately 1 Hz for the second mode before, during and after the burst [152].

A change has been detected successfully in the Schumann resonance spectra during the intense γ ray flare SGR 1806-20 (27 December 2004), recorded at the Moshiri

observatory, Japan (44.365°N and 142.24°E) [153]. It was compared with the experimental records at the same observatory with the model calculated approximately for the parametric ELF pulse produced by the γ ray flare [154-156].

Inhomogeneity can arise due to unequal extra ionization in different layers during solar X-ray flares (SF) and solar proton events (SPE) [157]. The variation in the first and second mode Schumann resonance frequencies occurred during the intense solar X-ray burst by 0.2 Hz and 0.3 Hz, respectively [158]. The observed maximum of first, second and third SR mode frequencies during sudden ionospheric disturbance were 8.51 Hz, 14.71 Hz and 21.22 Hz respectively [159].

During solar activity, there may be two kinds of changes to the lower boundary of the Earth-ionosphere waveguide: (i) ionization enhancement at the normal *D*-region reflection heights, and (ii) the variation of *D*-region's lower edge [160]. According to the simplest vacuum model [32] the variation of the first SR frequency can be written as:

$$\nabla f_1 / f_1 \approx 0.36(\nabla N / 2N + \nabla h / h)$$

where f_1 is the first mode frequency, Δf_1 change in first mode frequency, N is the ion density and ΔN change in ion density, h is the ionospheric reflection height and Δh change in reflection height.

It is established that solar X-ray radiation causes extra ionization mainly in the height range of 70–80 km, whereas SPE can cause extra ionization up to the depth of 40–50 km. To explain the effect of this kind of inhomogeneity on SR, the two-layer waveguide model has been proposed by Dyrda et.al [159] for the lower layer $\sigma=\varepsilon_0\omega$, i.e., where displacement and conduction currents are equal to each other. The other, relatively upper layer is that at which $\mu_0\omega\sigma\zeta^2 > 1$ where ζ is the conductivity scale height at the altitude for reflection of ELF wave. The unequal ionization of these two layers by solar extra radiation, i.e., by both X-ray and γ -rays can give rise to vertical inhomogeneity which modifies the SR frequency. The SR

frequencies can be expressed as [159]. where n is the mode number (n = 1, the first harmonic is regarded here); c, the velocity of light; r_e, mean radius of the earth; h_1 and h_2 are the two characteristic heights in the *D*-region.

$$f_n = \sqrt{\frac{n(n+1)}{2\pi}} \frac{c}{r_e} \sqrt{\frac{h_1}{h_2}}$$

For n =1

$$f_1 = \frac{1}{\sqrt{\pi}} \frac{c}{r_e} \sqrt{\frac{h_1}{h_2}}$$

During solar flare, the lower height h_1 is almost unaffected because it causes extra-ionization mainly around 70 km, i.e., the reduced upper reflection height δ_2 modified the first SR frequency as

$$(f_1)_{SR} = \frac{1}{\sqrt{2\pi}} \frac{c}{r_e} \sqrt{\frac{h_1}{h_2 - \delta 2}}$$

and thus the first SR frequency increases. During Solar proton events, energetic protons can penetrate deeply into the ionosphere upto 50 km and possibly even deeper and can ionize regions lower than the normal *D*-region [160]. Thus, the δ_1 decrement over h_1 lower reflection height modifies the first mode SR frequency

$$(f_1)_{SRP} = \sqrt{1/\pi}\ (c/r_e) \sqrt{(h_1 - \delta_1)/h_2}$$

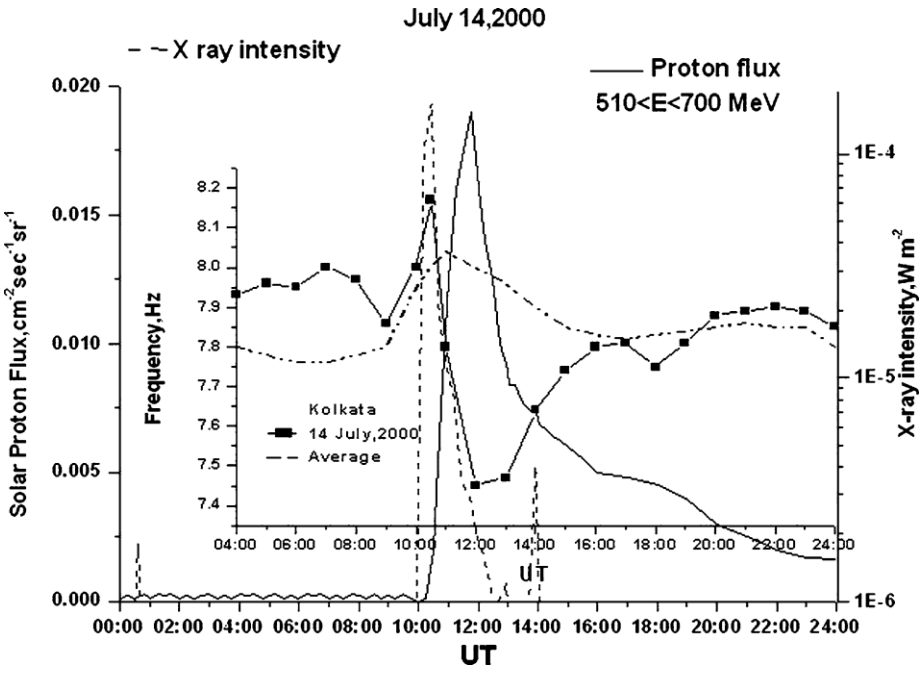

Fig. 4.5 Variation of the first mode SR frequency over Kolkata (22.56°N, 88.5°E) on July 14, 2000 depicted by the continuous line curve joining the square blocks. It is superposed on the curves for solar X-ray bursts and SPE. SR frequencies averaged over three days adjacent to the day of occurrence are shown by the dot dashed curve [40,41].

resulting in a diminishment of SR frequency. Variation of frequency for the first mode SR during solar flare on July 14, 2000, recorded over Kolkata is shown in Fig. 4.5 [40, 41]. In this figure, the continuous line curve joining with the square blocks indicates first mode SR frequency which is enhanced during the solar proton event. Immediately after this SPE there occurs a severe solar X-ray burst and during this X-ray flares first mode frequency decreases. This phenomenon has been justified in terms of extra-ionization at two different layers, 40–50 km for SPE and 70–80 km for X-ray flare. Figure 4.6 depicts the simultaneous frequency shifts of the first mode SR from different stations during the solar flares on the day of July 14, 2000 [40, 41]. For three stations Kolkata, Lovozero and Karymshino signal variations show similar trends that agree with the proposed theory.

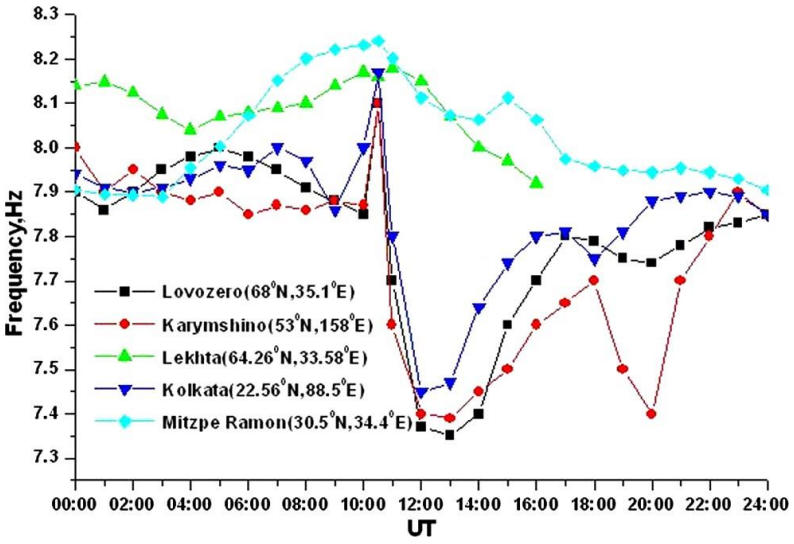

Fig. 4.6 Variation of the first mode SR frequency over different latitudes on July 14, 2000 [40, 41]

4.5.7 Meteor shower effect:

Meteor showers as another possible source of EM phenomena in the atmosphere have been debated for many years. Bright fireballs, theoretically, may produce ELF/VLF radio waves [161]. Many workers detected meteor responses in ELF/VLF radio waves, [161- 163] reported anomalies in the 1–10.5 kHz frequency range, associated with *m* 10–11 meteor. ELF/VLF radio emission has been detected during the 1998 and 1999 Leonid showers [164]. Also, a kind of signature has been pronounced in the 100 Hz–50 kHz frequency range for some faint meteors that could not be detected visually [163]. Meteor activity has been the focus in the 10 Hz–300 Hz frequency range, performed during the ESA 2001 Leonids campaign in Australia by Trautner et.al [165]. A remarkable increase of the electric field levels in the frequency range up to about 200 Hz was observed. The lower magnitudes for the higher frequencies indicate a 1/f envelope, which is characteristic for many natural signal sources. The signal level measured two hours before the Zenithal Hourly Rate (ZHR) maximum was exceeded by a factor of 7.6 at 14 Hz and by factors of 8.9 and 5.3 at 21.5

Hz and 59.2 Hz respectively [165]. Furthermore, the signal levels observed correlate well with ZHR rates measured independently.

4.6 VLF waves:

Maximum EM energy emissions from the lightning sources are predominantly occurring in the VLF range (3–30 kHz) [166]. Radio signals from lightning discharges (sferics) propagate in the Earth-ionosphere waveguide with low attenuation, typically 2–3 dB/1000 km [167]. The dynamic spectra of sferics are explained by considering the propagation through the Earth-ionosphere waveguide, where the *D*-region of the ionosphere acts as upper boundary of the waveguide. The VLF waves are mainly produced by the acceleration of charged particles inside the cloud due to lightning return stroke and provide useful information about the generation of lightning producing mechanism as well as information about the characteristics of the medium through which it is propagating [168]. VLF is also an interesting tool to detect anomalous signals from the natural lightning events and for the waveguide characteristics study. These emissions, being in the audio frequency range, can be converted to their corresponding audio outputs with suitable receivers. Depending on the characteristic audio sound generation for particular mode of propagation this natural signal is characterized as VLF sferic, whistler, Hiss, Chorus etc., some of which are from magnetospheric origin. The collected vertical electric field data are analyzed to derive information about the lightning discharges (source properties), propagation features and parameters of the medium through which the waves have propagated [169, 170]. Later on, the horizontal magnetic components of the wave fields were measured along with the vertical electric component. These measurements were used to determine the polarization and arrival directions of the waves [171] and are used to pinpoint where the down-coming whistler entered the earth-ionosphere waveguide [172]. Some works with sferics focused on the understanding of the delayed sferic component called a ‘tweek’. Recently Cannon and

their co-workers [173-176] proposed a method to estimate the effective ionospheric height of the Earth-ionosphere waveguide and the propagation distance of tweek atmospherics. Ohya et.al. [177] estimated equivalent night-time electron densities at reflection heights in the *D*-region ionosphere at low-middle latitudes by accurately reading the cut-off frequency of tweek atmospherics. Thus, sferics is a fruitful tool to estimate lower ionospheric electron density. It is also utilized in connection with the lightning centre detection.

4.6.1 Lightning centre detection by VLF sferics:

Many techniques have been employed for the detection and location of lightning discharges using satellite based as well as ground-based observations. The lightning imaging sensor (LIS) [178] aboard the TRMM satellite and its predecessor the Optical Transient Detector (OTD) [179] detected total lightning including both cloud-to-ground (CG) and intra-cloud (IC) lightning discharges using optical measurements. The stable propagation and low attenuation of VLF waves in the Earth-ionosphere waveguide (EIWG) allow a wide spacing of receiver sites of several thousand kilometres. Thus, true global location service may be provided by using only 10 receiver sites [180]. On the ground, many different methods of radiolocation of lightning have been implemented. To determine the location of the source lightning event, a single radio receiver can be used to locate intense lightning discharges at long range, by using the wave impedance of the lightning waveform for estimating the range to the lightning strike and by using magnetic direction finding to measure the arrival azimuth of the lightning strike [181]. Lightning discharges measured in this manner must be intense because a large ELF energy component, also called an ELF transient, is generally required for the range estimate [182]. The total amount of lightning activity present in a storm can also provide an estimate of the amount of convective rainfall in that storm [16, 183].

The VLF band is most commonly used for long range radiolocation of lightning due to the highly efficient propagation of VLF sferic energy in the Earth-ionosphere waveguide. The fact that the group velocity is close to the speed of light for low order modes at VLF frequencies and does not significantly vary with frequency (away from the cutoff regions) [184] further simplifies the analysis and TOA (Time of Arrival) estimations measuring the arrival phase delay between different VLF waves generated from the same lightning stroke using multiple stations. For example, using the equation for group velocity taken from Budden [184], V_{group} can be shown as

$$V_{group} = c \{1 - (f_n / f)^2 \}^{-½}$$

where, f_n is mode cutoff frequency.

For VLF propagation at 13 kHz, the difference in propagation time for daytime (60 km reflection height) versus night-time (80 km reflection height) for a 10,000 km path is 280 micro seconds, which would cause a smaller error than a one degree error in azimuth at 5,000 km. However, some techniques, such as those that rely on TOA measurements only, require more precise knowledge of the group velocity under various propagation conditions [180].

Using the arrival time difference as well as magnetic direction finding technique by widely spaced receivers (>9,000 km) researchers estimated the lightning discharge locations via triangulation for two receivers located at Palmer Station (64.77°S, 64.05°W) on Anvers Island off the Antarctic peninsula and on Vieques Island (18.12°N, 65.50°W) off the coast of Puerto Rico and calculated the azimuths of sferics originating in North America (10,000 km range) [185]. The results obtained by them, however, were plagued by ambiguities due to extremely distant locations of the receivers utilized. They compared arrival azimuth with flash level data from the National Lightning Detection Network (NLDN) and showed that 83.6 % of the cases matched the reported NLDN flashes to within 2 degrees. R.K.Said et.al [166]

developed a new paradigm for long range lightning detection and geolocation, through an extensive empirical cataloging of sferic waveforms from a variety of source locations and propagation path profiles. Several ground-based networks have been developed to determine the time and location of individual lightning strokes and flashes accurately using the characteristics of sferics, such as Lightning-Mapping Arrays [186], UK Met Office VLF system [187] and Los Alamos Sferic Array (LASA) [188]. Each lightning stroke location requires the time of group arrival (TOGA) from at least 5 WWLLN (World Wide Lightning Location Network) sensors. These sensors may be several thousand km distant from the stroke. The geographical arrangement of the sensors is important: a lightning stroke which is enclosed by sensors is much more accurately located than one which is not. Clearly a uniform spacing of sensors around the earth is the ideal solution. Since the earth is round, there are no edges: every lightning stroke is surrounded by sensors, but not necessarily by the sensors which sense it. Typically only about 15 to 30 % of strokes detected by one sensor are detected by 5 or more local centres. These strokes are usually the stronger ones. Recent research indicates that globally the detection efficiency for lightning strokes of about 30 kA is approximately 30% (http://wwlln.net/). It is also found that the obtained lightning source distributions both over the Pacific Ocean and the Sea of Japan are originated from the thunderstorm active regions confirmed by other measurements such as WWLLN [189]. Presently there are 40 WWLLN sensors, and they are in the process of expanding to 60 sensors shortly. To cover the whole world by sensors spaced uniformly about 1000 km apart would require roughly 500 sensors. If spaced 3000 km apart, we would need 'only' around 50 to 60 sensors and their working areas do not overlap (http://wwlln.net/).

4.6.2 Sferics for earthquake prediction:

Some investigators inferred that the ionospheric perturbation as detected by VLF-LF propagation may be a significant tool for short term earthquake prediction [190]. In case of

strong earthquakes, the atmospheric layer close to the Earth's surface becomes ionized and generates electric field which introduces particle acceleration thereby exciting local plasma instabilities [32]. Several days before the occurrence of the earthquake, the electron density of plasma in the upper ionosphere over the epicenter also increases abnormally [191]. Moreover, an interrelation between the tectonic activity and the anomalous changes of the geophysical, geochemical and geo-hydrological parameters characterizing the Earth's lithosphere has been noticed [192]. Electromagnetic anomalies (EA) preceding the destructive earthquakes in Greece covering a wide range of frequencies have been analyzed [193]. They are correlated with the fault model characteristics of the associated earthquake and with the degree of geotectonic het- erogeneity within the focal zone. The time evolution of sequences in EA revealed striking similarities to the acoustic and electromagnetic emissions observed in the laboratory [193].

Some significant spike observations in the 5, 7, 9 and 12 kHz VLF sferics signals recorded at Kolkata station (Lat. 22.56°N, Long. 88.5°E) during the Minahasa earthquake were made on November 16, 2008 at an epicentral distance of about 2400 km and have been analyzed [194] [195]. They observed similar spike signals in 6 and 9 kHz sferics for the India-Pakistan boarder earthquake of October 08, 2005 shown in Fig. 4.7. For this event spiky variations in the integrated field intensity of atmospherics (IFIA) at 6 and 9 kHz have been observed 10 days prior (from the midnight of September 28, 2005) to the day of occurrence of the earthquake on October 08, 2005 and the effect continued, decaying gradually and eventually ceased on 16 October 2005.

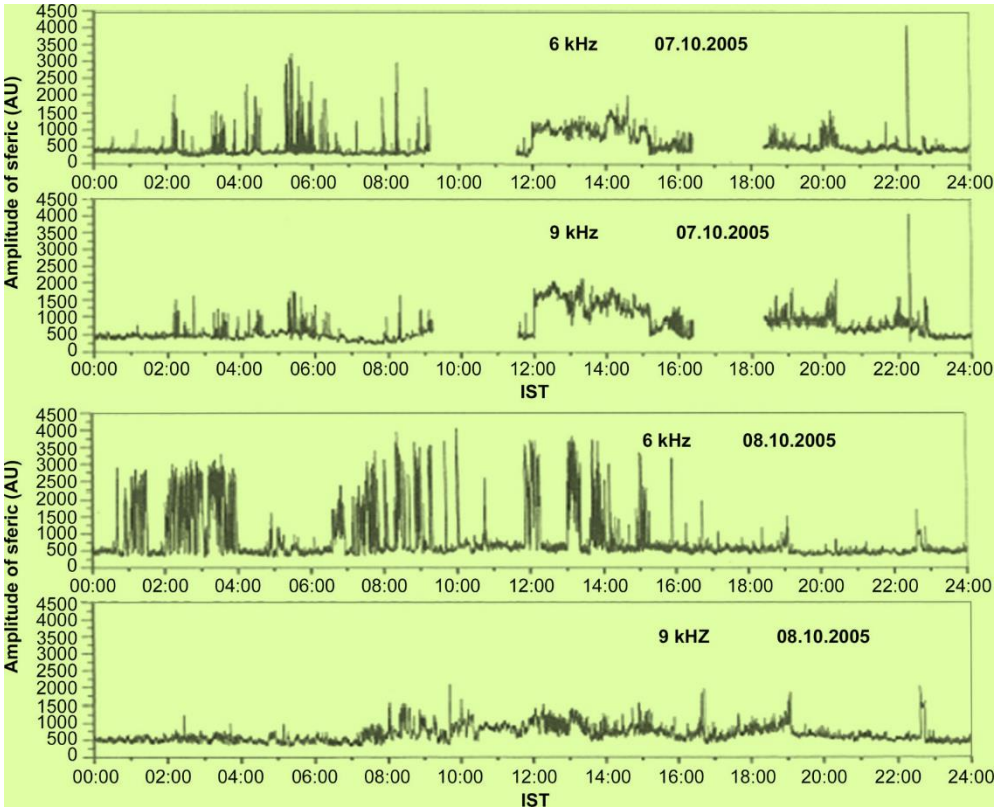

Fig. 4.7 Diurnal variation of sferics with spikes observed over Agartala on October 07 (upper two records) and October 08 (lower two panels) of the year 2005 [40,41].

Spiky nature of electromagnetic signals at 3 kHz frequency is detected which is similar to the VLF pre-seismic signals of Kozani Grevena earthquake. Spiky signatures of electromagnetic signals were also reported by Ohta et.al [196]. They observed ULF/ELF emission of spiky nature at Nakatsugawa observatory possibly associated with the ChiChi earthquake in Taiwan on 21 September 1999 (*M* 7.6). Similar records at VLF frequencies are also reported by Nagao and Izutsu and their co-workers [197,198] for the Hyogo-Ken Nanbu earthquake of 1995.

4.6.3 Whistler phenomena:

Major VLF energy, from the natural sources (mainly due to lightning and thunderstorms), trapped within the waveguide and simultaneously some part, beyond the thundercloud top, penetrates through the ionosphere with an incident angle less than the

critical angle and can propagate in the e-wave mode through the magnetosphere. This wave tends to propagate along the geomagnetic field lines without appreciable attenuation and reaches the opposite hemisphere. These whistlers are originated from the lightning discharges. Certain other types of whistlers generated in the magnetospheric region due to interaction of energetic particles within the radiation belt, e.g., chorus, Hiss etc. are known as the spontaneous emissions. The allowed frequency band for this plasma wave depends on either the electron gyrofrequency f_{HE} or the electron plasma frequency f_e, whichever is larger for longitudinal propagation, and on the lower hybrid frequency f_{LHR}. Both f_{HE} and f_e decrease with L shell and take the value about 50 kHz and 200 Hz respectively around the equatorial plasmapause. This mode of propagation is termed 'whistler'. Very large amplification (40 to 60 dB) of the primary whistler wave occurs during the process of cyclotron interaction with energetic electrons in the Earth's magnetosphere [199 - 201]. Thus whistler waves provide an energy coupling between the lower atmosphere (troposphere) and the magnetospheric altitude, initiated by thunderstorm and lightning discharges. As the wave propagates through the ionized medium embedded in the geomagnetic field, it is dispersed and a particular form of whistler spectrogram is obtained. VLF signals having spectra of different shapes are broadly classified as hiss or unstructured emissions, characterized by a continuous band-limited signal producing a hissing sound or chorus, structured emissions exhibiting coherent discrete spectra including periodic emissions, quasi-periodic emissions, triggered emissions [202, 203].

Whistler mode waves are right-hand polarized EM wave, with the upper frequency cut off as either the local electron plasma frequency or gyro-frequency. The ionospheric plasma consists of electrons with ions having different ion gyro frequencies. Hydrogenion whistlers, oxygen ion whistlers, and helium-ion whistlers have been observed on satellites.

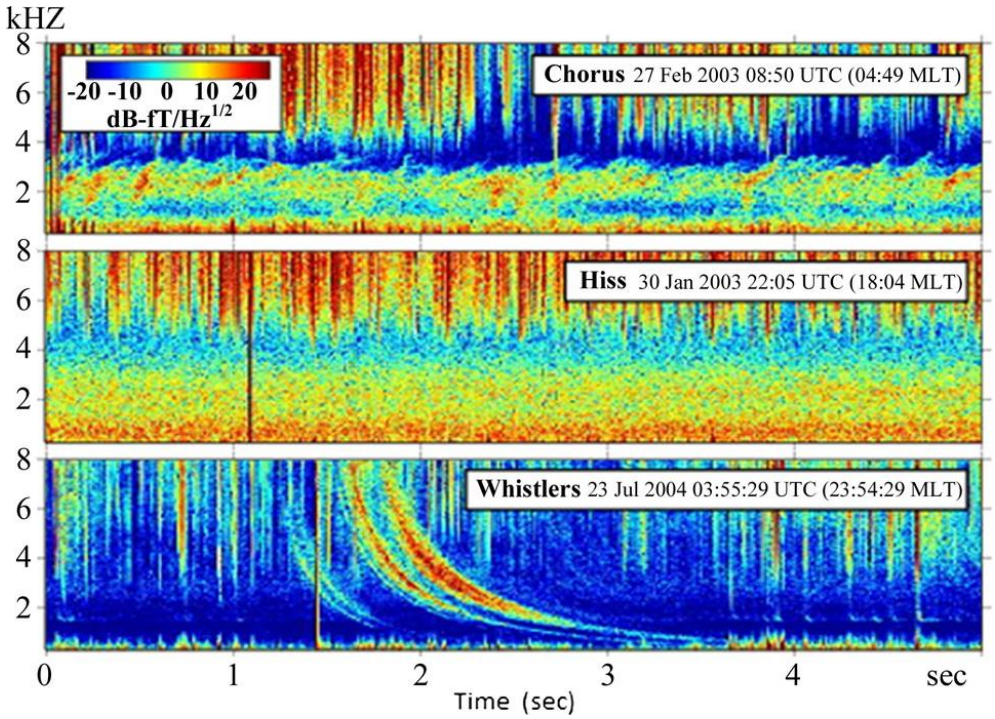

Fig. 4.8 Observation of Whistler-mode emissions observed at Palmer, Antarctic peninsula, at 64.77°S, 64.05°W. Chorus (top panel) is an important source and loss mechanism for energetic particles, while hiss (middle panel) and whistlers (bottom panel) are important loss mechanisms (See text below)

These waves have been received both on the Earth's surface as well as on orbiting satellites. They can propagate through the magnetospheric plasma in a ducted mode, a non-ducted mode and a pro-longitudinal mode. Waves propagating in the non-ducted mode can be received only by onboard satellites. Several theories regarding the origin of these emissions can be classified into the following categories: Cerenkov radiation (incoherent and coherent) [204], traveling wave tube mechanism [205], backward wave oscillator, cyclotron radiation and transverse resonance instability [206]. Detection of Whistler, Hiss and Chorus in the VLF spectrum up to 8 kHz has been shown in the bottom, middle and upper panel respectively in Fig. 4.8, recorded at Palmer, Antarctic Peninsula, (64.77°S, 64.05°W) by the Stanford VLF Group (http://vlf.stanford.edu/research).

4.6.3.1 Ducted mode of propagation:

Whistler mode waves enter the ionosphere/magnetosphere with small wave normal angles and are trapped in the geomagnetic field-aligned duct, formed by the enhancement depletion of electron density. At mid and high latitudes, ducts are formed because electron density fluctuations support ducted mode propagation of whistlers with almost negligible attenuation [202,207]. Furthermore, geomagnetic field lines at low latitudes are quite curved. Under these diverse conditions, ducted mode propagation of VLF waves at low latitudes is ruled out and non-ducted or a pro-longitudinal mode of propagation is considered [208]. Two dimensional ray-tracing computation studies suggested non-ducted propagation at these low latitudes [209]. These computational results showed that a preferred non-ducted propagation channel exists in the geomagnetic latitude range 10°–15°. Three dimensional ray tracing computations using realistic modes for the plasma density and geomagnetic field show that the waves with wave-normal angles less than 4° could be trapped in the duct and be received on the Earth's surface [210, 211] showed a reduction in wave path excursions both in latitude and longitude as rays propagate upwards in a duct from low altitudes (1000 km) to the equatorial plane. The ray tracing method is applicable when the duct radius is greater than the characteristic wavelength Strangeways et.al and AP Nickolaenko et. al [211,212] have studied whistler mode wave propagation in magnetospheric ducts of enhanced cold plasma density for the arbitrary ratio of the duct radius to the whistler wavelength (where the ray tracing method is not applicable). They have shown that in the case of the source exciting several duct eigen modes simultaneously, the receiver should register the set of discrete signals each corresponding to one of the excited eigen modes. The interval is longer for a narrow duct and smaller in the case of a wide duct, and the interval can vary up to hundreds of milliseconds.

When a lightning discharge is composed of multiple flashes and VLF energy propagates in the same duct, the series of whistlers having the same dispersion and separated in time are called 'multiflash' whistlers. The dynamic spectra of whistlers are controlled by the path length, distribution of electron density and magnetic field along the path of propagation. Spiky whistlers combined with multimode sferics are presented in the dynamic spectra containing numerous fractional-hop whistlers recorded onboard by the DEME-TER satellite [213,214] analyzed whistler signals for the last decade of the 20th century and showed the maximum monthly occurrence rate during January to March. The dependence of occurrence rate on geomagnetic disturbances was analyzed using the variation of the K_p index (where The K_p index is the global geomagnetic activity **index** that is based on 3-hour measurements from ground-based magnetometers around the world). They showed that the probability of occurrence increases monotonically with the K_p (daily sum) values. The occurrence rate is found to be greater than the average value for K_p 20. The results are in good agreement with earlier studies from low latitude stations measured by Helliwell, Singh and their co-workers [202,208]. Helliwell, Singh and their co-workers [202,208] have also shown that, as the intensity of a magnetic storm increases, the probability of whistler occurrence decreases. The enhancement in the whistler occurrence rate during geomagnetic disturbances at low latitudes is attributed to the formation of additional field aligned ducts [208]. A marked seasonal variation is observed at all latitudes. This is obviously due to the seasonal asymmetry of sources (lightning activity) in the conjugate hemisphere.

The analysis of whistlers recorded at a ground station yields information about the duct properties through which it has propagated. The analyses of occurrence rate and diffuseness of the whistler trace give an estimate of the lifetime and width of the duct. The lifetime of ducts may vary from a few minutes to many hours [208]. However, statistical analysis suggests that the duct formation and decay are cyclic phenomena with the time scale

of an hour [215, 216]. At low latitudes duct formation is difficult due to the required density enhancement (100%), the presence of curvature in geomagnetic field, and plasma turbulence. In the absence of a duct, the observation of small-dispersion low-latitude whistlers are proposed to be due to propagation in the pro-longitudinal (PL) mode with the angle between the wave normal and the geomagnetic field tending to zero Singh and Kumar and their co-workers [208, 217] reported an observation from the low latitude station Suva, Fiji, and interpreted the propagation mechanism to be PL mode, supported by the negative electron density gradient in the ionosphere that is enhanced during magnetic storms.

4.6.3.2 Non-ducted mode of propagation:

VLF waves entering the ionosphere/magnetosphere with large wave-normal angles to the geomagnetic field cannot be trapped in the field aligned ducts; they propagate in a non-ducted mode. Such waves suffer reflection at the point where the wave frequency equals to the lower hybrid resonance frequency [218], and they do not reach the Earth's surface. They can only be received by onboard satellites. Such whistlers are referred to as magneto-spherically reflected (MR) whistlers and are composed of multiple discrete components [219]. Sometimes waves of higher frequency while propagating downward may not undergo lower hybrid resonance reflection; they propagate with their wave-normal nearly perpendicular to the geomagnetic field but their ray direction remains nearly parallel to the Earth's magnetic field. Such a mode of propagation is called the pro-resonance (PR) mode, and the whistler traces are the so-called 'walking trace' whistlers [220]. When the wave frequency is lower than the lower hybrid resonance frequency and the wave normal angle is relatively small (but not small enough to be trapped in ducts) the waves propagate in the pro-longitudinal mode (PL) and such whistlers can be received on low altitude satellites. They are called PL whistlers and are considerably different from PR whistlers [221].

The other class of whistlers observed on satellites is proton/ion whistlers, propagating in the ion-cyclotron mode. The propagating frequency lies in the range between the proton gyro-frequency and the crossover frequency characterized by the frequency where the polarization becomes linear during the transition from right- to left-handed. Observed whistler traces are proton whistlers, helium whistlers, deuterium whistlers, etc. [222].

4.6.3.3 Hiss emissions:

A band-limited, unstructured, incoherent whistler mode emission occurs predominantly in the plasmasphere or high density plasma regions in the near-Earth space environment and is known as Plasmaspheric Hiss (PH), in the frequency span $f_{cH} < f < f_{ce}$, where f_{cH} and f_{ce} are the local proton and electron gyro-frequencies, respectively [223]. This incoherent, structureless emission is generally confined within the plasmasphere (from L 1.6 to the plasmapause), regions of high-density plasma in the near earth space environment such as plasmaspheric drainage plumes [207, 224, 225] and possibly a high latitude day side plume region [226], within the frequency span between 100 Hz and 2 kHz, and may extend to several kHz at lower power levels [227] distributed over three principal zones, namely auroral hiss located around 70° latitude, mid-latitude hiss near 50° latitude and equatorial hiss observed below 30° latitude. The intensity of the equatorial/low latitude hiss is smaller than those observed at middle and high latitudes [206, 216, 228]. Recent observations clearly suggest that the equatorial region from low altitudes to the inner plasmasphere is an intense source of hiss emissions [206, 229].

Based on their dynamic spectrum hiss emissions are classified as continuous hiss and impulsive hiss. The occurrence probability of auroral hiss and equatorial hiss is increased when the K_p index increases from 0 to 5 [230]. Impulsive hiss was reported during the expansion phase of a sub-storm in the midnight sector, whereas continuous hiss did not show any correlation with the local magnetic disturbances [231]. This shows that magnetospheric

conditions control the generation and propagation of hiss emissions.

Back and forth propagation of whistler mode waves along the geomagnetic field lines may produce a hiss like spectrum due to interference and diffraction processes [232, 233] discussed evidence that hiss could be produced from lightning generated whistlers. But, the intensity distribution of hiss over the land mass and the ocean does not correlate with the distribution of lightning activity which shows stronger activity over the land mass than over the oceans [233, 234]. An extensive study showed that hiss intensity below 2 kHz has no correlation with land mass [235]. Meredits et.al analyzed CRRES (Combined release and radiation effects satellite) wave data together with the global distribution of lightning to test both the theories and suggested that natural plasma turbulence should dominate the loss of relativistic (MeV) electrons in the slot region $2 < L < 3$. They also estimated radiation belt electron loss time scales due to plasmaspheric hiss and lightning generated whistlers in the slot region [236].

Different plasma density models as well as reverse ray tracing computations showed that the observed low altitude hiss on the dayside at sub-auroral latitudes may have a possible source region near the geomagnetic equator at a radial distance between 5 and 7 Earth radii consistent with the source of chorus [237]. Thus it has been suggested that ELF hiss is nothing but chorus propagating to low altitudes, with their modified dynamic spectra. Santolik, Bortnik and their co-workers [237,238] proposed an explanation for the generation of plasmaspheric hiss that reproduces its fundamental properties. However, Rodger et.al [239] commented that this modeling of hiss generation from chorus required experimental confirmation. The connection between chorus and hiss is very interesting because chorus helps in the formation of high energy electrons (by acceleration) outside the plasmasphere [240] whereas hiss depletes these electrons at lower equatorial altitudes [241].

4.6.3.4 Chorus emissions:

Structured emissions exhibit coherent, discrete frequency time characteristics; these are emissions like chorus, periodic emissions, and quasi-periodic emissions [202] [208]. Chorus emissions are natural wave emissions generated by plasma instabilities in the Earth's magnetosphere observed first on the ground at middle and high latitudes in the frequency range from hundreds of Hz to several kHz [202]. They have complex frequency spectra resembling a riser, faller, hook, inverted hook or even more complex structures on time scales of a fraction of second. Chorus is also observed at low latitude ground stations [242]. Also there is report of a rare observation of hisslers quasi-periodic falling noise from a low latitude station [243].

The importance of chorus arises because these waves are believed to accelerate electrons outside the plasmasphere. The observation of a local peak in phase space density [244], flat top pitch angle distributions [245] and energy dependence in the particle spectrum [246], support the idea that electrons are accelerated by the chorus emissions during wave (chorus)–particle (electron) interactions. The other effect of chorus is to cause burst precipitation [245] and the depletion of radiation belt electrons. These precipitated energetic electrons create additional ionization in the lower atmosphere [247] and cause the absorption of whistler mode waves as they propagate through the medium [247,248] computed the energy spectra of precipitated electrons based on current models of chorus propagation and wave- particle interaction theory. They showed that the results are not consistent with the experimentally observed radio wave perturbations. Chorus can act as a mediating agent in transferring energy due to acceleration from the lower energy electrons (10–100 keV) to the predominantly precipitated relativistic electrons (MeV) [240, 249].

The generation mechanism of chorus has been extensively studied in the past. The non-linear cyclotron resonance interaction between whistler mode waves and counter

streaming electrons is the most widely used theory [242,250]. During the development of the cyclotron instability, a singularity in the form of a step in the distribution function of the energetic electrons is formed at the boundary in velocity space between resonant and nonresonant electrons [251]. The backward wave oscillator (BWO) regime is realized; discrete emissions such as chorus are generated. Singh et.al [252] used the BWO mechanism to explain some features of chorus observed at the Indian Antarctic Station, Maitri. Chorus is believed to be generated near the geomagnetic equator, where the first derivative of the magnetic field strength along the field line is nearly zero [253]. The analysis of multi-satellite Cluster data of chorus emissions [254 - 256] shows that the generation region is localized near the equatorial cross-section of the L4 magnetic flux tube, and has a typical scale size of 2000 km along the magnetic field lines. The source centre is defined by the balance of the Poynting flux parallel and antiparallel to the field lines [255, 257]. The central position is found to move back and forth randomly over a few thousand kilometres in time scales of minutes. The chorus waves propagating along the geomagnetic field lines may be reflected back to the source region [258]. The intensity ratio between the magnetic components of waves coming directly from the equator and waves returning to the equator was observed to be between 0.005 and 0.01 [257]. Ray tracing results show that the chorus waves are generated with oblique wave vectors pointing towards the Earth in an equatorial region between 5 and 7 Earth radii [259]. Moreover, the wave normals are nearly field-aligned when the waves again cross the equator inside the plasmasphere which is consistent with the observed wave-normal of plasmaspheric hiss and makes further amplification of these waves possible [260]. This also shows that waves generated with finite wave-normal angle can, after one/two reflections, have wave-normal almost parallel to the geomagnetic field lines and so could be received on the earth's surface. Singh, Trakhtengerts and their co-workers [261, 262] analyzed Cluster data obtained on two different geomagnetically active days of March

31, 2001 and April 18, 2002 and showed that the frequency spectrum of individual chorus elements depends on the position of the observation point in and around the generation region.

Regarding spontaneous emission of whistlers [207], based on statistical analysis Hayakawa et.al [215] showed that the unstructured emissions are closely associated with geomagnetic storms whereas structured ones are closely associated with sub-storms. Storm-time chorus is especially important for the physics of the Earth's magnetosphere since it can significantly influence the distribution functions of the energetic electrons in the outer radiation belt [245]. The spontaneous emissions of whistler waves are usually observed either during the initial phase or the recovery phase of the storm [214]. A similar signature has been established for a long-term correlation study of whistler occurrence and geomagnetic storm ΣKP data recorded at a low latitude station, Varanasi (geomagnetic lat. 14°55̇N, long. 154°E) during January 1990–December 1999 [263]. Some anomalous whistlers are observed at Sugadaira and Moshiri observatories during the period of 1970–1978 for local EQs with $M > 6$ [264].

4.6.4 VLF transmitted signals and different influences

Some electromagnetic signals generated with the passage of meteor showers in the ELF/VLF ranges are detected by many workers [265, 266] and have been explained on the basis of Kelvin–Helmholtz instability at the height where meteors interact with the atmosphere [265, [267]. Meteor showers introduce perturbations in ion composition, temperature and other physical parameters within the ionospheric medium at different altitudes extending from the lower *D*-region to the magnetosphere height [268]. This perturbation in ion composition can affect appreciably the propagation of electromagnetic waves in the VLF range [269, 270]. Thus, during the entry of meteors, the reflection height of

the lower ionosphere will be modified and as a result the phase and intensity of VLF sub-ionospheric transmitted signals will be perturbed. Some typical variations in amplitudes of 16.4 kHz and 18.2 kHz sub-ionospheric signals due to Leonid, Perseid and Geminid meteor showers have been reported [271 - 274]. Thus the meteor shower effect can be detected by the VLF transmitted signals.

An abnormal precursory influence of earthquakes upon sub-ionospheric VLF propagation was first reported by Gokhberg et.al [275] who suggested this as possible method of earthquake prediction. Later, Russian [276] and Japanese [277] colleagues accumulated more evidence on anomalies in sub-ionospheric propagation associated with earthquakes. The electrical conductivity and the electric field of the atmosphere change during variations of the density and the kinds of aerosols. The charged aerosols modify the lower atmosphere few hours before the earthquake [278, 279]. The large aerosol particles are generally negatively charged whereas the smaller particles become positively charged and are suspended above. Hence it causes an electric field of opposite polarity. Thus electric field in the closed atmosphere– ionosphere electric circuit is generated: (i) the external electric current excited in the lower atmosphere in a process of vertical atmospheric convection and gravitational sedimentation of charged aerosols injected into the atmosphere before an earthquake, (ii) the effects of the ionization of lower atmosphere by radioactive sources (radon, etc.), the adhesion of electrons to molecules and the interaction of charged ions with charged aerosols. These electric disturbances gradually reach up to the ionospheric level and enhance the ionospheric electron density through this electric channel. Hayakawa et.al [280] introduced a new method, namely the 'terminator time method' for earthquake prediction. VLF day length, i.e., the time difference between the two terminator times becomes anomalously high typically two days before the earthquakes [281]. Subsequently, Ray. S et.al [282] reported that the 'VLF day length' obtained from the VLF signals for VTX–Malda, India propagation path

becomes anomalously high one day before the earthquake. They also support the 'terminator' for earthquake prediction in 1996 and showed that both the sunrise and sunset terminators times shifted towards the night time a few days before the earthquake. Some anomalous night time variations in radio signals before a few days of the occurrence of earthquake have been studied for the last two decades by different workers [275, 283 - 285].

Hayakawa et.al [286] studied the extremely large earthquake in Japan on March 11, 2011, formally known as the 2011 earthquake off the Pacific coast of Tohoku, by using temporal and spatial characteristics of the seismo-ionospheric perturbations of VLF signal. Anomalous fluctuations in the amplitude of night time VLF signals have been detected about three days prior to the earthquake day. Ray. S et.al [287] also observed a 40 minute terminator time shift by the VLF signal three days before the large earthquake of *Mw* 7.2, occurring in South-western Pakistan (latitude 28.440°N, longitude 63.560°E) at a depth of 68 km on 18 January 2011. Figure 4.9 presents the terminator time shift by the VLF transmitter signal for the Hyogoken Nanbu earthquake (7.3 M) in 1995 with a focal depth of 20 km [280].

Acoustic waves and acoustic-gravity waves were indeed observed at the sub-ionospheric altitudes during earthquake preparation times [288]. It is assumed that several days before earthquakes atmospheric acoustic and acoustic- gravity waves are generated in earthquake

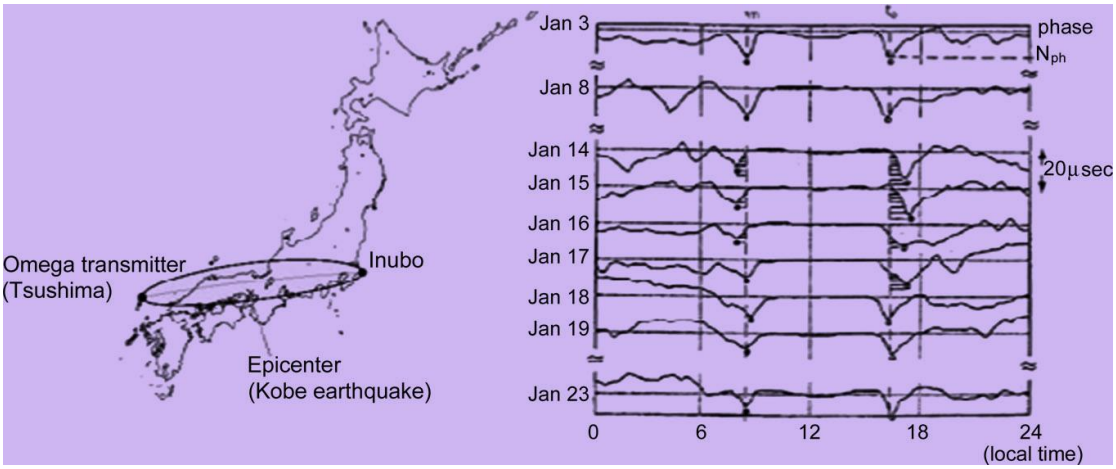

Fig. 4.9 Significant shift in the terminator times in the VLF transmitted signal before the Hyogo-Ken Nanbu earthquake (7.3 M) in 1995 (depth 20 km) [105]

preparation zones and propagate through the atmosphere up to ionospheric altitudes and initiate lithosphere-atmosphere-ionosphere coupling [289]. Thus by this coupling phenomenon ionospheric reflection height for the VLF waves of the waveguide perturbed the over-horizon radio wave propagation within the Earth-ionosphere cavity in terms of phase and amplitude change. Spiky transient was detected at 3 kHz electromagnetic signals, which is similar to the VLF pre-seismic signals of Kozani–Grevena earthquake [290]. Similar records regarding VLF frequencies were reported for the 1995 Hyogo-Ken Nanbu earthquake [291, 292]. The VLF–VHF electromagnetic anomalies were detected for the Kozani–Grevena earthquake (*M* 6.6) in Greece [293]. Some spiky transients have been observed at Kolkata (lat: 22.56°N, long: 88.5°E) for several earthquakes upon the two sub-ionospheric transmitted signals, one 19.8 kHz from North West Cape, Australia (lat: 21.82°S; long: 114.16°E) and the other 40 kHz from Fukushima, Japan (lat: 37.37°N; long: 140.85°E) [273, 274]. Sub-ionospheric VLF/LF propagation has been extensively used to investigate seismo-ionospheric perturbations [294].

4.7 Summary and conclusions:

The influences of different geophysical events in these various signals may be implemented to investigate particular events over the different man-made as well as natural signals according to their nature of signatures. However, we need repeated investigations by various methods to identify the true signatures.

Lightning research: ULF radiation during lightning discharge offers a direct method of monitoring the temporal variation of terrestrial lightning. It has been suggested that the Schumann (ELF) resonance could offer a method of monitoring global temperature. Lightning centre detection by ELF/VLF waves are also employed in different parts of the world [5, 166, 295]. Upper Tropospheric Water Vapour (UTWV) is a key element to initiate thunderstorms and lightning which can be monitored with SR signals [114].

Earthquake research: Sudden release of large stress energy within the tectonic plates near the fault boundary in the form of acoustic shock manifests as an earthquake. This energy may produce electromagnetic anomaly by generating EM wave or by modifying the Earth-ionosphere waveguide. Generation of ULF/ELF/VLF frequency due to piezoelectric effects by the mechanical vibrations is the direct outcome of the seismic hazards in the radio wave. It may enhance the intensity level of the transmitted signal propagating along the same direction in the form of spikes and bursts. Further, this energy may perturb the ionospheric altitude due to Lithosphere-Atmosphere-Ionosphere (LAI) coupling through different channels, e.g., chemical channel, wave channel and electrical channel. The released energy corresponding to different sub-micron gases (CO_2, Radon, He, CH_4 etc., i.e., greenhouse gases) and also heat energy release before the event are the main clue for the short term earthquake prediction research. Thus the ionospheric modification and change in the dielectric property of the waveguide in terms of electron density aerosol particles entry through different coupling mechanisms and corresponding signal perturbation constitutes the indirect earthquake prediction research. Schumann resonance frequency shift, phase variation

of VLF transmitted signals, detection of terminator-time shift by the VLF transmitted signal before the earthquake mentioned before are the evidence. Furthermore, heat release in the lithospheric zone enhances the electrical conductivity and thus the attenuation of signal of lithospheric origin decreases and the corresponding enhancement of polarization ratio (ratio of vertical magnetic and horizontal field components) shows satisfactory result in a precursory study. In this way repeated investigation of various anomalies through these signals may save lives if it were possible to predict earthquakes well in advance through the continuous efforts of the scientific community.

Meteor shower research: The extra ionization, produced by the supersonic meteoroids during their entry through the passage to the lower ionosphere, causes a strong fluctuation of charge density distribution in the medium. As a result, the relative electron-ion drift velocity may exceed the value for the onset of Kelvin-Helmholtz instability. At the frontal path of the meteor, compressible ionospheric plasma driven due to velocity shears and Earth's magnetic field increases the growth rate of Kelvin-Helmholtz instability thereby generating electromagnetic waves that produce the observed effects in the sub-ionospheric signals.

Solar flare research: The frequency variation of the first SR mode carries positive hints to detect solar proton and X-ray flare events [40, 41, 296]. These two events modify the waveguide in different ways according to the two-layer theory [37].

Solar eclipse: The amplitude and phase variations of sub-ionospheric signals during the solar eclipse are also quite interesting. By analyzing the received wave features of whistler phenomena, it may be possible to extract information about the medium such as the electron and proton density, temperature, and electric and magnetic field distributions in the medium [28, 170]. This may carry some information regarding earthquake.

Thus we need repeated and detailed investigations of these signals by using multiple approaches for the prediction of different natural disasters so that it becomes possible to save lives in various natural calamities.

4.8 REFERENCE:

[1] Kułak, A., Młynarczyk, J.: ELF propagation parameters for the Ground-Ionosphere waveguide with finite ground conductivity. IEEE Trans. Antennas Propag. **61**(4), 2269 (2013)

[2] Schumann, W. O. (1952), Uber die strahlungslosen Eigenschwingungen einer leitenden Kugel, die von einer Luftschicht und einer Ionospha renhu lleumgeben ist, Z. Naturforsch. A, **7**, 149–154.

[3] Balser, M., and C. A. Wagner On Frequency variations of the Earth-ionosphere cavity modes, J. Geophys. Res., **67(10)**, 4081-4083, 1962.

[4] Bliokh, P.V., Nicholaenko, A.P., Filtippov, Yu.F., Llanwyn Jones, D.: Schumann Resonances in the Earth-Ionosphere Cavity. Stevenage [England], Peter Peregrinus, New York (1980)

[5] Huang, E., Williams, E., Boldi, R., Heckman, S., Lyons, W., Taylor, M., Nelson, T., Wong, C.: Criteria for sprites and elves based on Schumann resonance observations. J. Geophys. Res. **104**(D14), 16943 (1999)

[6] Rycroft, M.J., Israelsson, S., Price, C.: The global atmospheric electric circuit, solar activity and climate change. J. Atmos. Sol.-Terr. Phys. **62**, 1563 (2000)

[7] Shvets, A.V., Hobara, Y., Hayakawa,M.: Variations of the global lightning distribution revealed from three-station Schumann resonance measurements. J. Geophys. Res. **115**(A12), A12316 (2010)

[8] Williams, E.R., Mareev, E.: Recent progress on the global electrical circuit. Atmos. Res. **208**, 135–136, (2014)

[9] Dyrda, M., Kułak, A., Młynarczyk, J., Ostrowski, M., Kubisz, J., Michalec, A., Nieckarz, Z.: Application of the Schumann resonance spectral decomposition in

characterizing the main African thunderstorm center. J. Geophys. Res. **119**(23), 13338 (2014)

[10] Nickolaenko, A. P., G. Sa´tori, B. Zieger, L. M. Rabinowicz, and I. G. Kudintseva (1998), Parameters of global thunderstorm activity deduced from the long-term Schumann resonance records, J. Atmos. Sol. Terr. Phys., **60**, 387–399.

[11] Cummer, S.A., Inan, U.S., Bell, T.F., Barrington-Leigh, C.P.: ELF radiation produced by electrical currents in sprites. Geophys. Res. Lett. **25**(8), 1281 (1998)

[12] Nickolaenko, A. P. and M. Hayakawa, 2002: Resonances in the Earth-Ionosphere Cavity, Modern Approaches in Geophysics, Vol. **19**, Springer Science & Business Media, New York, 380 pp

[13] Magunia, A.: The thunderstorm-driven diurnal variation of the ELF electromagnetic activity level. J. Atmos. Sol.-Terr. Phys. **58**(15), 1683 (1996)

[14] Cummer, S.A., Li, J., Han, F., Lu, G., Jaugey, N., Lyons, W.A., Nelson, T.E.: Quantification of the troposphere-to-ionosphere charge transfer in a gigantic jet. Nat. Geosci. **2(9)**, 617 (2009)

[15] Pasko, V.P., Yair, Y., Kuo, C.-L.: Lightning related transient luminous events at high altitude in the Earth's atmosphere: henomenology, mechanisms and effects. Space Sci. Rev. **168**, 475 (2012)

[16] Młynarczyk, J., Bór, J., Kułak, A., Popek, M., Kubisz, J.: An unusual sequence of sprites followed by a secondary TLE: an analysis of ELF radio measurements and optical observations. J. Geophys. Res. **120**(3), 2241 (2015)

[17] Kułak, A., Młynarczyk, J., Zi˛eba, S., Micek, S., Nieckarz, Z.: Studies of ELF propagation in the spherical shell cavity using a field decomposition method based on asymmetry of Schumann resonance curves. J. Geophys. Res. **111**(A10), A10304 (2006)

[18] Dyrda, M., Kułak, A., Młynarczyk, J., Ostrowski, M., Kubisz, J., Michalec, A., Nieckarz, Z.: Application of the Schumann resonance spectral decomposition in characterizing the main African thunderstorm center. J. Geophys. Res. **119**(23), 13338 (2014)

[19] Schlegel, K., Füllekrug, M.: Schumann resonance parameter changes during high-energy particle precipitation. J. Geophys. Res. **104**(A5), 10111 (1999)

[20] Molchanov, O.A., Schekotov, A.Yu., Solovieva, M., etal.: Nearseismic effects in ULF fields and seismo-acoustic emission: statistics and explanation. Nat. Hazards Earth Syst. Sci. **5**, 1 (2005)

[21] Ohta, K., Izutsu, J., Furukawa, K., Hayakawa, M.: Anomalous excitation of Schumann resonances associated with huge earthquakes, Chi-Chi (China, 1999), Niigata-Chuetsu (Japan, 2004), Noto- Hantou (Japan, 2007) observed at Nakatsugawa in Japan. In: Proc. 7th International Conf. Problems of Geocosmos', p. 461 (2008)

[22] Yuanqing, M., Xuemin, Z., Xuhui, S., Xinyan, O.: Pre-earthquake Schumann resonance anomaly in Yunnan. Earthq. Res. China **27**(1), 101 (2013)

[23] Nickolaenko, A. P. and M. Hayakawa,) : Resonances in the Earth-Ionosphere Cavity, Modern Approaches in Geophysics, Springer Science & Business Media, New York, Vol. **19**, 380 pp (2002)

[24] Nickolaenko, A.P., Hayakawa, M.: Spectra and waveforms of ELF transients in the Earth-ionosphere cavity with small losses. Radio Sci. **49**, 118 (2014)

[25] Carlson, C.R., Helliwell, R.A., Inan, U.S.: Space-time evolution of whistler mode wave growth in the magnetosphere. J. Geophys. Res. **95**(A9), 15073 (1990)

[26] Omura, Y., Nunn, D., Matsumoto, H., Rycroft, M.J.: A review of observational, theoretical and numerical studies of VLF triggered emissions. J. Atmos. Terr. Phys. **53**, 351 (1991)

[27] Bell, T.F., Inan, U.S., Helliwell, R.A., Scudder, J.D.: Simultaneous triggered VLF emissions and energetic electron distributions observed on POLAR with PWI and HYDRA. Geophys. Res. Lett. **27**(2), 165 (2000)

[28] Helliwell, R.A.: Whistler and Related Ionospheric Phenomena. Stanford University Press, Stanford (1965)

[29] Helliwell, R.A.: Low-frequency waves in the magnetosphere. Rev. Geophys. **7**, 281 (1969)

[30] Hayakawa, M., Kawate, R., Molchanov, O.A., Yumoto, K.: Results of ultra-low-frequency magnetic field 257) Omura, Y., Nunn, D., Matsumoto, H., Rycroft, .M.J.: A review of observational, theoretical and numerical studies of VLF triggered emissions. J. Atmos. Terr. Phys. **53**, 351 (1991)

[31] Barr, R., Jones Llanwyn, D., Rodger, C.J.: ELF and VLF radio waves. J. Atmos. Sol.-Terr. Phys. **62**, 1689 (2000)

[32] Pulinets, S.A., Ouzounov, D.: Lithosphere-atmosphere-ionosphere coupling (LAIC) model an unified concept for earthquake recursors validation. J. Asian Earth Sci. **41**, 371 (2011)

[33] Balling, R. C. and M. Hildebrandt, 2000: Evaluation of the linkage between Schumann Resonance peak frequency values and global and regional temperatures. Clim. *Res.*, **16**, 31-36, .

[34] Meister, C.-V., Mayer, B., Dziendziel, P., Fülbert, F., Hoffmann, D.H.H., Liperovsky, V.A.: On the acoustic model of lithosphereatmosphere- ionosphere coupling before earthquakes. Nat. Hazards Earth Syst. Sci. **11**, 1011 (2011)

[35] Tanaka, Y.T., Hayakawa, M., Hobara, Y., Nickolaenko, A.P., Yamashita, K., Sato, M, Takahashi, Y., Terasawa, T., Takahashi, T.: Detection of transient ELF emission

caused by the extremely intense cosmic gamma-ray flare of 27 December 2004. Geophys. Res. Lett. **38**(8), L08805 (2011)

[36] Pal, S., Maji, S.K., Chakrabarti, S.K.: First ever VLF monitoring of the lunar occultation of a solar flare during the 2010 annular solar eclipse and its effects on the D-region electron density profile. Planet. Space Sci. **73**(1), 310 (2012)

[37] Greifinger, C., Greifinger, P.: Approximate method for determining ELF eigenvalues in the Earth-ionosphere waveguide. Radio Sci. **13**(5), 831 (1978)

[38] Earth Ionosphere Wave guide dispersion Parameter – Optical Fiber Communication, Page 125, John. M. Senior

[39] Sátori, G., Williams, E., Mushtak, V.: Response of the Earthionosphere cavity resonator to the 11-year solar cycle in Xradiation. J. Atmos. Sol.-Terr. Phys. **67**, 553 (2005)

[40] De, S.S., De, B.K., Bandyopadhyay, B., Paul, S., Haldar, D.K., Barui, S.: Studies on the shift in the frequency of the first Schumann resonance mode during a solar proton event. J. Atmos. Sol.-Terr. Phys. **72**, 829 (2010a)

[41] De, S.S., De, B.K., Bandyopadhyay, B., Paul, S., Haldar, D.K., Bhowmick, A., Barui, S., Ali, R.: Effects on atmospherics at 6 kHz and 9 kHz recorded at Tripura during the India-Pakistan Border earthquake. Nat. Hazards Earth Syst. Sci. **10**, 843 (2010b)

[42] Dyrda, M., Kułak, A., Młynarczyk, J., Ostrowski, M.: Novel analysis of a sudden ionospheric disturbance using Schumann resonance measurements. J. Geophys. Res. **120**(3), 2255 (2015)

[43] Bliokh, P.V., Nicholaenko, A.P., Filtippov, Yu.F., Llanwyn Jones, D.: Schumann Resonances in the Earth-Ionosphere Cavity. Stevenage [England], Peter Peregrinus, New York (1980)

[44] Sentman, D.D.: Approximate Schumann resonance parameters for a two-scale-height ionosphere. J. Atmos. Terr. Phys. **52**(1), 35 (1990)

[45] Labendz, D., 1998: Investigation of Schumann resonance polarization parameters. *J. Atmos. Sol.-Terr. Phys.*, **60**, 1779-1789,

[46] Grimalsky, V., S. Koshevaya, A. Kotsarenko, and R. P. Enriquez, 2005: Penetration of the electric and magnetic field components of Schumann resonances into the ionosphere. *Ann. Geophys.*, **23**, 2559-2564,

[47] Merrill, R.T.: Our Magnetic Earth: The Science of Geomagnetism, p. 126. The University of Chicago Press, Chicago (2010)

[48] Parks, G.K.: Physics of Space Plasmas: An Introduction. Addison- Wesley, Reading (1991). ISBN 0201508214, Chap. 1

[49] Fabien, D., Johan, D.K., Philippe, E.C.: Cluster shows plasmasphere interacting with Van Allen belts. European Space Agency. http:// sci.esa.int/cluster/52802-cluster (2013)

[50] Takahashi, T.: Riming electrification as a charge generation mechanism in thunderstorms. J. Atmos. Sci. **35**, 1536 (1978)

[51] Uman, M.A.: The Lightning Discharge. Academic Press, Oxford (1987)

[52] MacGorman, D.R., Rust, W.D.: The Electrical Nature of Storms. Oxford University Press, London (1998)

[53] Rakov, V.A., Uman, M.A.: Lightning: Physics and Effects. Cambridge Univ. Press, Cambridge (2003)

[54] Stolzenburg, M., Marshall, T.C.: Charge structure and dynamics in 0thunderstorms. Space Sci. Rev. **137**, 355 (2008)

[55] Yair, Y.: Charge generation and separation processes. Space Sci. Rev.**137**(1), 119 (2008)

[56] Brooks, I.M., Saunders, C.P.R.: An experimental investigation of the inductive mechanism of thunderstorm electrification. J. Geophys. Res. **99**(D5), 10627 (1994)

[57] Harrison, R.G., Nicoll, K.A., Ambaum, M.H.P.: On the microphysical effects of observed cloud edge charging. Q. J. R. Meteorol. Soc. **141**(692), 2690 (2015)

[58] Yasuhide Hobara, Spatio-temporal characteristics of sub-ionospheric perturbations associated with annular solar eclipse over Japan: Network observations and modeling **August 2014**

[59] Saunders, C.: Charge separation mechanisms in clouds. Space Sci. Rev. **137**, 335 (2008)

[60] MacGorman, D.R., Burgess, D.W., Mazur, V., Rust, W.D., Taylor, W.L., Johnson, B.C.: Lightning rates relative to tornadic storm evolution on 22 May 1981. J. Atmos. Sci. **46**, 221 (1989)

[61] MacGorman, D.R., Rust, W.D., Krehbiel, P., Rison, W., Bruning, E., Wiens, K.: The electrical structure of two supercell storms during STEPS. Mon. Weather Rev. **133**, 2583 (2005)

[62] MacGorman, D.R., Filiaggi, T., Holle, R.L., Brown, R.A.: Negative cloud-to-ground lightning flash rates relative to VIL, maximum reflectivity, cell height, and cell isolation. J. Lightning Res. **1**, 132 (2007)

[63] MacGorman, D.R., Emersic, C., Heinselman, P.L.: In: 22nd International Lightning Conference. Bromfield, Colorado (2012)

[64] Belyaev, P.P., Polyakov, S.V., Rapoport, V.O., Trakhtengerts, V.Y.: Theory for the formation of resonance structure in the spectrum of atmospheric electromagnetic background noise in the range of short-period geomagnetic pulsations. Radiophizika **32**(7), 802 (1989b)

[65] Polyakov, S.V.: On properties of an ionospheric Alfvén resonator. In: Symposium KAPG on Solar-Terrestrial Physics, Vol. **III**, p. 72. Nauka, Moscow (1976)

[66] Polyakov, S.V., Rapoport, V.O.: The ionospheric Alfvén resonator. Ge- omagn. Aeron. **21**, 610 (1981)

[67] Yahnin, A.G., Semenova, N.V., Ostapenko, A.A., Kangas, J., Manninen, J., Turunen, T.: Morphology of the spectral resonance structure of the electromagnetic background noise in the range of 0.1– 4 Hz at *L* 5.2. Ann. Geophys. **21**, 779 (2003)

[68] Polyakov, S.V., Rapoport, V.O., Trakhtengerts, V.Yu.: Alfvén sweep maser. Fiz. Plazmy **9**, 371 (1983)

[69] Belyaev, P.P., Polyakov, S.V., Rapoport, V.O., Trakhtengerts, V.Y.: The fine structure of the radiation of an Alfvén maser. Geomagn. Aeron. **24**, 202 (1984)

[70] Belyaev, P.P., Polyakov, S.V., Rapoport, V.O., Trakhtengerts, V.Y.: Linear theory of radiation fine structure for an Alfvén maser with fre- quency drift. Radiophizika **33**(4), 408 (1990b)

[71] Trakhtengerts, V.Yu.: Stimulation of auroral phenomena by periodic heating of the ionosphere. Geomagn. Aeron. **29**, 383 (1989)

[72] Trakhtengerts, V.Yu., Feldstein, A.Ya.: Quiet auroral arcs: ionosphere effect of magnetospheric convection stratification. Planet. Space Sci. **32**(2), 127 (1984)

[73] Trakhtengerts, V.Yu., Feldstein, A.Y.: Turbulent regime of magneto- spheric convection. Geomagn. Aeron. **27**, 221 (1987)

[74] Fujita, S., Tamao, T.: Duct propagation of hydromagnetic waves in the upper ionosphere, 1, electromagnetic field disturbances in high latitudes associated with localized incidence of a shear Alfvén wave. J. Geophys. Res. **93**(A12), 14665 (1988)

[75] Pilipenko, V., Fedorov, E., Mursula, K., Pikkarainen, T.: Generation of magnetic noise bursts during distant rocket launches. Geophysica **41**, 57 (2005)

[76] Belyaev, P.P., Polyakov, S.V., Rapoport, V.O., Trakhtengerts, V.Y.: The ionospheric Alfvén resonator. J. Atmos. Terr. Phys. **52**(9), 781 (1990a)

[77] Lysak, R.L. (ed.): Geophys. Monogr. Set., vol. **80**, p. 121, AGU, Wash- ington (1993)

[78] Belyaev, P.P., Polyakov, S.V., Rapoport, V.O., Trakhtengerts, V.Y.: Experimental studies of the spectral resonance structure of the atmospheric electromagnetic noise background within the range of short-period geomagnetic pulsations. Radiophizika **32**, 663 (1989a)

[79] Fraser-Smith, A.C.: ULF magnetic fields generated by electrical storms and their significance to geomagnetic pulsation generation. Geophys. Res. Lett. **20**(6), 467 (1993)

[80] Bösinger, T., Haldoupis, C., Belyaev, P.P., Yakunin, M.N., Semenova, N.N., Demekhov, A.G., Angelopoulos, V.: Spectral properties of the ionospheric Alfvén resonator observed at a low latitude station (*L* 1.3). J. Geophys. Res. **107**(A10), 1281 (2002)

[81] Demekhov, A.G., Trakhtengertz, V.Yu., Bösinger, T.: Pc1 waves and ionospheric Alfvén resonator: generation or filtration Geophys. Res. Lett. **27**(23), 3805 (2000)

[82] Molchanov, O.A., Fedorov, E., Schekotov, A., et al.: Lithosphere- atmosphere-ionosphere coupling as governing mechanism for preseismic short term events in atmosphere and ionosphere. Nat. Hazards Earth Syst. Sci. **4**, 757 (2004a)

[83] Molchanov, O.A., Schekotov, A.Yu., Fedorov, E.N., Hayakawa, M.: Ionospheric Alfvén resonance at middle latitudes: results of observations at Kamchatka. Phys. Chem. Earth Parts A/B/C **29**, 649 (2004b)

[84] Bösinger, T., Haldoupis, C., Belyaev, P.P., Yakunin, M.N., Semenova, N.N., Demekhov, A.G., Angelopoulos, V.: Spectral properties of the ionospheric Alfvén

resonator observed at a low latitude station (*L* 1.3). J. Geophys. Res. **107**(A10), 1281 (2002)

[85] Fedorov, E.N., Schekotov, A.Ju., Molchanov, O.A., Hayakawa, M., Surkov, V.V., Gladichev, V.A.: An energy source for the mid latitude IAR: world thunderstorm centers, nearby discharges or neutral wind fluctuations Phys. Chem. Earth Parts A/B/C **31**(4–9), 462 (2006)

[86] Surkov, V.V., Hayakawa, M., Schekotov, A.Y., Fedorov, E.N., Molchanov, O.A.: Ionospheric Alfvén resonator excitation due to nearby thunderstorms. J. Geophys. Res. **111**, A01303 (2006)

[87] Surkov, V.V., Pokhotelov, O.A., Parrot, M., Fedorov, E.N., Hayakawa, M.: Excitation of the ionospheric resonance cavity by neutral winds at middle latitudes. Ann. Geophys. **22**, 2877 (2004)

[88] Bösinger, T., Demekhov, A.G., Trakhtengerts, V.Y.: Fine structure in ionospheric Alfvén resonator spectra observed at low latitude (*L* 1.3). Geophys. Res. Lett. **31**, L18802 (2004)

[89] Schekotov, A., Pilipenko, V., Shiokawa, K., Fedorov, E.: ULF impulsive magnetic response at mid-latitudes to lightning activity. Earth Planets Space **63**(2), 119 (2011)

[90] Bösinger, T., Ermakova, E.N., Haldoupis, C., Kotik, D.S.: Magnetic inclination effects in the spectral resonance structure of the iono- spheric Alfvén resonator. Ann. Geophys. **27**, 1313 (2009)

[91] Kopytenko, Y., Ismagilov, V.S., Hayakawa, M., Smirnova, N., Troyan, V., Peterson, T.: Investigation of the ULF electromagnetic phe- nomena related to earthquakes: contemporary achievements and the perspective. Ann. Geophys. **44**, 325 (2001)

[92] Moore, G.W.: Magnetic disturbances preceding the 1964 Alaska earth- quake. Nature **203**, 508 (1964)

[93] Hayakawa, M., Molchanov, O.A. (eds.): Seismo Electromagnetics: Lithosphere-Atmosphere-Ionosphere Coupling, p. 477. TerraPub, Tokyo (2002)

[94] Gotoh, K., Akinaga, Y., Hayakawa, M., Hattori, K.: Principal component analysis of ULF geomagnetic data for Izu Islands earth- quakes in July 2000. J. Atmos. Electr. **22**, 1 (2002)

[95] Molchanov, O.A., Hayakawa, M.: Seismo Electromagnetics and Related Phenomena: History and Latest Results, p. 189. Terra Sci. Pub. Comp., Tokyo (2008)

[96] Ida, Y., Yang, D., Li, Q., Sun, H., Hayakawa, M.: Detection of ULF electromagnetic emissions as a precursor to an earthquake in China with an improved polarization analysis. Nat. Hazards Earth Syst. Sci. **8**, 775 (2008)

[97] Rozhnoi, A., Solovieva, M., Molchanov, O., et al.: Anomalies in VLF radio signals prior the Abruzzo earthquake (*M* 6.3) on 6 April 2009. Nat. Hazards Earth Syst. Sci. **9**, 1727 (2009)

[98] De, S.S., Bandyopadhyay, B., Barui, S., Paul, S., Haldar, D.K., De, D., De, B.K., Chattopadhyay, S., Kundu, A.K.: Studies on the effects of 2009 Leonid Meteor Shower on subionospheric transmitted VLF signals and vertical electric potential gradient. Earth Moon Planets **108**(2), 111 (2012a)

[99] De, S.S., Paul, S., Haldar, D.K., De, D., Kundu, A.K., Chottopadhyay, S., Barui, S.: Analyses of the effects of several earthquakes on the sub-ionospheric VLF–LF signal propagation. J. Atmos. Sol.-Terr. Phys. **81**, 20 (2012b)

[100] Wen, S., Chen, C.-H., Yen, H.-Y., Yeh, T.-K., Liu, J.-Y., Hattori, K.,Peng, H., Wang, C.-H., Shin, T.-C.: Magnetic storm free ULF analysis in relation with earthquakes in Taiwan. Nat. Hazards Earth Syst. Sci. **12**(5), 1747 (2012)

[101] Kotsarenko, A., Grimalsky, V., Perez Enriquez, R., Valdez-Gonzalez, C., Koshevaya, S., Cruz-Abeyro, J.A.L., Yutsis, V.: Nat. Hazards Earth Syst. Sci. **7**, 103 (2007)

[102] Potapov, A.S., Dovbnya, B.V., Tsegmed, B.: Earthquake impact on ionospheric Alfvén resonances. Izv. Phys. Solid Earth **44**(4), 346 (2008)

[103] Dovbnya, B.V., Potapov, A.S., Rakhmatulin, R.A.: Proceedings of the 8th International Conference 'Problems of Geocosmos' (St. Petersburg, Russia, 20–24 September 2010) (2010),

[104] Huang Q.: Seismicity pattern changes prior to large earthquakes—an approach of the RTL algorithm. Terr. Atmos. Ocean. Sci. **15**(3),469 (2004)

[105] Hayakawa, M., Kawate, R., Molchanov, O.A., Yumoto, K.: Results of ultra-low-frequency magnetic field measurements during the Guam earthquake of 8 August 1993. Geophys. Res. Lett. **23**(3), 241 (1996b)

[106] Hayakawa, M., Ito, T., Smirnova, N.: Fractal analysis of ULF geo- magnetic data associated with the Guam earthquake on August 8, 1993. Geophys. Res. Lett. **26**(18), 2797 (1999)

[107] Hattori, K., Akinaga, Y., Hayakawa, M., Yumoto, K., Na- gao, T., Uyeda, S.: ULF magnetic anomaly preceding the 1997 Kagoshima earthquakes. In: Hayakawa, M., Molchanov, O.A. (eds.) Seismo Electromagnetics: Lithosphere-Atmosphere- Ionosphere Coupling, p. 477. Terra Sci. Pub. Comp., Tokyo (2002)

[108] Hobara, Y., Koons, H.C., Roeder, J.L., Yumoto, K., Hayakawa, M.: Characteristics of ULF magnetic anomaly before earthquakes. Phys. Chem. Earth **29**, 437 (2004)

[109] Kopytenko, Yu.A., Ismaguilov, V.S., Hattori, K., Voronov, P.M., Hayakawa, M., Molchanov, O.A., Kopytenko, E.A., Zaitsev, D.B.: Monitoring of the ULF electromagnetic disturbances at the station network before EQ in seismic zones of Izu and Chibo Peninsulas (Japan). In 2002)

[110] Kushwah, V.K., Singh, B., Singh, V.: Ultra Low Frequency (ULF) bursts as precursors of earthquakes. In: The 12th International Conference of International

Association for Computer Methods and Advances in Geomechanics (IACMAG), 1–6 October, 2008, Goa, India (2008)

[111] Wen, S., Chen, C.-H., Yen, H.-Y., Yeh, T.-K., Liu, J.-Y., Hattori, K.,Peng, H., Wang, C.-H., Shin, T.-C.: Magnetic storm free ULF analysis in relation with earthquakes in Taiwan. Nat. Hazards Earth Syst. Sci. **12**(5), 1747 (2012)

[112] De, S.S., De, B.K., Sarkar, B.K., Bandyopadhyay, B., Haldar, D.K., Paul, S., Barui, S.: Analyses of Schumann resonance spectra from Kolkata and their possible interpretations. Indian J. Radio Space Phys. **38**(4), 208 (2009)

[113] Nickolaenko, A.P., Hayakawa, M.: Spectra and waveforms of ELF transients in the earth-ionosphere cavity with small losses. Radio Sci. **49**, 118 (2014)

[114] Price, C.: Evidence for a link between global lightning activity and upper tropospheric water vapour. Nature **406**, 290 (2000)

[115] Nickolaenko, A.P., Hayakawa, M., Kudintseva, I.G., Myand, S.V., Rabinowicz, L.M.: ELF sub-ionospheric pulse in time domain. Geophys. Res. Lett. **26**, 999 (1999a)

[116] Nickolaenko, A.P., Hayakawa, M., Hobara, Y.: Long-term periodical variations in global lightning activity deduced from the Schumann resonance monitoring. J. Geophys. Res. **104**(D22), 27585 (1999b)

[117] Price, C., Pechony, O., Greenberg, E.: Schumann resonances in lightning research. J. Lightning Res. **1**, 1 (2007)

[118] Cannon, P.S., Rycroft, M.J.: Schumann resonance frequency variations during sudden ionospheric disturbances. J. Atmos. Terr. Phys. **44**, 201 (1982)

[119] Price, C., Pechony, O., Greenberg, E.: Schumann resonances in lightning research. J. Lightning Res. **1**, 1 (2007)

[120] Roldugin, V.C., Maltsev, Y.P., Vasiljev, A.N., Schokotov, A.Y., Belyajev, G.G.: Diurnal variations of Schumann resonance frequency in NS and EWmagnetic components. J. Geophys. Res. **109**, A08304 (2004a)

[121] Sekiguchi, M., Hayakawa, M., Nickolaenko, A.P., Hobara, Y.: Evidence on a link between the intensity of Schumann resonance and global surface temperature. Ann. Geophys. **24**, 1809 (2006)

[122] Madden, T. and W. Thompson, 1965: Low-frequency electromagnetic oscillations of the earth-ionosphere cavity. *Rev. Geophys*., **3**, 211-254,

[123] Price, C., Pechony, O., Greenberg, E.: Schumann resonances in lightning research. J. Lightning Res. **1**, 1 (2007)

[124] Shvets, A.V.: A technique for reconstruction of global lightning distance profile from background Schumann resonance signal. J. Atmos. Sol.-Terr. Phys. **63**(10), 1061 (2001)

[125] 1 Balser, M. and C. A. Wagner, 1960: Observations of earth-ionosphere cavity resonances. *Nature*, **188**, 638-641, doi: 10.1038/188638a0.

[126] Nickolaenko, A.P., Hayakawa, M., Kudintseva, I.G., Myand, S.V., Rabinowicz, L.M.: ELF sub-ionospheric pulse in time domain. Geophys. Res. Lett. **26**, 999 (1999a)

[127] Nickolaenko, A.P., Hayakawa, M., Hobara, Y.: Long-term periodical variations in global lightning activity deduced from the Schumann resonance monitoring. J. Geophys. Res. **104**(D22), 27585 (1999b)

[128] Hobara, Y., Hayakawa, M., Inoue, T., Shiokawa, K.: Deducing locations and charge moment changes of lightning discharges by ELF network observations in Japan. IEEJ Trans. Power Energy **133**, 994 (2013)

[129] Balling, R.C. Jr., Hildebrandt, M.: Evaluation of the linkage between Schumann resonance peak frequency values and global and regional temperatures. Clim. Res. **16**(1), 31 (2000)

[130] Sátori, G., William, E.R., Boccippio, D.J.: On the dynamics of the north-south seasonal migration of global lightning, AE32A-0166, AGU Fall meeting, San Francisco, December, 8–12 (2003)

[131] Sekiguchi, M., Hayakawa, M., Nickolaenko, A.P., Hobara, Y.: Evidence on a link between the intensity of Schumann resonance and global surface temperature. Ann. Geophys. **24**, 1809 (2006)

[132] Hayakawa, M., Sekiguchi, M., Hobara, Y., Nickolaenko, A.P.: Intensity of Schumann resonance oscillations and the ground surface temperature. J. Atmos. Electr. **26**(2), 79 (2006)

[133] Tyagi, R., Singh, B., Singh, O.P., Dua, R.L.: Measurement of Ground surface temperature with Schumann resonance relation at Agra. J. Adv. Res. Elec., Electron. Instrum. Eng. **2**(3), 1138 (2013)

[134] Held, I.M., Soden, B.J.: Water vapor feedback and global warming. Annu. Rev. Energy Environ. **25**, 441 (2000)

[135] Melnikov, A., C. Price, G. Sátori, and M. Füllekrug, 2004: Influence of solar terminator passages on Schumann resonance parameters. *J. Atmos. Sol.-Terr. Phys*., **66**, 1187-1194,

[136] Sátori, G., Mushtak, V., Williams, E.: Schumann resonance signatures of global lightning activity. In: Bets, H.D., et al. (eds.) Lightning: Principles, Instruments and Applications, Springer, New York, pp. 347–386 (2009)

[137] Gray, K. G. and Bowhill, S. A., Radio Sci., 9, 63, (1974)

[138] Madden, T. and W. Thompson, 1965: Low-frequency electromagnetic oscillations of the earth-ionosphere cavity. *Rev. Geophys*., **3**, 211-254, .

[139] Kirillov, V.V.: Parameters of the earth-ionosphere waveguide at ELF. Prob. Diffr. Wave Propag. **25**, 35 (1993) (in Russian)

[140] Mushtak, V.C., Williams, E.R.: ELF propagation parameters for uniform models of the earth-ionosphere waveguide. J. Atmos. Sol.- Terr. Phys. **64**(18), 1989 (2002)

[141] Kirillov, V.V., Kopeykin, V.N., Mushtak, V.K.: Electromagnetic waves in ELF range in the earth-ionosphere waveguide. Geomagn. Aeron. **37**(3), 114 (1997) (in Russian)

[142] Ohta, K., Izutsu, J., Hayakawa, M.: Anomalous excitation of Schumann resonances and additional anomalous resonances before the 2004 Mid-Niigata prefecture earthquake and the 2007 Noto Hantou Earthquake. Phys. Chem. Earth, Parts A/B/C **34**(6–7), 441 (2009)

[143] Pechony, O., Price, C.: Schumann resonance parameters calculated with a partially uniform knee model on Earth, Venus, Mars, and Titan. Radio Sci. **39**(5), RS5007 (2004)

[144] Ohta, K., Umeda, K., Watanabe, N., Hayakawa, M.: ULF/ELF emissions observed in Japan, possibly associated with the Chi-Chi earthquake in Taiwan. Nat. Hazards Earth Syst. Sci. **1**, 37 (2001) Ohta, K., Watanabe, N., Hayakawa, M.: Survey of anomalous Schumann resonance phenomena observed in Japan, in possible asso-ciation with earthquakes in Taiwan. Phys. Chem. Earth **31**, 397 (2006)

[145] Hayakawa, M., Ohta, K., Nickolaenko, A.P., Ando, Y.: Anomalous effect in Schumann resonance phenomena observed in Japan, possibly associated with the Chichi earthquake in Taiwan. Ann. Geo- phys. **23**, 1335 (2005)

[146] Molchanov, O.A., Fedorov, E., Schekotov, A., et al.: Lithosphere- atmosphere-ionosphere coupling as governing mechanism for preseismic short-term events in atmosphere and ionosphere. Nat. Hazards Earth Syst. Sci. **4**, 757 (2004a)

[147] Molchanov, O.A., Schekotov, A.Yu., Fedorov, E.N., Hayakawa, M.: Ionospheric Alfvén resonance at middle latitudes: results of observations at Kamchatka. Phys. Chem. Earth Parts A/B/C **29**, 649 (2004b)

[148] Pulinets, S.A., Boyarchuk, K.A.: Ionospheric Precursors of Earth- quake. Springer, Berlin (2004)

[149] Pulinets, S.A., Boyarchuk, K.A., Hegai, V.V., Karelin, A.V.: Conception and model of seismo-ionosphere-magnetosphere coupling. In: Hayakawa, M., Molchanov, O.A. (eds.) Seismo- Electromagnetics: Lithosphere-Atmosphere-Ionosphere Coupling, pp. 353–361. Terra Pub, Tokyo (2002)

[150] Roldugin, V. C., Y. P. Maltsev, A. N. Vasiljev, and E. V. Vashenyuk, 1999: Changes of the first Schumann resonance frequency during relativistic solar proton precipitation in the 6 November 1997 event. *Ann. Geophys*., **17**, 1293-1297,

[151] Roldugin, V. C., Y. P. Maltsev, A. N. Vasiljev, A. V. Shvets, and A. P. Nikolaenko, 2003: Changes of Schumann resonance parameters during the solar proton event of 14 July 2000. *J. Geophys. Res*., **108**, 1103,

[152] Price, C., Mushtak, V.: The impact of the August 27, 1998, γ -ray burst on the Schumann resonances. J. Atmos. Sol.-Terr. Phys. **63**(10), 1043 (2001)

[153] Nickolaenko, A.P., Kudintseva, I.G., Pechony, O., Hayakawa, M., Hobara, Y., Tanaka, Y.T.: The effect of a gamma ray flare on Schumann resonances. Ann. Geophys. **30**, 1321 (2012)

[154] Nickolaenko, A.P., Hayakawa, M.: Model disturbance of Schumann resonance by the SGR l806-20 γ -ray flare on December 27, 2004. J. Atmos. Electr. **30**(1), 1 (2010)

[155] Nickolaenko, A.P., Schekotov, A.Yu.: Experimental detection of an ELF radio pulse associated with the gamma-ray burst of December 27, 2004. Radiophys. Quantum Electron. **54**(1), 15 (2011a)

[156] Nickolaenko, A.P., Schekotov, A.Yu.: ELF Q-burst caused by galactic gamma ray burst, XXX URSI General Assembly, Istanbul Turkey, 13–20 August 2011, Abstract EGH-3 (2011b)

[157] Sátori, G., Williams, E., Mushtak, V.: Response of the earth- ionosphere cavity resonator to the 11-year solar cycle in X- radiation. J. Atmos. Sol.-Terr. Phys. **67**, 553 (2005)

[158] Roldugin, V.C., Maltsev, Y.P., Vasiljev, A.N., Schokotov, A.Y., Belyajev, G.G.: Schumann resonance frequency increase during solar X-ray bursts. J. Geophys. Res. **109**, A01216 (2004b)

[159] Dyrda, M., Kułak, A., Młynarczyk, J., Ostrowski, M.: Novel analysis of a sudden ionospheric disturbance using Schumann resonance measurements. J. Geophys. Res. **120**(3), 2255 (2015)

[160] Roldugin, V. C., Y. P. Maltsev, A. N. Vasiljev, and E. V. Vashenyuk, 1999: Changes of the first Schumann resonance frequency during relativistic solar proton precipitation in the 6 November 1997 event. *Ann. Geophys*., **17**, 1293-1297,

[161] Beech, M., Brown, P., Jones, J.: VLF detection of fireballs. Earth Moon Planets **68**, 181 (1995)

[162] Watanabe, T., Okada, T., Suzuki, K.: Meteor and radio wave. Ham J. **54**, 109 (1988)

[163] Price, C., Blum, M.: ELF/VLF radiation produced by the 1999 Leonid meteors. Earth Moon Planets **82**, 545 (1998)

[164] Vinkovic, D.: LF/VLF emission and electrophonic sounds from Leonids identified. In: The Leonids MAC Workshop (1999)

[165] Trautner, R., Koschny, D., Witasse, O., Zender, J., Knofel, A.: Proceedings of Asteroids, Comets, Meteors (ACM 2002), 29 July–2 August 2002, TU Berlin, Germany (2002)

[166] Said, R.K., Inan, U.S., Cummins, K.L.: Long-range lightning geolocation using a VLF radio atmospheric waveform bank. J. Geophys. Res. **115**, D23108 (2010)

[167] Davies, K.: Planet. Space Sci. **19**, 374 (1990)

[168] Arnold, H.R., Pierce, E.T.: Leader and junction processes in the light- ning discharge as a source of VLF atmospherics. J. Res. Natl. Bur. Stand. D, Radio Sci. **68D**(7), 771 (1964)

[169] DE. S. S., B. K. DE, S. K. ADHEKARL S. K. SARKAR, R. BERA, A. GUHA and P. K. MANDAL (2006): A report on some specific features of the atmospheric electric potential gradient in Kolkata, *Indian J. Phys.*, **80**, 167-172.

[170] Singh, R.P., Singh, A.K., Singh, D.K.: Plasmaspheric parameters as determined from whistler spectrograms: a review. J. Atmos. Sol.- Terr. Phys. **60**(5), 495 (1998)

[171] Sagredo, J.L., Bullough, K.: VLF goniometer observations at Halley bay, Antarctica II. Magnetospheric structure deduced from whistler observations. Planet. Space Sci. **21**(6), 913 (1973)

[172] Hayakawa, M., Ito, T., Smirnova, N.: Fractal analysis of ULF geomagnetic data associated with the Guam earthquake on August 8, 1993.

[173] Outsu, J.: Numerical study of tweeks based on waveguide mode theory. Proc. Res. Inst. Atmos. Nagoya Univ. **7**, 58 (1960)

[174] Yedemsky, D.Ye., Ryabov, B.S., Shchokotov, A.Yu., Yarotsky, V.S.: Experimental investigation of the tweek field structure. Adv. Space Res. **12**(6), 251 (1992)

[175] Shvets, A.V., Serdiuk, T.M., Gorishnyaya, Y.V., Hobara, Y., Hayakawa, M.: Estimating the lower ionosphere height and lightning location using multimode "tweek" atmospherics. J. Atmos. Sol.-Terr. Phys. **108**, 1 (2014)

[176] CANNON, P. S. and M. J. RYCROFT (1982): Schumann resonance frequency variations during sudden ionospheric disturbances, J. Atmos. Sot -Terr. Phys., 44, 201-206.

[177] Ohya, H., Nishino, M., Murayama, Y., Igarashi, K.: Equivalent electron densities at reflection heights of tweek atmospherics in the low- middle latitude D-region ionosphere. Earth Planets Space **55**, 627 (2003)

[178] Christian, H.J., Blakeslee, R.J., Goodman, S.J., et al.: The lightning imaging sensor. NASA Conference Publication, 746 (1999)

[179] Christian, H.J., Blakeslee, R.J., Boccippio, D.J., et al.: Global frequency and distribution of lightning as observed from space by the optical transient detector. J. Geophys. Res. **108**(D1), 4005 (2003)

[180] Dowden, R.L., Brundell, J.B., Rodger, C.J.: VLF lightning location by time of group arrival (TOGA) at multiple sites. J. Atmos. Sol.- Terr. Phys. **64**(7), 817 (2002)

[181] Price, C., Asfur, M., Lyons, W., Nelson, T.: An improved ELF/VLF method for globally geolocating sprite-producing lightning. Geophys. Res. Lett. **29**(3), 1031 (2002)

[182] Burke, C.P., Jones, D.L.: Global radiolocation in the lower ELF frequency band. J. Geophys. Res. **100**(D12), 26263 (1995)

[183] Kempf, N.M., Krider, E.P.: Cloud-to-ground lightning and surface rainfall during the Great Flood of 1993. Mon. Weather Rev. **131**, 1140 (2003)

[184] Budden, K.G.: The Waveguide Mode Theory of Wave Propagation. Logos Press, London (1961)

[185] Wood, T.G., Inan, U.S.: Localization of individual lightning discharges via directional and temporal triangulation of sferic measurements at two distant sites. J. Geophys. Res. **109**, D21109 (2004)

[186] Thomas, R.J., Krehbiel, P.R., Rison, W., Hamlin, T., Boccippio, D.J., Goodman, S.J., Christian, H.J.: Comparison of ground-based 3 dimensional lightning mapping observations with satellite-based LIS observations in Oklahoma. Geophys. Res. Lett. **27**(12), 1703 (2000)

[187] Lee, A.C.L.: Ground truth confirmation and theoretical limits of an experimental VLF arrival time difference lightning flash locating system. Q. J. R. Meteorol. Soc. **115**(489), 1147 (1989)

[188] Smith, D.A., Eack, K.B., Harlin, J., Heavner, M.J., Jacobson, A.R., Massey, R.S., Shao, X.M., Wiens, K.C.: The Los Alamos sferic array: a research tool for lightning investigations. J. Geophys. Res. **107**(D13), 4183 (2002)

[189] Hobara, Y., Hayakawa, M., Inoue, T., Shiokawa, K.: Deducing locations and charge moment changes of lightning discharges by ELF network observations in Japan. IEEJ Trans. Power Energy **133**, 994 (2013)

[190] Yamauchi, T., Maekawa, S., Horie, T., Hayakawa, M., Soloviev, O.: Subionospheric VLF/LF monitoring of ionospheric perturbations for the 2004 Mid-Niigata earthquake and their structure and dynamics. J. Atmos. Sol.-Terr. Phys. **69**, 793 (2007)

[191] Utsunomiya, T.: Cause of long spikes for cyclotron harmonic waves in the Ionograms. IEICE Trans. Commun. **E83-B**(4), 838 (2000)

[192] Moldovan, I.A., Moldovan, A.S., Panaiotu, C.G., Placinta, A.O., Marmureanu, Gh.: The geomagnetic method on precursory phenomena associated with 2004 significant intermediate-depth Vrancea seismic activity. Rom. J. Phys. **54**, 249 (2009)

[193] Eftaxias, K., Kapiris, P., Polygiannakis, J., Peratzakis, A., Kopanas, J., Antonopoulos, G., Rigas, D.: Experience of short term earthquake precursors with VLF–VHF electromagnetic emissions. Nat. Haz- ards Earth Syst. Sci. **3**, 217 (2003)

[194] DE, S. S., B. K. DE, A. GUHA and P. K. MANDAL (2006): Detection of 2004 Leonid meteor shower by observing its effects on VLF transmission., Indian J. Radio Space Phys, **35**, 396-400

[195] De, S.S., Bandyopadhyay, B., Das, T.K., Paul, S., Haldar, D.K., De, B.K., Barui, S., Sanfui, M., Pal, P., Chattopadhyay, G.: Studies on the anomalies in the behaviour of transmitted subionospheric VLF electromagnetic signals and the changes in the fourth Schumann resonance mode as signatures of two pending earthquakes. Indian J. Phys. **85**(3), 447 (2011b)

[196] Ohta, K., Umeda, K., Watanabe, N., Hayakawa, M.: ULF/ELF emissions observed in Japan, possibly associated with the Chi-Chi earthquake in Taiwan. Nat. Hazards Earth Syst. Sci. **1**, 37 (2001)

[197] Nagao, T., Enomoto, Y., Fujinawa, Y., et al.: Electromagnetic anomalies associated with 1995 Kobe earthquake. J. Geodyn. **33**, 401 (2002)

[198] Izutsu, J.: Influence of lightning on the observation of seismic electromagnetic wave anomalies. Terr. Atmos. Ocean. Sci. **18**(5), 923 (2007)

[199] Carlson, C.R., Helliwell, R.A., Inan, U.S.: Space-time evolution of whistler mode wave growth in the magnetosphere. J. Geophys. Res. **95**(A9), 15073 (1990)

[200] Omura, Y., Nunn, D., Matsumoto, H., Rycroft, M.J.: A review of observational, theoretical and numerical studies of VLF triggered emissions. J. Atmos. Terr. Phys. **53**, 351 (1991)

[201] Bell, T.F., Inan, U.S., Helliwell, R.A., Scudder, J.D.: Simultaneous triggered VLF emissions and energetic electron distributions observed on POLAR with PWI and HYDRA. Geophys. Res. Lett. **27**(2), 165 (2000)

[202] Helliwell, R.A.: Whistler and Related Ionospheric Phenomena. Stanford University Press, Stanford (1965)

[203] Helliwell, R.A.: Low-frequency waves in the magnetosphere. Rev. Geophys. **7**, 281 (1969)

[204] Trakhtengerts, V.Yu.: Magnetosphere cyclotron maser: backward wave oscillator generation regime. J. Geophys. Res. **100**(A9), 17205 (1995)

[205] Singh, R.P., Patel, R.P.: Hiss-triggered chorus emissions at Indian stations. J. Atmos. Sol.-Terr. Phys. **66**(12), 1027 (2004)

[206] Singh, K., Singh, R., Singh, A.K., Singh, R.P.: Propagation characteristics and generation mechanism of ELF/VLF Hiss observed at low-latitude ground station (*L* 1.17). Earth Moon Planets **100**, 17 (2007b)

[207] Hayakawa, M., Tanaka, Y., Shimakura, S., Hzuka, A.: Statistical characteristics of medium-latitude VLF emissions (unstructured and structured): local time dependence and the association with geomagnetic disturbances. Planet. Space Sci. **34**, 1361 (1986)

[208] Singh, R.P.: Whistler studies at low latitudes: a review. Indian J. Radio Space Phys. **22**(3), 139 (1993)

[209] Liang, B., Bao, Z., Xu, J.: Propagation characteristics of night-time whistlers in the region of equatorial anomaly. J. Atmos. Terr. Phys. **47**, 999 (1985)

[210] Ohta, K., Nishimura, Y., Kitagawa, T.: Study of propagation characteristics of very low latitude whistlers by means of three-dimensional ray-tracing computations. J. Geophys. Res. **102**(A4), 7537 (1997)

[211] Strangeways, H.J.: Lightning induced enhancements of D-region ionisation and whistler ducts. J. Atmos. Sol.-Terr. Phys. **61**(14), 1067 (1999)

[212] A P Nickolaenko and M Hayakawa: Resonances in the Earth ionosphere cavity (Dordrecht, The Netherlands : Kluwer Academic Publishers) (2002)

[213] Ferencz, O.E., Ferencz, Cs., Steinbach, P., Lichtenberger, J., Hamar, D., Parrot, M., Lefeuvre, F., Berthelier, J.-J.: The effect of subionospheric propagation on whistlers recorded by the DEME- TER satellite—observation and modelling. Ann. Geophys. **25**, 1103 (2007)

[214] Singh, S., Patel, R.P., Singh, K.K., Singh, A.K., Singh, R.P.: Role of geomagnetic disturbance on whistler occurrence at a low latitude station. Planet. Space Sci. **55**(10), 1218 (2007a)

[215] Hayakawa, M., Tanaka, Y., Okada, T., Ohtsu, J.: Time scales for the formation, lifetime and decay of low latitude whistler ducts. Ann. Geophys. **1**, 515 (1983)

[216] Singh, D.K., Singh, A.K., Patel, R.P., Singh, R.P., Singh, A.K.: Two types of ELF hiss observed at Varanasi, India. Ann. Geophys. **17**, 1260 (1999)

[217] Kumar, S., Anil, D., Kishore, A., Ramachandran, V.: Whistlers ob- served at low-latitude ground-based VLF facility in Fiji. J. Atmos. Sol.-Terr. Phys. **69**(12), 1366 (2007)

[218] Stix, T.H.: Waves in Plasmas, American Inst. Physics, New York, p. 86. (1992)

[219] Smith, R.L., Angermi, J.J.: Magnetospheric properties deduced from OGO 1 observations of ducted and nonducted whistlers. J. Geo- phys. Res. **73**, 1 (1968)

[220] Walter, P., Angerami, J.J.: Nonducted mode of VLF propagation between conjugate hemispheres; Observations on OGO's 2 and 4 of the 'walking-trace' whistler and of Doppler shifts in fixed frequency transmissions. J. Geophys. Res. **74**, 6352 (1969)

[221] Morgan, M.G.: Some features of pararesonance (PR) whistlers. J. Geophys. Res. **85**(A1), 130 (1980)

[222] Gurnett, D.A., Shawhan, S.D., Brice, N.M., Smith, R.L.: Ion cyclotron whistlers. J. Geophys. Res. **70**(7), 1665 (1965)

[223] Singh, K.K., Patel, R.P., Singh, J., Kumar, B., Singh, A.K., Singh, R.P., Koul, B.L., Lalmani: observations of unusual whistlers during daytime at Jammu. J. Earth Syst. Sci. **117**(3), 219 (2008)

[224] Chan, K.-W., Holzer, R.E.: ELF hiss associated with plasma density enhancements in the outer magnetosphere. J. Geophys. Res. **81**, 2267 (1976)

[225] Parrot, M., Lefeuvre, F.: Statistical study of the propagation characteristics of ELF hiss observed on GEOS-1, inside and outside the plasmasphere. Ann. Geophys. Ser. A **4**(5), 363 (1986)

[226] Russell, C.T., Holzer, R.E., Smith, E.J.: OGO 3 observations of ELF noise in the magnetosphere: 1. Spatial extent and frequency of occurrence. J. Geophys. Res. **74**(3), 755 (1969)

[227] Hayakawa, M., Sazhin, S.S.: Mid-latitude and plasmaspheric hiss: a review. Planet. Space Sci. **40**(10), 1325 (1992)

[228] Sazhin, S.S., Bullough, K., Hayakawa, M.: Auroral hiss: a review. Planet. Space Sci. **41**(2), 153 (1993)

[229] Singh, D.K., Singh, R.P.: Hiss emissions during quiet and disturbed periods. Pramana **59**(4), 563 (2002)

[230] Hayakawa, M., Tanaka, Y., Ohtsu, J.: Satellite and ground observations of magnetospheric VLF hiss associated with the severe magnetic storm on May 25–27, 1967. J. Geophys. Res. **80**, 86 (1975)

[231] Makita, M., Fukunishi, H.: Jpn. Antarct. Res. Exped. Sci. Rep. **46**, 172 (1973)

[232] Bortnik, J., Inan, U.S., Bell, T.F.: Energy distribution and lifetime of magnetospherically reflecting whistlers in the plasmasphere. J. Geophys. Res. **108**(A5), 1199 (2003)

[233] Green, J.L., Boardsen, S., Garcia, L., Taylor, W.W.L., Fung, S.F., Reinisch, B.W.: On the origin of whistler mode radiation in the plasmasphere. J. Geophys. Res. **110**, A03201 (2005)

[234] Thorne, R.M., Horne, R.B., Meredith, N.P.: Comment on 'On the origin of whistler mode radiation in the plasmasphere' by Green et al. J. Geophys. Res. **111**, A09210 (2006)

[235] Meredith, N.P., Horne, R.B., Clilverd, M.A., Horsfall, D., Thorne, R.M., Anderson, R.R.: Origins of plasmaspheric hiss. J. Geophys. Res. **111**, A09217 (2006)

[236] Meredith, N.P., Horne, R.B., Glauert, S.A., Anderson, R.R.: Slot region electron loss timescales due to plasmaspheric hiss and lightning- generated whistlers. J. Geophys. Res. **112**, A08214 (2007)

[237] Santolík, O., Chum, J., Parrot, M., Gurnett, D.A., Pickett, J.S., Cornilleau-Wehrlin, N.: Propagation of whistler mode chorus to low altitudes: spacecraft observations of structured ELF hiss. J. Geophys. Res. **111**, A10208 (2006)

[238] Bortnik, J., Thorne, R.M., Meredith, N.P.: The unexpected origin of plasmaspheric hiss from discrete chorus emissions. Nature **452**, 62 (2008)

[239] Rodger, C.J., Clilverd, M.A.: Magnetospheric physics: Hiss from the chorus. Nature **452**, 41 (2008)

[240] Horne, R.B., Thorne, R.M., Shprits, Y.Y., et al.: Wave acceleration of electrons in the Van Allen radiation belts. Nature **437**, 227 (2005)

[241] Abel, B., Thorne, R.M.: Electron scattering loss in Earth's inner magnetosphere: 1. Dominant physical processes. J. Geophys. Res. **103**(A2), 2385 (1998)

[242] Singh, R., Patel, R.P., Singh, R.P., Lalmani: an experimental study of hiss-triggered chorus emissions at low latitude. Earth Planets Space **52**, 37 (2000)

[243] LaBelle, J., Treumann, R.A.: Auroral radio emissions, 1. Hisses, roars, and bursts. Space Sci. Rev. **101**(3), 295 (2002)

[244] BERING, E. A. III, A A FEW and J. R. BENBROOK (1998): The global electric circuit, Phys. Today, **51**, 24-30.

[245] Horne, R.B., Thorne, R.M.: Relativistic electron acceleration and precipitation during resonant interactions with whistler-mode chorus. Geophys. Res. Lett. **30**(10), 1527 (2003)

[246] Summers, D., Ma, C., Meredith, N.P., Horne, R.B., Thorne, R.M., Heynderickx, D., Anderson, R.R.: Model of the energization of outer-zone electrons by whistler-mode chorus during the October 9, 1990 geomagnetic storm. Geophys. Res. Lett. **29**(24), 2174 (2002)

[247] Rodger, C.J., Enell, C.-F., Turunen, E., Clilverd, M.A., Thomson, N.R., Verronen, P.T.: Lightning-driven inner radiation belt energy deposition into the atmosphere: implications for ionisation-levels and neutral chemistry. Ann. Geophys. **25**, 1745 (2007)

[248] Smith, A.J., Horne, R.B., Meredith, N.P.: Ground observations of chorus following geomagnetic storms. J. Geophys. Res. **109**, A02205 (2004)

[249] Meredith, N.P., Horne, R.B., Iles, R.H.A., Thorne, R.M., Heynderickx, D., Anderson, R.R.: Outer zone relativistic electron acceleration associated with substorm-enhanced whistler mode chorus. J. Geo- phys. Res. **107**(A7), 1144 (2002)

[250] Titova, E.E., Kozelov, B.V., Jiricˇek, F., Smilauer, J., Demekhov, A.G., Trakhtengerts, V.Yu.: Verification of the backward wave oscillator model of VLF

chorus generation using data from MAGION 5 satellite. Ann. Geophys. **21**, 1073 (2003)

[251] Hobara, Y., Trakhtengerts, V.Y., Demekhov, A.G., Hayakawa, M.: Cy- clotron amplification of whistler waves by electron beams in an inhomogeneous magnetic field. J. Geophys. Res. **103**(A9), 20449 (1998)

[252] Singh, R.P., Patel, R.P.: Hiss-triggered chorus emissions at Indian stations. J. Atmos. Sol.-Terr. Phys. **66**(12), 1027 (2004)

[253] Lauben, D.S., Inan, U.S., Bell, T.F., Gurnett, D.A.: Source characteristics of ELF/VLF chorus. J. Geophys. Res. **107**(A12), 1429 (2002)

[254] Parrot, M., Santolík, O., Cornilleau-Wehrlin, N., Maksimovic, M., Harvey, C.C.: Source location of chorus emissions observed by Cluster. Ann. Geophys. **21**(2), 473 (2003)

[255] Santolík, O., Gurnett, D.A., Pickett, J.S., Parrot, M., Cornilleau Wehrlin, N.: Central position of the source region of storm-time chorus. Planet. Space Sci. **53**, 299 (2005)

[256] Santolík, O., Chum, J., Parrot, M., Gurnett, D.A., Pickett, J.S., Cornilleau-Wehrlin, N.: Propagation of whistler mode chorus to low altitudes: spacecraft observations of structured ELF hiss. J. Geophys. Res. **111**, A10208 (2006)

[257] Santolík, O.: New results of investigations of whistler-mode chorus emissions. Nonlinear Process. Geophys. **15**, 621 (2008)

[258] Parrot, M., Buzzi, A., Santolík, O., Berthelier, J.J., Sauvaud, J.A., Lebreton, J.P.: New observations of electromagnetic harmonic ELF emissions in the ionosphere by the DEMETER satellite during large magnetic storms. J. Geophys. Res. **111**, A08301 (2006)

[259] Chum, J., Santolík, O.: Propagation of whistler-mode chorus to low altitudes: divergent ray trajectories and ground accessibility. Ann. Geophys. **23**, 3727 (2005)

[260] Santolík, O., Parrot, M., Storey, L.R.O., Pickett, J.S., Gurnett, D.A.: Propagation analysis of plasmaspheric hiss using Polar PWI measurements. Geophys. Res. Lett. **28**(6), 1127 (2001)

[261] Singh, R.P., Patel, R.P.: Hiss-triggered chorus emissions at Indian stations. J. Atmos. Sol.-Terr. Phys. **66**(12), 1027 (2004)

[262] Trakhtengerts, V.Yu., Demekhov, A.G., Titova, E.E., et al.: Formation of VLF chorus frequency spectrum: cluster data and comparison with the backward wave oscillator model. Geophys. Res. Lett. **34**(2), L02104 (2007)

[263] Patel, R.P., Singh, S., Singh, A.K., Singh, R.P.: VLF whistler wave activity and effects of geomagnetic disturbances at low latitudes. Bull. Astron. Soc. India **35**, 655 (2007)

[264] Hayakawa, M.: Study of generation mechanisms of magnetospheric VLF/ELF emissions based on the direction findings. Proc. NIPR Symp. Up. Atmos. Phys. **6**, 117 (1993)

[265] Chakrabarti, S.K., Pal, S., Acharya, K., Mandal, S., Chakrabarti, S., Khan, R., Bose, B.: VLF observation during Leonid meteor shower-2002 from Kolkata, India. Indian J. Phys. **76B**(6), 693 (2002)

[266] Guha, A., De, B.K., Choudhury, A., Roy, R.: Investigation on spectral character of ELF electromagnetic radiations during Leonid 2009 meteor shower. Astrophys. Space Sci. **341**(2), 287 (2012)

[267] Landau, L.D., Lifshitz, E.M.: Fluid Mechanics. Pargamon, New York (1989), Chap. VII

[268] Rodger, C.J.: Subionospheric VLF perturbations associated with lightning discharges. J. Atmos. Sol.-Terr. Phys. **65**(5), 591 (2003)

[269] Price, C., Blum, M.: ELF/VLF radiation produced by the 1999 Leonid meteors. Earth Moon Planets **82**, 545 (1998)

[270] Trautner, R., Koschny, D., Witasse, O., Zender, J., Knofel, A.: Proceedings of Asteroids, Comets, Meteors (ACM 2002), 29 July 2 August 2002, TU Berlin, Germany (2002)

[271] DE, S. S., B. K. DE, A. GUHA and P. K. MANDAL Detection of 2004 Leonid meteor shower by observing its effects on VLF transmission., Indian J. Radio Space Phys, **35**, 396-400

[272] De, S.S., Bandyopadhyay, B., Das, T.K., Paul, S., Haldar, D.K., De, B.K., Barui, S., Sanfui, M., Pal, P., Chattopadhyay, G.: Studies on the anomalies in the behaviour of transmitted subionospheric VLF electromagnetic signals and the changes in the fourth Schumann resonance mode as signatures of two pending earthquakes. Indian J. Phys. **85**(3), 447 (2011b)

[273] De, S.S., Bandyopadhyay, B., Barui, S., Paul, S., Haldar, D.K., De, D., De, B.K., Chattopadhyay, S., Kundu, A.K.: Studies on the effects of 2009 Leonid Meteor Shower on subionospheric transmitted VLF signals and vertical electric potential gradient. Earth Moon Planets **108**(2), 111 (2012a)

[274] De, S.S., Paul, S., Haldar, D.K., De, D., Kundu, A.K., Chottopadhyay, S., Barui, S.: Analyses of the effects of several earthquakes on the sub-ionospheric VLF–LF signal propagation. J. Atmos. Sol.-Terr. Phys. **81**, 20 (2012b)

[275] Gokhberg, M.B., Gufeld, I.L., Rozhnoy, A.A., Marenko, V.F., Yampolsky, V.S., Ponomarev, E.A.: Study of seismic influence on the ionosphere by super long-wave probing of the earth-ionosphere waveguide. Phys. Earth Planet. Inter. **57**, 64 (1989)

[276] Gufeld, I.L., Gusev, G., Pokhotelov, O., Hayakawa, M., Fujinawa, Y. (eds.): Electromagnetic Phenomena Related to Earthquake Prediction, pp. 381–390. Terra Sci. Pub., Tokyo (1994)

[277] Hayakawa, M., Sato, H.: Ionospheric perturbations associated with earthquakes, as detected by subionospheric VLF propagation. In: Hayakawa, M., Fujinawa, Y. (eds.) Electromagnetic Phenomena Related to Earthquake Prediction, p. 391. TerraPub, Tokyo (1994)

[278] Alekseev, A.S., Aksenov, V.V.: On the electromagnetic field in the hearth zone of earthquakes. Dokl. Akad. Nauk **392**(1), 101 (2003)

[279] Grishin, A.N., Matvienko, G.G., Alekseev, V.A., Alekseeva, N.G., Dontshenko, V.A., Vodnev, S.A.: Aerosol and electric characteristics of the atmosphere in seismo-dangerous regions. Preprint No. 6, Tomsk Institute of Atmospheric Optics SO RAN (2003)

[280] Hayakawa, M., Yoshino, T., Morgounov, V.A.: On the possible influence of seismic activity on the propagation of magnetospheric whistlers at low latitudes. Phys. Earth Planet. Inter. **77**, 97 (1993) Hayakawa, M., Molchanov, O.A., Ondoh, T., Kawai, E.: On the precursory signature of Kobe earthquake in subionospheric VLF propa-gation. J. Commun. Res. Lab. **43**, 169 (1996a)

[281] Sasmal, S., Chakrabarti, S.K.: Ionosperic anomaly due to seismic activities part 1: calibration of the VLF signal of VTX 18.2 KHz station from Kolkata and deviation during seismic events. Nat. Hazards Earth Syst. Sci. **9**(4), 1403 (2009)

[282] Ray, S., Chakrabarti, S.K., Sasmal, S., Choudhury, A.K.: Correlations between the anomalous behaviour of the ionosphere and the seismic events for VTX-MALDA VLF propagation. AIP Conf. Proc. **1286**, 298 (2010)

[283] Clilverd, M.A., Rodger, C.J., Thomson, N.R.: Investigating seismo-ionospheric effects on a long subionospheric path. J. Geophys. Res. **104**(A12), 28171 (1999)

[284] Rozhnoi, A., Solovieva, M., Molchanov, O., et al.: Anomalies in VLF radio signals prior the Abruzzo earthquake (*M* 6.3) on 6 April 2009. Nat. Hazards Earth Syst. Sci. **9**, 1727 (2009)

[285] Kasahara, Y., Muto, F., Hobara, Y., Hayakawa, M.: The ionospheric perturbations associated with Asian earthquakes as seen from the subionospheric propagation from NWC to Japanese stations. Nat. Hazards Earth Syst. Sci. **10**, 581 (2010)

[286] Hayakawa, M., Hobara, Y., Yasuda, Y., Yamaguchi, H., Ohta, K., Izutsu, J., Nakamura, T.: Possible precursor to the March 11, 2011, Japan earthquake: ionospheric perturbations as seen by subionospheric very low frequency/low frequency propagation. Ann. Geophys. **55**(1), 95 (2012)

[287] Ray, S., Chakrabarti, S.K., Sasmal, S.: Precursory effects in the night- time VLF signal amplitude for the 18th January, 2011 Pakistan earthquake. Indian J. Phys. **86**(2), 85 (2012)

[288] Hayakawa, M., Hobara, Y., Yasuda, Y., Yamaguchi, H., Ohta, K., Izutsu, J., Nakamura, T.: Possible precursor to the March 11, 2011,

[289] Liperovsky, V.A., Pokhotelov, O.A., Meister, C.-V., Liperovskaya, E.V.: Physical models of coupling in the lithosphere atmosphere ionosphere system before earthquakes. Geomagn. Aeron. **48**(6), 795 (2008)

[290] Eftaxias, K., Kapiris, P., Dologlou, E., Kopanas, J., Bogris, N., Antonopoulos, G., Peratzakis, A., Hadjicontis, V.: EM anomalies before the Kozani earthquake: a study of their behavior through laboratory experiments. Geophys. Res. Lett. **29**(8), 1228 (2002)

[291] Izutsu, J., Oike, K.: The waveforms of VLF electromagnetic waves recorded at the time of the 1995 Hyogo-ken Nanbu earthquake. Proc. Jpn. Acad. Ser. B **79**, 125 (2003)

[292] Izutsu, J.: Influence of lightning on the observation of seismic electromagnetic wave anomalies. Terr. Atmos. Ocean. Sci. **18**(5), 923 (2007)

[293] Eftaxias, K., Kopanans, J., Bogris, N., Kapiris, P., Antonopoulos, G., Varotsos, P.: Proc. Jpn. Acad. Ser. B **76**, 45 (2000)

[294] Hayakawa, M.: Propagation effects of very low frequency radio waves. In: Chakrabarti, S.K. (ed.) AIP Conf. Proceedings, Am. Inst. Physics, New York, vol. **1286**, p. 223. (2010)

[295] M., Hobara, Y., Nickolaenko, A.P.: Intensity of Schumann resonance oscillations and the ground surface temperature. J. Atmos. Electr. **26**(2), 79 (2006)

[296] Sátori, G., Williams, E., Mushtak, V.: Response of the earth- ionosphere cavity resonator to the 11-year solar cycle in X- radiation. J. Atmos. Sol.-Terr. Phys. **67**, 553 (2005).

Chapter - V

SUMMARY, CONCLUSION AND FUTURE SCOPE

The Thesis essentially embodies the analysis of some characteristic of Schumann resonance phenomena recorded over Kolkata and variation of the first mode Schumann resonance frequency during solar proton event and some atmospheric electricity parameters based on the effects of different geophysical and extra-terrestrial events like Earthquake, Thunderstorm, Lightning, Solar Eclipse, Leonid meteor showers upon the ULF/ELF/VLF signals.

At the onset, in chapter-I, a general background about the contents of the thesis is narrated in along with the outline of the chapters followings:

In chapter-II, rudimentally theoretical background of Schumann resonance is discussed in detail. Also in this chapter an experimental setup to detect ELF range is presented. Here Square Loop Antenna, Co-axial Cable and ELF Receiver Circuit etc. have been discussed in details. Data Acquisition Card and Computer System have been discussed in detail. Here flow chart of Data Acquisition Card (DAC) is presented along with pin configuration of IC OPAM 741 and IC LA3161. In this chapter the design of ELF receiver and mathematical calculation of first mode SR frequency have been discussed.

In chapter-III, the study of the first mode Schumann resonance frequency during a solar proton event that took place on 6-7 th March, 2012 is presented. Protons with energy upto 100 Mev are most often emitted from the Sun in conjunction with solar flares which can penetrate deep into the D-region and caused additional ionization leading to conductivity changes thereby modifying SR parameters. The result shows the decrease in frequency during the proton event and the severe Solar X-ray bursts show enhancement of the first mode SR frequency which is presented in this Chapter.

Chapter-IV deals with the studies on different geophysical and extra-terrestrial events within the earth-ionosphere cavity in terms of ULF/ELF/VLF radio waves. Here different atmospheric layers and waveguide, thunderstorm and lightning, ULF signal and earthquake research Atmospheric layers and waveguide, Ionospheric Alfven Resonator (IAR) & Spectral Resonance Structure (SRS), ULF Signal and Earthquake Research, ELF waves and Schumann Resonance, Global Thunderstorm and Lightning Activity, Tropical Surface Temperature of the Earth, SR for Climatic Research, Solar Terminator Effect, Schumann Resonance for earthquake Research, SPE Event, Meteor Shower Effect, VLF Waves, Lightning Center detection by VLF Sferics for Earthquake Prediction, Whistler Phenomena, Ducted Mode of Propagation, Non Ducted Mode of Propagation, Hiss Emission, VLF transmitted signals and different influences etc. have been discussed in detail. The resonance of earth-ionosphere cavity is analyzed by considering the difference propagation characteristic of day and night hemispheres. At the time of solar eclipse the amplitude and phase of the sub-ionospheric transmitted signal have been discussed.

The works presented in different chapters of this thesis are summarized in Chapter V. Problems for extensional work on different topics at various chapter of this thesis have been contemplated. Hope, based on this thesis new researcher who will work in this ELF/VLF field, they will get support properly. Repeated investigation of various anomalies through the ELF, VLF signals may save lives from earthquake, super cyclone, lightning discharging etc. Also the observations of the sub inospheric spectrum have been used to study the essential characteristic of VLF, ELF propagation field. By the use of VLF transmitted signal such as 19.8 KHz which is transmitted from Australia, we can determined the electron and heavy ion number density and nature of earth ionosphere cavity also. Recent in space research, brain wave research, bio physical research, planet in mars research etc. SR frequencies have important role in this field.